INCREASED TRACTION FORCES BY CANCER-ASSOCIATED FIBROBLASTS ALIGN FIBRONECTIN TO DIRECT CANCER CELL MIGRATION

By

Begum Erdogan

Dissertation

Submitted to the Faculty of the

Graduate School of Vanderbilt University

in partial fulfillment of the requirements

for the degree of

DOCTOR OF PHILOSOPHY

in

Biological Sciences

January 31, 2018

Nashville, Tennessee

Approved:

Todd R. Graham, Ph.D.

Charles K. Singleton, Ph.D.

Alissa M. Weaver, M.D., Ph.D.

Deyu Li, Ph.D.

Katherine L. Friedman, Ph.D.

Dedicated to the memories of my father, Ismail Erdogan,

and my Ph.D. advisor, Dr. Donna J. Webb.

ACKNOWLEDGMENTS

I would like to thank my Ph.D. advisor, Dr. Donna J. Webb, for her guidance and support throughout my Ph.D. training. I am very grateful that Dr. Webb made herself available to talk, listen, discuss, and troubleshoot whenever I needed it. I will always remember her positive attitude and her devotion to science.

I would like to express my sincere gratitude to my committee members: Dr. Todd R. Graham, Dr. Charles K. Singleton, Dr. Deyu Li and Dr. Alissa M. Weaver, for their helpful suggestions, continuous guidance and valuable criticism. I am thankful to Dr. Weaver for guiding me through the review process of my paper. I would like to thank Dr. Li and Li lab members, Bryson Brewer and Lijie Yang, for their valued feedback in group meetings and productive collaborations. I would like to extend my gratitude to Dr. Kathy Friedman, for her supervision and help during my time in graduate school and in completion of this thesis.

I would like to thank all the members of the Webb lab, past and present, for their support and friendship over the years. I am grateful to Drs. Simon Hayward, Omar Franco and Anna Means for their contributions to this project. I would also like to thank everyone in the Department of Biological Sciences, for the support and training I received throughout the graduate school.

Finally, I would like to thank my parents, my brother and my husband for their continuous love and support. Thank you for being there for me in one of the most challenging times of my life.

TABLE OF CONTENTS

Page

LIST OF TABLES

Table Page

LIST OF FIGURES

LIST OF ABBREVIATIONS

ACC	Adenoid cystic carcinoma
BM	Basement membrane
CAF	Cancer-associated fibroblast
Cav1	Caveolin 1
CCL	C-C motif chemokine
CDM	Cell-derived matrix
CXCL	C-X-C motif chemokine
CXCR	C-X-C motif chemokine receptor
DMSO	Dimethyl sulfoxide
ECM	Extracellular matrix
EDA	Extra domain A
EDB	Extra domain B
ELC	Essential light chain
EMT	Epithelial-to-mesenchymal transition
FA	Focal adhesion
FAK	Focal adhesion kinase
FAP	Fibroblast activation protein
FBS	Fetal bovine serum
FFT	Fast Fourier Transform
FGF	Fibroblast growth factor
FGFR	Fibroblast growth factor receptor

FITC	Fluorescein isothiocyanate
Fn	Fibronectin
GAP	GTPase activating protein
GDP	Guanosine diphosphate
GEF	Guanine nucleotide exchange factor
GFP	Green fluorescent protein
GTP	Guanosine triphosphate
HGF	Hepatocyte growth factor
HNSCC	Head and neck squamous cell carcinoma
ICAP1	Integrin cytoplasmic domain-associated protein 1
IF	Immunofluorescence
Ig	Immunoglobulin
IL	Interleukin
KD	Knock down
kDa	Kilo Dalton
MAPK	Mitogen-activated protein kinase
MCP1	Monocyte chemoattractant protein 1
MEF	Mouse embryonic fibroblast
MHC	Myosin heavy chain
MLC2	Myosin light chain 2
MMP	Matrix metalloproteinase
MRCK	Myotonic dystrophy kinase-related Cdc42-binding kinase
MyoII	Non-muscle myosin II

NA	Numerical aperture
NF	Normal fibroblast
NHS	N-hydroxysuccinimide esters
PAA	Ployacrylamide
PAGE	Polyacrylamide gel electrophoresis
PBS	Phosphate buffered saline
PDAC	Pancreatic ductal adenocarcinoma
PDGF	Platelet-derived growth factor
PDGFR	Platelet-derived growth factor receptor
PDMS	Polydimethylsiloxane
PG	Proteoglycan
PI3K	Phosphoinositide 3-kinase
PLC-γ	Phospholipase C-γ
PP1	Protein phosphatase 1
RA	Retinoic acid
RGD	Arginine-glycine-aspartic acid
RGE	Arginine-glycine-glutamic acid
Rho	Ras homolog
RLC	Regulatory light chain
ROCK	RhoA-associated protein kinase
RPMI	Roswell Park Memorial Institute
RTK	Receptor tyrosine kinase
SCC	Squamous cell carcinoma

Sdc	Syndecan
SDF1	Stromal cell-derived factor 1
SDS	Sodium dodecyl sulfate
SEM	Standard error of the mean
SF	Scatter factor
SGC	Scirrhous gastric carcinoma
SH2	Src-homology 2
SHARPIN	Shank-associated RH domain interacting protein
TBS	Tris buffered saline
TGFβ	Transforming growth factor-β
TIRF	Total internal reflection fluorescence
TK	Tyrosine kinase
TNC	Tenascin-C
tRNA	Transfer RNA
tTG	Tissue transglutaminase
UV	Ultraviolet
WB	Western blot
WT	Wild-type
αSMA	Smooth muscle α−actin

CHAPTER I

INTRODUCTION

Overview and hypothesis

Cell migration is a multistep process that begins with the extension of a protrusion and the assembly of adhesions at the leading edge, followed by contraction of the cell body and detachment of adhesions at the cell rear. Coordination of these steps enables the cell to move forward. Migration is indispensable for many biological processes, including embryogenesis, immune surveillance, and wound healing. It also contributes to pathological conditions such as rheumatoid arthritis, multiple sclerosis, and cancer metastasis. Cancer cell migration and invasion into the adjacent tissue are initial steps in metastasis, which results in the formation of tumors at a secondary site. Recently, a great deal of effort has been made to understand the contribution of cells in the tumor microenvironment to the regulation of cancer cell migration.

Traditionally, cancer research focused predominantly on cancer cells themselves. However, recent studies point to the importance of the interactions between the cancer cells and the surrounding stroma. One of the most prominent cell types in the tumor stroma is fibroblasts, which are spindle-shaped cells of the connective tissue that deposit extracellular matrix (ECM), regulate inflammation, and mediate wound healing. Following injury, fibroblasts become activated and differentiate into myofibroblasts; they secrete higher levels of ECM constituents and become more contractile. Similarly, myofibroblast-like cells were observed in tumor stroma and referred to as “cancer-associated fibroblasts” (CAFs). This is

intriguing because tumors were previously described as "wounds that do not heal", containing similarities with the wound healing response, such as increased ECM deposition and infiltration of inflammatory cells. CAFs have been shown to express markers, such as α-smooth muscle actin (αSMA) and fibroblast activation protein (FAP), to localize near the tumor margin and more importantly, to have the ability to promote tumor growth. Therefore, there is a lot of current interest in understanding how CAFs influence tumor progression, especially cancer cell migration and invasion. Studies have shown that CAFs from various carcinomas promote the invasion of cancer cells. However, the mechanisms by which CAFs regulate cancer cell migration and invasion are still not well understood.

The goal of this thesis was to identify the mechanisms by which CAFs regulate cancer cell migration. By co-culturing CAFs and cancer cells, we observed that cancer cells migrate along CAFs in a directionally persistent manner. Since assembly and maintenance of the ECM is a major function of fibroblasts and ECM plays an important role in cell migration, we hypothesized that CAFs modulate cancer cell migration by altering the composition and/or architecture of the ECM. We found that CAFs align the matrix fibers, specifically fibronectin, in a parallel fashion. Thus, we sought to identify the molecular processes that CAFs use to align the matrix. Given that increased contractility is a common feature of CAFs, we hypothesized that enhanced contractility leads to higher traction forces by CAFs, which is transduced to the matrix through integrins, resulting in the alignment of the matrix. Cellular contractility and integrin activity can be mediated by growth factor receptor activity. Since CAFs are characterized by high expression of PDGFRs, we investigated the role of PDGFRα in CAF-mediated changes in the ECM organization.

The ultimate purpose of this study was to advance our understanding of the stromal factors that affect cancer cell migration, an initial step in metastasis. Metastasis is the main cause of death in many cancers, thus, it is critical to understand how stromal cells such as CAFs influence cancer cell migration to develop strategies and treatments to prevent metastasis formation.

Tumor microenvironment and cancer-associated fibroblasts

Carcinomas are the most common human cancers that arise from uncontrolled proliferation of epithelial cells. Normal tissues and organs are structured in a way that the epithelial cell layer is laid atop of the basement membrane (BM), which separates the epithelial cells from the stroma. While the epithelium performs specialized functions, the stroma provides structural and connective support for tissues and is composed of blood and lymphatic vessels, nerves and connective tissue. When carcinomas arise, they are confined to the epithelial side of the BM. As tumor progresses, cancer cells break down the BM and invade into the stroma, where they come in contact with many different types of cells (Steeg, 2006). The stromal cells, such as inflammatory cells and fibroblasts, have been implicated in aiding cancer cells in BM degradation, invasion into the stroma and intravasation (Glentis et al., 2017; Wyckoff et al., 2007; Li et al., 2007). Therefore, the stroma surrounding the tumors –tumor microenvironment- takes on an active role in mediating these critical stages in cancer.

One of the most prominent cell types in the stroma is fibroblasts, which are spindle-shaped connective tissue cells that deposit ECM, regulate inflammation, and mediate wound healing (Tripathi et al., 2012). In the wound healing process, fibroblasts differentiate into

myofibroblasts, and secrete a provisional ECM to provide a scaffold for tissue regeneration. The myofibroblastic differentiation of fibroblasts is also referred to as "fibroblast activation" (Schäfer and Werner, 2008; Li and Wang, 2011). Fibroblasts that are found in the tumor stroma also often display an "activated" myofibroblast-like phenotype, which they acquire after being exposed to growth factors and cytokines secreted by cancer cells over a period of time (Madar et al., 2013; Kalluri and Zeisberg, 2006). These activated fibroblasts are referred to as carcinoma-associated fibroblasts or cancer-associated fibroblasts (CAFs) (Figure 1). CAFs can promote tumor progression to malignancy and metastatic spread by facilitating underlying processes such as cell growth, increased angiogenesis, invasion and metastasis. CAFs promote cell migration and invasion through two main mechanisms: (1) secretion of growth factors and cytokines, (2) reorganization of the stromal ECM (Erdogan and Webb, 2017).

The role of CAF-secreted factors in cancer cell migration and invasion

Migration and invasion of cancer cells into the adjacent tissue is an important initial step in metastasis, a process that can result in the formation of tumors at secondary sites (Valastyan and Weinberg, 2011). CAFs have been shown to secrete growth factors and pro-migratory cytokines which regulate the migratory and invasive behavior of cancer cells in a paracrine manner (Figure 2a). One of the major pro-metastatic factors derived from CAFs is the cytokine transforming growth factor-β (TGFβ). TGFβ is a secreted protein that regulates many cellular functions such as cell growth, proliferation, differentiation and apoptosis (Jakowlew, 2006). CAFs have been shown to secrete increased levels of TGFβ

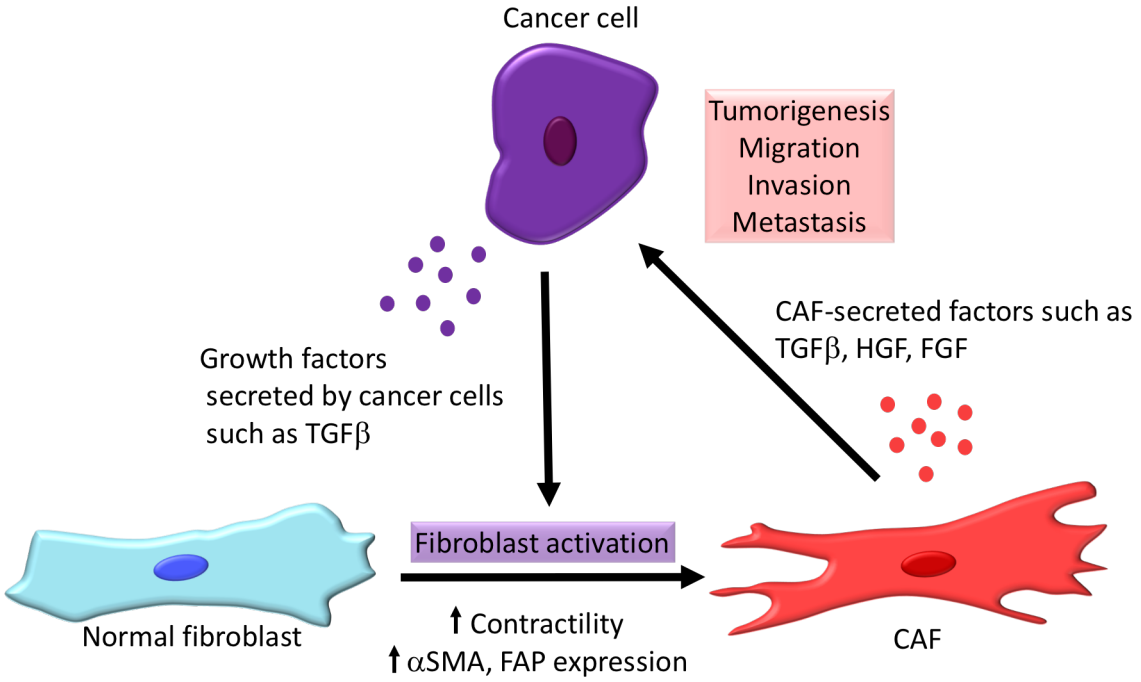

Figure 1. Crosstalk between cancer cells and CAFs in the tumor microenvironment. Secretion of growth factors such as TGFβ from cancer cells can activate stromal fibroblasts into CAFs, increasing their contractility and expression of CAF markers, including αSMA and FAP. CAFs, in turn, secrete higher amounts of growth factors such as TGFβ, HGF and FGF, which further stimulate tumorigenesis, migration, invasion and metastasis of cancer cells.

Reprinted from (Erdogan and Webb, 2017)

(Ao et al., 2007; Yu et al., 2014). TGFβ, present in CAF-conditioned media, stimulated epithelial-to-mesenchymal transition (EMT) in breast cancer cells, inducing expression of mesenchymal markers such as vimentin, fibronectin, and matrix metalloproteinases (MMPs) 2 and 9. In addition, CAF-derived TGFβ enhanced migration and invasion of breast cancer cells (Yu et al., 2014). Inhibition of the TGFβ pathway in cancer cells negated the effects of CAF-conditioned media on cancer cells (Yu et al., 2014). Similar pro-migratory effects of CAF-derived TGFβ were also observed in other cancer types such as gastric, colorectal, and bladder cancer (Fuyuhiro et al., 2012; Shimao et al., 1999; Kim et al., 2015; Zhuang et al., 2015). Intriguingly, other studies reported that blocking TGFβ signaling in CAFs enhances invasion of carcinoma cells by increasing the expression of hepatocyte growth factor (HGF) by CAFs (Cheng et al., 2008; Oyanagi et al., 2014). However, how TGFβ – HGF crosstalk is regulated in different cancers and CAFs is currently not well understood.

HGF, also called scatter factor (SF/HGF), is primarily secreted by stromal cells and regulates functions such as differentiation, proliferation, and migration in epithelial cells, which express its cell-surface receptor c-Met (Rizwani et al., 2015). CAFs secrete high levels of HGF and the ECM glycoprotein tenascin-C (TNC), which stimulated the invasion of colon cancer cells into Matrigel and type I collagen gels (De Wever et al., 2004). Interestingly, these two factors are not sufficient to promote the invasion of cancer cells individually, underscoring the interdependent roles of the ECM and soluble factors in modulating cancer cell behavior (De Wever et al., 2004).

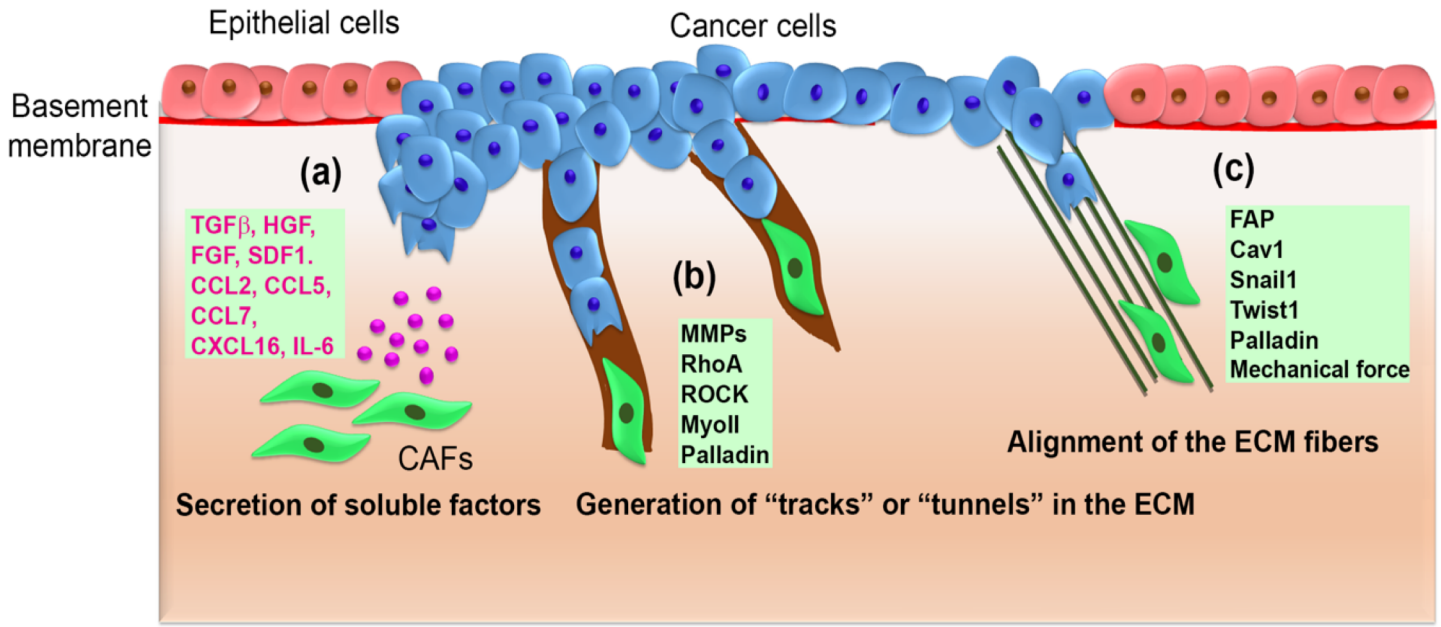

Figure 2. Schematic of CAF-mediated cancer cell migration and invasion. (a) CAFs modulate cancer cell migration and invasion by altering the tumor microenvironment via secretion of growth factors and cytokines such as TGFβ, HGF, FGF, SDF1, CCL2, CCL5, CCL7, CXCL16, and IL-6. (b) CAFs modify the stromal ECM through MMP, RhoA, ROCK, MyoII and palladin, generating "tracks" or "tunnels" in the matrix for cancer cells to follow. (c) CAFs alter the matrix architecture in the tumor stroma, organizing the ECM into parallel fibers that facilitate cancer cell migration and invasion. FAP, Cav1, Snail1, Twist1, palladin as well as mechanical force play a role in ECM alignment.

Reprinted from (Erdogan and Webb, 2017)

HGF, released by CAFs, was also shown to induce migration and invasion of head and neck squamous cell carcinoma cells (Grugan et al., 2010; Kumar et al., 2015). Clinical trials are currently underway using the anti-HGF antibody ficlatuzumab for treatment of HNSCC and non-small cell lung cancers (clinicaltrials.gov).

TGFβ and HGF signaling have been shown to play a critical role in the CAF-mediated cancer cell invasion. However, soluble factors, such as fibroblast growth factor (FGF), are also secreted by CAFs and mediate cancer cell migration and invasion. A study by Henriksson *et al.* showed that treating fibroblasts with conditioned media from colon cancer cells transformed the fibroblasts into CAFs (Henriksson et al., 2011). Culture media from these CAFs, which produced increased levels of FGF1, enhanced the migration and invasion of colon cancer cells in Boyden chambers and in three dimensional organotypic invasion assays. Furthermore, blocking the interaction of FGF1 with its receptor FGF receptor-3 (FGFR3) abolished the pro-invasive effects of the CAF-conditioned media on colon cancer cells (Henriksson et al., 2011). CAFs also express other FGF isoforms such as the surface-associated growth factor FGF2, which is typically not secreted into the extracellular space. When CAFs expressing FGF2 came into direct contact with colorectal cancer cells, the cancer cells became elongated, migrated longer distances, and invaded into the fibroblast-supplemented Matrigel (Knuchel et al., 2015). These effects were attributed to the activation of FGF receptor on cancer cells through binding to FGF2 on CAFs, the effects of which were counteracted by treatment with FGF receptor inhibitors (Knuchel et al., 2015).

Another group of soluble molecules that are important in the regulation of tumor progression and cancer cell-stroma interactions are in the cytokine/chemokine family (Table 1 and Figure 2a) (Mezawa and Orimo, 2016). One of these chemokines is the stromal cell-

derived factor-1 (SDF1), also known as C-X-C motif chemokine 12 (CXCL12), which interacts with the chemokine receptor-4 (CXCR4). Orimo *et al*. demonstrated that breast carcinoma CAFs express high levels of SDF1 that recruit CXCR4-expressing endothelial precursor cells to tumors, resulting in augmented angiogenesis and tumor growth (Orimo et al., 2005). Increased SDF1α expression was also observed in endometrial cancer-derived CAFs and shown to increase cancer cell migration and invasion (Teng et al., 2016). In this study, SDF1 increased the expression of metalloproteinases 2 and 9 (MMP2 and MMP9) in CAFs through an autocrine mechanism, which enhanced cancer cell invasion in CAF-modified Matrigel.

Two independent studies of oral squamous cell carcinomas showed that CAFs secrete increased levels of the chemokine (C-C motif) ligand 2 (CCL2), also known as monocyte chemoattractant protein 1 (MCP1). CCL2 was found to promote cancer cell migration and invasion through activation of focal adhesion kinase (FAK) and galectin-1 (Min et al., 2015;

Table 1. Soluble factors released by CAFs and their receptors in cancer cells

Growth factor /cytokines	*Receptors*
TGFβ	TGF-β type I and II receptors
HGF	c-MET
FGF1	FGFR3
FGF2	FGFR
SDF1/CXCL12	CXCR4
CCL2/MCP1	CCR2
CCL5, CCL7 AND CXCL16	CCR5, CCR1/3 and CXCR6
IL-6 AND IL-8	IL6R and IL8R

Wu et al., 2011). CAFs also secrete higher levels of the chemokines CCL2, CCL5, CCL7 and CXCL16 compared to normal fibroblasts from the same patient, and all of these chemokines were found to increase the migration of hepatocellular carcinoma cells (Liu et al., 2016).

In addition to chemokines, CAFs also secrete cytokines from the interleukin family. Interleukin-6 (IL-6) in CAF-conditioned media promoted the invasion of melanoma cells from tumor spheroids into the surrounding type I collagen matrix (Jobe et al., 2016). Co-culturing CAFs with melanoma cells induced IL-8 secretion by CAFs, and inhibition of IL-6 and IL-8 abrogated the invasion of melanoma spheroids (Jobe et al., 2016). Retinoic acid (RA), a lipophilic molecule derived from vitamin A, is thought to exert therapeutic effects by decreasing the secretion of IL-6 by CAFs, thereby limiting pancreatic cancer cell migration and induction of EMT (Guan et al., 2014; Carapuça et al., 2016).

Paracrine communication between CAFs and tumor cells play a significant role in mediating cancer cell migration, invasion, and metastasis. Some growth factors and cytokines that were shown to induce cancer cell migration and invasion are listed in Table 1. Targeting these growth factor/cytokine signaling pathways in CAFs could have therapeutic benefits for cancer patients by impairing the tumor-supportive roles of CAFs. However, additional studies are needed to better discern the role of paracrine communication between CAFs and cancer cells *in vivo*.

CAFs promote cancer cell invasion by modifying the stromal ECM

Fibroblasts are indispensable components of connective tissue, and their major function is the deposition and assembly of the ECM. They secrete multiple components of

the stromal ECM, including fibronectin as well as types I, III, and V collagens (Miles and Sikes, 2014). Fibroblasts also maintain ECM homeostasis by facilitating its turnover and degradation through secretion of enzymes such as MMPs (Cunha et al., 2003). CAFs exhibit abnormal activity in terms of ECM regulation; they secrete high levels of ECM proteins such as fibronectin and type I collagen, and express isoforms of fibronectin that are not normally expressed in adult tissues (oncofetal Fn). In addition, CAFs modify the stromal ECM by enhanced expression and activation of MMPs (Miles and Sikes, 2014).

Changes in the matrix environment, implemented by CAFs, can facilitate cancer cell migration and invasion. Gaggioli *et al*. observed that CAFs deformed type I collagen matrices using MMPs and Rho-ROCK-mediated contractile force, thereby creating "tracks" in the ECM. These tracks enabled squamous cell carcinoma (SCC) cells to migrate as a collective chain, following the lead of the CAF that generated the track (Figure 2b) (Gaggioli et al., 2007). This study provided a new model of CAF-mediated cancer cell invasion in which CAFs physically remodel the matrix, allowing cancer cells to invade while still maintaining their epithelial properties (Gaggioli et al., 2007). A recent study made similar observations using salivary gland adenoid cystic carcinoma (ACC) cells (Li et al., 2016). Utilizing a microfluidic device, the authors co-cultured ACC cells and CAFs in a chamber that was separated from the chemoattractant (20% FBS) by Matrigel. CAFs invaded the Matrigel using MMP activity and ACC cells followed behind them (Figure 2b). However, in this study, generation of tracks in the ECM by CAFs was not sufficient to promote cancer cell invasion, as blocking the CXCL12/CXCR4 pathway inhibited cancer cell invasion into the tracks generated by CAFs, indicating that biochemical signaling between CAFs and cancer cells was required to drive ACC cell invasion (Li et al., 2016).

Another study examined the role of caveolin-1 (Cav1) on the mechanical regulation of the ECM by CAFs. Cav1 is a major component of the caveolar membrane, which also activates the small GTPase Rho by regulating its inhibitor p190RhoGAP (p190) (Goetz et al., 2011). Cav1 is enriched in the stroma of breast and renal carcinomas, and it is overexpressed by breast cancer CAFs. Interestingly, Cav1-expressing MEFs organized fibronectin into parallel fibers that supported cancer cell migration with increased velocity and directionality (Figure 2c) (Goetz et al., 2011). The remodeling of the fibronectin matrix by Cav1-expressing mouse fibroblasts was dependent on cellular contractility mediated by Rho. Furthermore, orthotopic injection of cancer cells into the mammary glands of wild-type (WT) or Cav1 knockout mice resulted in differences in the tumor stromal ECM. The loss of Cav1 slightly decreased tumor growth and metastasis, and more importantly, these tumors were minimally invasive with fewer collagen fibers surrounding the tumor. In contrast, tumors in WT mice consisted of radially aligned collagen fibers with interacting tumor cells along them, suggesting a more invasive tumor microenvironment (Goetz et al., 2011). Remodeling of the ECM through increased contractility of CAFs was also observed in scirrhous gastric carcinoma (SGC) (Yamaguchi et al., 2014). Co-culture of SGC cells and CAFs generated "invasive foci" in Matrigel. These invasive foci were comprised of CAFs, which reorganized the matrix through actomyosin contractility, and cancer cells that surrounded the CAFs that had invaded into Matrigel. Furthermore, treatment with the myosin-II (MyoII) inhibitor blebbistatin significantly reduced the invasion of these foci, whereas treatment with the broad MMP inhibitor GM6001 did not perturb the matrix remodeling and invasion phenotype (Yamaguchi et al., 2014).

CAFs from different carcinomas, such as breast and pancreas, have been shown to

align matrix fibers into parallel orientation, creating an anisotropic (directionally-dependent) matrix topography. Fibroblast activation protein (FAP), which is a serine protease that is overexpressed in CAFs, was found to contribute to the aligned matrix organization by CAFs (Figure 2c) (Lee et al., 2011a). Another protein that is involved in CAF-mediated matrix organization is Snail1 (Stanisavljevic et al., 2015). Snail1 is a transcriptional regulator that is responsive to TGFβ signaling and regulates EMT in cancer cells (Zhang et al., 2016). It is expressed by a subset of CAFs and mediates anisotropic fiber organization and increased matrix stiffness by upregulating αSMA expression and RhoA activation in response to TGFβ treatment (Stanisavljevic et al., 2015). Snail1 knockout MEFs do not generate a matrix with parallel fiber orientation and thus, do not support directional cell migration and invasion (Stanisavljevic et al., 2015). Twist1, another transcriptional regulator of the EMT, is also expressed by CAFs (García-Palmero et al., 2016). Expression of Twist1 in immortalized human fibroblasts induced CAF-like properties, including the ability to cause increased collagen contraction and alignment, stiffening of matrix fibers, and stimulation of cancer cell invasion. These effects of Twist1 resulted from upregulated expression of type VI collagen α1 and palladin (García-Palmero et al., 2016). Palladin is an actin scaffold protein that regulates cell migration by controlling actin polymerization (Gurung et al., 2016). Brentnal *et al*. demonstrated that increased palladin expression in CAFs correlates with enhanced RhoA activation, matrix degradation, and cell invasion into Matrigel (Brentnall et al., 2012). Pancreatic cancer cells that are co-cultured with palladin-expressing fibroblasts invade the Matrigel by following "tunnels" created by the fibroblasts (Goicoechea et al., 2014).

Normal fibroblasts displayed CAF-like properties when subjected to mechanical stretching. These fibroblasts also aligned fibronectin, similar to prostate CAFs and promoted

the directionally persistent migration of cancer cells (Figure 2c) (Ao et al., 2015).

Cell migration and adhesion

Cell migration refers to the process by which a cell moves from one location to another. This process is essential for normal development and homeostasis, however, it also contributes to pathological conditions such as cancer (Webb et al., 2012). Cell migration requires coordination of multiple cellular processes (Figure 3) (Vicente-Manzanares et al., 2005). The first step in migration is the formation of a protrusion in the leading edge called the lamellipodium, formed by branched actin networks. Actin polymerization at the lamellipodium pushes the plasma membrane forward, generating the initial forward movement (Ridley, 2003). Next, adhesion complexes form, linking actin cytoskeleton to the ECM. The adhesions serve as attachment points (focal complexes) which mature into focal adhesions (FA) that enable cells to produce traction forces to drive cell migration forward (Nobes and Hall, 1995; Galbraith et al., 2002). These tractions forces are generated by the activity of myosin II motor proteins, which bind to anti-parallel actin filaments and enable the translocation of the cell. In the final step of the migration cycle, the focal adhesions disassemble at the cell rear and the trailing edge retracts as the cell moves forward (Ridley, 2003). Efficient migration of cells is dependent on the coordinated assembly and disassembly of the cell-matrix adhesions. Adhesions are complex structures -- nearly 200 proteins have been identified in cellular adhesion complexes (Zaidel-Bar et al., 2007). The adhesion proteins include the integrin family of transmembrane receptors, signaling proteins such as kinases, adaptor and structural molecules (Byron et al., 2010).

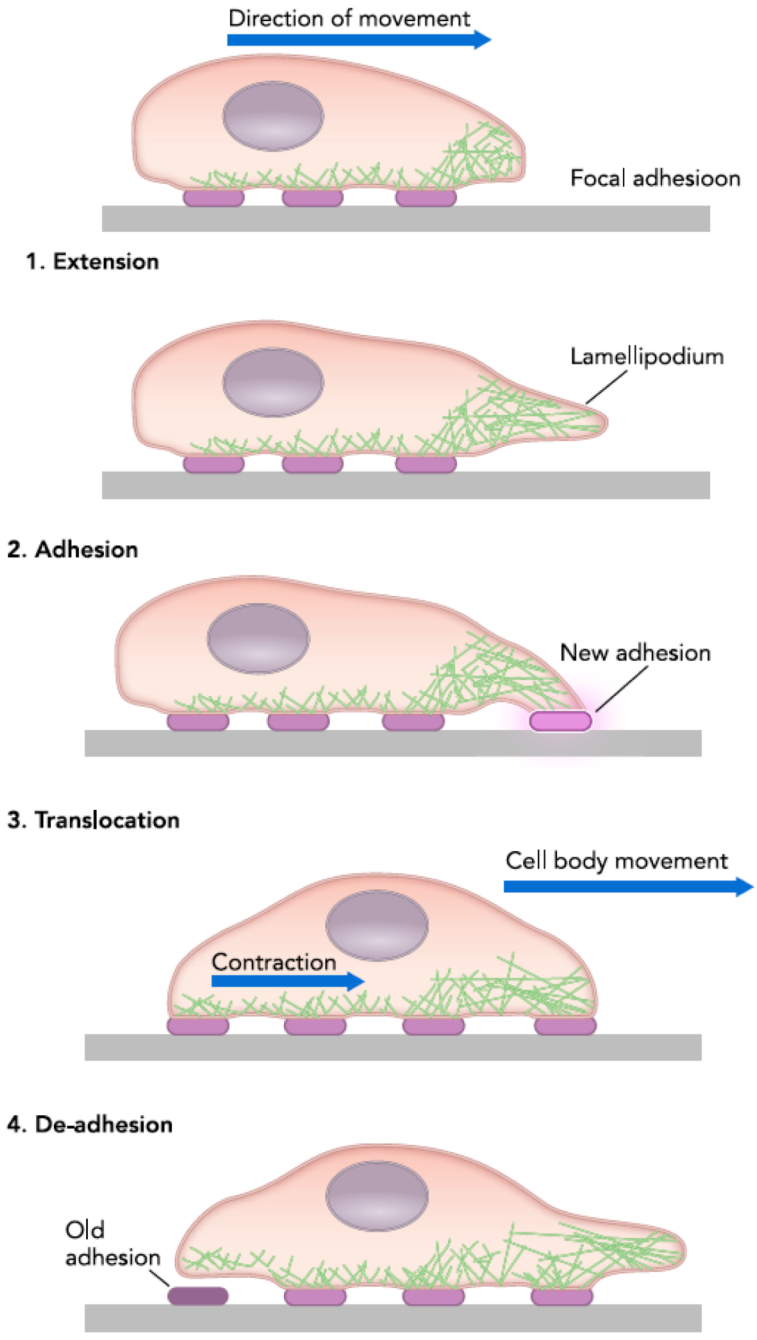

Figure 3. Steps of cell migration. 1. Extension. Cell migration initiates by extension of an actin-rich protrusion (lamellipodia) at the leading edge. 2. New adhesions are formed where cell makes contact with the substrate. 3. Through actin-myosin contractions, cell body moves forward. 4. Adhesions in the cell rear are released to enable forward movement.

Reprinted from (Tschumperlin, 2013)

Different modes of migration have been observed in cancer cells: Cancer cells can migrate as single cells or in clusters of adhesive cells undergoing collective migration (Yilmaz and Christofori, 2010). In single cell migration, cells lose their cell-cell contacts and migrate individually. In collective migration, cells maintain their cell-cell adhesions and move as sheets of cells or follow a leading a cell as a group (Friedl et al., 2012). Intrinsic properties of the cancer cells such as loss of cell-cell adhesions or increased contractility are important for determining the mode of cancer cell migration (Polacheck et al., 2013). In addition, environmental cues, including biochemical signals such as chemokines or growth factors secreted from stromal cells, and physical factors such as matrix topography and stiffness, all play a critical role in determining the properties of cell migration, including the migration mode, speed, orientation and directionality (Taddei et al., 2013; Yeung et al., 2005). For example, anisotropic matrix environments can provide cells with directional cues, in which cells move directionally along the ECM fibers (Larsen et al., 2006; Doyle et al., 2009). Perpendicular realignment of collagen fibers at the tumor periphery has been shown to increase breast cancer cell invasion compared to collagen fibers aligned in parallel to the tumor (Provenzano et al., 2008; Conklin et al., 2011a). ECM rigidity/stiffness is also higher in tumors compared to normal tissue (Yeung et al., 2005; Seewaldt, 2014). The physical forces on the ECM fibers and biochemical crosslinking of ECM proteins lead to stiffening of the stromal ECM. Stiffer ECM promotes changes in proliferation rate, integrin-mediated adhesions and migration of cancer cells (Kaukonen et al., 2016a; Levental et al., 2009; Zaman et al., 2006).

The extracellular matrix

The ECM is the non-cellular component of all tissues and organs, consisting of secreted proteins and polysaccharides that form an intricate network (Frantz et al., 2010). The ECM not only acts as a structural framework for the cells, but also provides biochemical and biomechanical cues to support the cells. Many cellular processes such as cell survival, growth, differentiation and migration are dependent on the interactions between the cells and the ECM (Hynes, 2009).

Two types of macromolecules make up the majority of the ECM: Proteoglycans (PG) and fibrous proteins such as collagen, fibronectin and elastin (Frantz et al., 2010). PGs are highly hydrophilic and form a gel-like substance which resists compressive forces and supports rapid diffusion of nutrients and metabolites between the cells and blood. Collagen is the most abundant fibrous protein in the ECM, giving tensile strength to tissues (Brinckmann, 2005). Collagen is produced and secreted by fibroblasts and assembled into the matrix in a Fn-dependent manner (Velling et al., 2002; Kadler et al., 2008). Fn is a large ECM glycoprotein which provides attachment points for cells and regulate the overall structure and organization of the matrix by mediating the assembly of ECM molecules such as collagen I, fibrillin, and tenascin-C (Kadler et al., 2008; Kii et al., 2010b). Elastic fibers provide resilience to the ECM, enabling recoil of the tissue following a stretch.

Although the ECM can be viewed as an inert scaffold that stabilizes the physical structure of the tissues, it is becoming more apparent that the ECM is highly dynamic in that it is constantly being remodeled by the cells, and in turn, it influences the behavior of the cells within it. The ECM shows great variability in its composition, topology and physical properties between different tissues (e.g. lungs versus bone), and within the same tissue when

under different physiological states (e.g. normal versus cancerous). In cancer, changes in the ECM properties affect numerous cellular activities such as proliferation and migration (Insua-Rodríguez and Oskarsson, 2016; Seewaldt, 2014; Alexander and Cukierman, 2016).

Fibronectin

Fibronectin (Fn) is an ECM protein that regulates a wide variety of cellular processes such as cell survival, adhesion, migration, and differentiation (Pankov and Yamada, 2002; Magnusson and Mosher, 1998). Fn is essential for vertebrate development; inactivation of *FN* gene in mice results in embryonic lethality due to defects in mesoderm formation (George et al., 1993). Plasma is an abundant source of Fn; in wound healing, Fn from plasma is assembled into the provisional matrix to initiate the tissue repair (Lenselink, 2015). Cellular Fn is found in the fibrillar matrices of most tissues and provides a structural framework for the ECM (Schwarzbauer and DeSimone, 2011; To and Midwood, 2011). Fn interacts with many other ECM proteins, such as collagen, heparin, fibrin, and tenascin-C, and mediates their assembly into the matrix (Figure 5A) (Kii et al., 2010b; Kadler et al., 2008; Pankov and Yamada, 2002). Therefore, Fn plays a fundamental role in the overall structure and organization of the ECM. Dysregulation of Fn expression has been associated with diseases such as fibrosis and cancer (Gopal et al., 2017; Muro et al., 2008; Longtin, 2004).

Fn is a large homodimeric protein, in which the 250 kDa Fn subunits are joined with a pair of disulfide bonds at their C-termini. Fn is composed of three types of repeating domains (type I, II and III) as well as a variable domain (Pankov and Yamada, 2002; Schwarzbauer and DeSimone, 2011) (Figure 5A). Alternative splicing of the Fn mRNA results in multiple forms of Fn protein. Exclusion or inclusion of two type III repeats

produces EDA (also called EIIIA, located between type III repeats 11 and 12) and EDB (also called EIIIB, located between type III repeats 7 and 8) isoforms of Fn. The variable domain (V) is also alternatively spliced; five different lengths of the V region have been found in humans (White et al., 2008). Thus, alternative splicing of the Fn mRNA can give rise to many different Fn variants with differing properties in cell adhesion and ligand binding. Spatiotemporal regulation of expression of these Fn isoforms enables fine-tuning of the composition of the ECM (White and Muro, 2011; Muro et al., 2008). Increased expression of the Fn-EDA and -EDB isoforms has been reported in cancers and was shown to support cancer cell proliferation, migration, and invasion (Wang and Hielscher, 2017).

Fn fibrillogenesis is a cell-mediated process, initiated by integrin binding to Fn on the cell surface (Figure 5B). Although eleven different integrins can bind to Fn, only four of these ($\alpha5\beta1$, $\alpha v\beta3$, $\alpha4\beta1$ and $\alpha IIb\beta3$) have been shown to mediate Fn matrix assembly into fibrils *in vitro* (Sechler et al., 2000; Yang and Hynes, 1996). Among these integrins, $\alpha5\beta1$ is considered the major Fn receptor as it only binds to Fn and generates the most intricate network of Fn matrix (Leiss et al., 2008). When Fn is secreted, its compact conformation prevents its assembly into fibrils in solution. Binding of $\alpha5\beta1$ integrin to Fn, through the RGD and synergy sites in type III repeats 9 and 10, promotes a conformational change from its compact form into an extended form which reveals the hidden Fn-Fn interaction sites (Singh et al., 2010). Integrin binding to bivalent Fn molecules results in integrin clustering, bringing together more Fn molecules and increasing its local concentration, hence increasing Fn-Fn interactions. There are at least four Fn-Fn interaction sites on the Fn subunit, all of which interact with the 70 kDa N-terminal assembly domain, which is essential for Fn fiber assembly (Wierzbicka-Patynowski and Schwarzbauer, 2003). Following binding of integrin

A

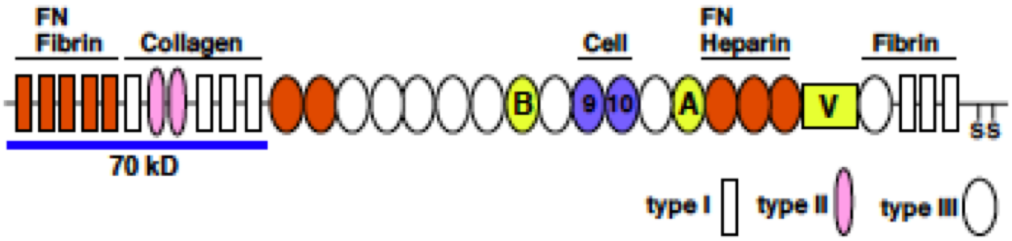

B

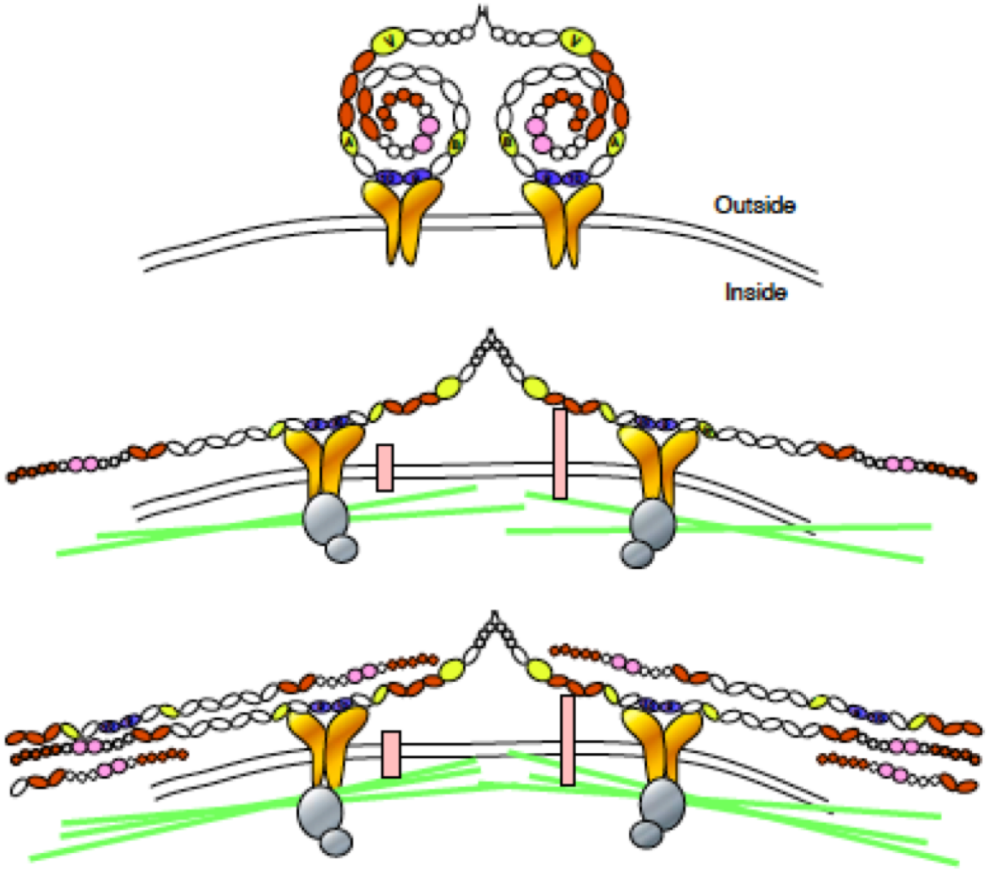

Figure 4. Fibronectin structure and fibrillogenesis (A) Domain structure of a Fn subunit and important molecular interaction sites. (B) Steps of Fn fibrillogenesis. (I) Binding of integrins to the compact form of Fn results in reorganization of the actin cytoskeleton and recruitment of adhesion proteins. (II) Actomyosin contractility produces a pulling force on the Fn dimer though integrins, leading to a conformational change of the dimer which exposes the cryptic Fn-Fn interaction sites. (III) Fn-Fn interactions lead to formation of Fn fibrils.

Reprinted from (Mao and Schwarzbauer, 2005)

to Fn, adhesion proteins are recruited to the intracellular integrin tail which link the integrins to the actin cytoskeleton (Schwarzbauer and DeSimone, 2011). Fn-bound α5β1 integrin clusters translocate centripetally from focal adhesions to central fibrillar adhesions in a process that is dependent on actomyosin contractility (Pankov et al., 2000; Clark et al., 2005). Translocation of integrins on actin filaments applies tension to the Fn molecules, leads to exposure of hidden Fn-Fn interaction sites on Fn and promotes Fn fibrillogenesis (Zhong et al., 1998; Lemmon et al., 2009). Rho GTPase, which is a regulator of myosin-II-mediated contractility, is critical for Fn fibrillogenesis (Zhang et al., 1994; Zhong et al., 1998). Cellular contractility also increases the bond strength between α5β1 integrin and Fn by engaging the synergy site in addition to the RGD site, which is required for matrix assembly (Friedland et al., 2009).

Integrins

Integrins are heterodimeric transmembrane adhesion receptors with two subunits, α and β, combined in a noncovalent complex (Hynes, 1987). There are 18 α and 8 β subunits that can assemble into 24 different integrin receptors with varying substrate specificity and tissue expression patterns (Campbell and Humphries, 2011). Integrins bind to ECM molecules such as laminins, collagens and fibronectin and have been classified based on their ligand affinity (Figure 4A) (Margadant et al., 2011). Loss of many of the integrin subunits causes embryonic or perinatal lethality, highlighting the importance of integrins (Bouvard et al., 2013).

The name “integrin” was devised as these proteins integrate the intracellular actin cytoskeleton and extracellular proteins (Campbell and Humphries, 2011). Each integrin

subunit contains a large extracellular domain which binds to ECM molecules, a single-pass transmembrane domain and, usually, a short cytoplasmic tail (Figure 4B) (Hynes, 2002). The intracellular cytoplasmic tail interacts with adaptor proteins which form the link between the integrin and actin cytoskeleton. The extracellular domain of integrins bind to the ECM proteins and determine the ligand specificity. Conformational changes in the integrin structure regulate its ligand-binding activities (Askari et al., 2009). Integrins can adopt three major conformations: inactive (low affinity), primed (intermediate affinity) or active (high affinity). Integrins are considered inactive when in bent conformation (Figure 4B), although there is evidence that integrins can bind to ligand in a bent conformation as well (Arnaout et al., 2007). Similar to other cell surface receptors, integrins can be activated upon binding to a ligand ("outside-in" signaling). However, integrins can also be activated through binding of adhesion proteins, such as talin or kindlins, to the intracellular β tail ("inside-out" signaling) (Moser et al., 2009; Harburger et al., 2009; Campbell and Humphries, 2011). Following their activation, ligand-bound integrins cluster on the cell surface, which increases the avidity of the cell-ECM attachment (Legate et al., 2009). Integrin binding to the ECM not only results in physical anchorage of the cell to its surroundings, but also transmits biochemical signals that regulate migration, survival and differentiation (Harburger and Calderwood, 2009). In addition to their roles in biochemical signaling pathways, integrins are also mechanotransducers that convert a mechanical stimulus into a biochemical signal (Roca-Cusachs et al., 2012). External mechanical tension and internal cell-generated cytoskeletal forces can activate integrins (Katsumi et al., 2005; Friedland et al., 2009). In response to mechanical forces transduced by integrin-based adhesions, cells can strengthen the adhesions and reorganize the actin cytoskeleton and the ECM (Hinz, 2006).

A

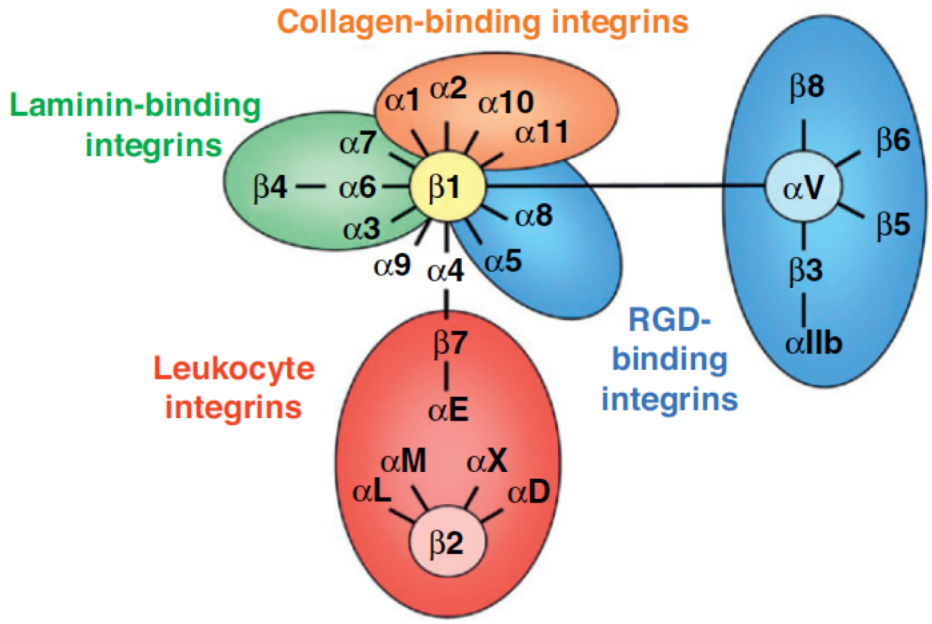

B

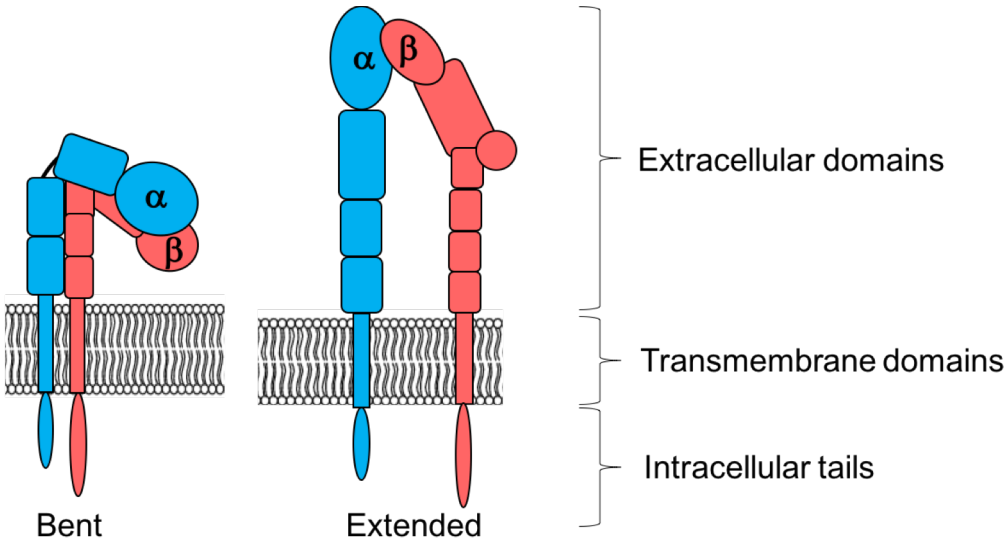

Figure 5. Integrin classes and structure. (A) Classes of mammalian integrins and their ligands. Reprinted from (Margadant et al., 2011). (B) Structure of an integrin heterodimer. Integrins can be found in inactive (bent) and active (extended) conformations. Adapted from (Srichai and Zent, 2010).

α5β1 integrin

α5β1 integrin is the major fibronectin (Fn) receptor that binds to the tripeptide Arg-Gly-Asp (RGD) site and the synergy site (Pro-His-Ser-Arg-Asn, PHSRN) on Fn (Ruoslahti, 1996; Cao et al., 1999). Similar to other integrins, activation of α5β1 integrin recruits kinases such as Src and FAK, and structural and adaptor proteins such as talin, paxillin and vinculin to the cytoplasmic tail (Costa et al., 2013; Ilić et al., 2004; Arthur et al., 2000; Desgrosellier and Cheresh, 2010). Integrin α5β1 activity is negatively regulated by proteins such as integrin cytoplasmic domain-associated protein 1 (ICAP1), Shank-associated RH domain interacting protein (SHARPIN) and nischarin (Pouwels et al., 2012; Bouvard et al., 2013; Alahari et al., 2000). Furthermore, internalization and recycling of α5β1 integrin regulates its availability on the cell surface, mediating its effects on cell adhesion and migration (Margadant et al., 2011; Donovan et al., 2013b). Recent studies identified α5β1 integrin to be mechanosensitive (Schwartz, 2010; Roca-Cusachs et al., 2012). When mechanical force is applied to the cells, α5β1 integrin-Fn linkage becomes stronger as α5β1-Fn bonds engage the synergy site on Fn in addition to the RGD site (Friedland et al., 2009). In cancer cells, α5β1 integrin enhances the generation and transmission of contractile forces to increase invasiveness (Mierke et al., 2011). Although deregulation of α5β1 integrin expression and activity has been frequently observed in cancer, there is no consensus on the role of α5β1 in cancer progression; some reports indicate that α5β1 integrin promotes cancer cell migration, invasion and metastasis (Sawada et al., 2008; Caswell et al., 2007; Qian et al., 2005), other studies found that α5β1 integrin negatively regulates these processes (Tani et al., 2003; Taverna et al., 1998). Some of these discrepancies can be attributed to differences in cell type

or technique, still, it is important to ascertain what kind of role α5β1 integrin plays in cancer.

Non-muscle myosin-II

Non-muscle myosin-II (MyoII) belongs to the class II of the myosin family of actin-based molecular motors (Sellers, 2000). MyoII is similar to other myosin II proteins in that it can walk along actin filaments or facilitate sliding of actin filaments to contract or produce tension in the actin cytoskeleton (Vicente-Manzanares et al., 2009). Myosin II proteins are largely responsible for contraction of cardiac, skeletal and smooth muscle cells. On the other hand, MyoII is found in all eukaryotic cells, and performs important functions in cellular contractility, cell migration, adhesion, and division (Conti and Adelstein, 2008). MyoII is a large hexamer, composed of three pairs of peptides; two 230 kDa myosin heavy chains (MHC), two 20 kDa regulatory light chains (RLCs) and two 17 kDa essential light chains (ELCs) (Figure 6A). Together, these six peptides form the three domains of the MyoII: (i) the amino-terminal head domain that binds to actin and has the ATPase activity, (ii) the neck domain that acts as a lever arm to transduce the generated force and regulate MyoII activity, and (iii) the tail domain that interacts with the tail (rod) domain of another MyoII molecule to form a bipolar MyoII filament (Xiao et al., 2016). The amino-termini of the MHCs form the MyoII head domain that contains the actin-binding and catalytic sites. ATP hydrolysis by the head domain causes a conformational change in the MyoII molecule, powering the movement of MyoII along an actin filament. The carboxy-termini of the MHCs form the rod domain via homodimerization into a coiled-coil structure. In addition, anti-parallel association of MyoII rod domains form MyoII bipolar filaments that are critical for contraction of actin filaments (Newell-Litwa et al., 2015) (Figure 6B).

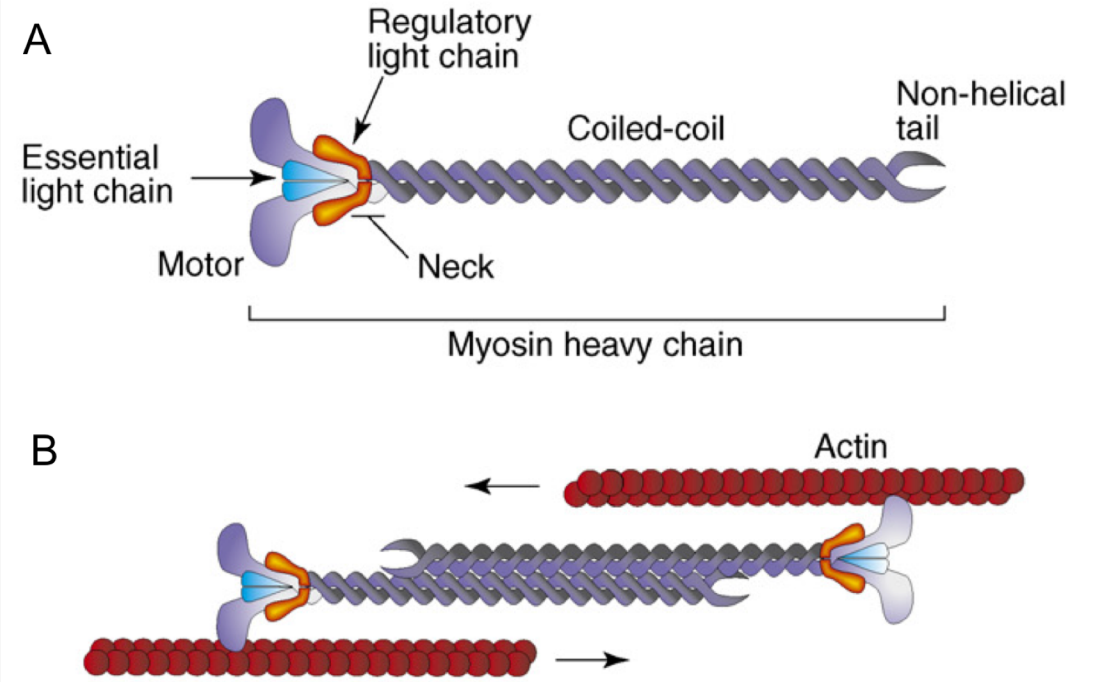

Figure 6. Myosin II protein and bipolar filaments. (A) Schematic showing the domain structure of MyoII protein. The head domain binds to actin and confers ATPase activity. The essential and regulatory light chains bind to the neck region. The MHC tails dimerize to form the coiled-coil rod domain which ends with a short non-helical tail. (B) MyoII rod domains can interact and form bipolar filaments, which can bind to anti-parallel actin filaments, and mediate contraction of actin filaments.

Reprinted from (Clark et al., 2007)

Both of the MyoII light chains bind noncovalently to the MHCs in the neck region (Figure 6A). While ELCs are important for stabilizing MyoII structure, RLCs are critical for MyoII function. Phosphorylation of the Ser19 and/or Thr18 residues on the RLCs controls MyoII conformation and activity. Although phosphorylation of Ser19 is sufficient to activate MyoII, simultaneous phosphorylation of both residues have been shown to further increase the ATPase activity of MyoII (Vicente-Manzanares and Horwitz, 2010). A number of kinases and phosphatases have been identified that act upon the MyoII RLCs and regulate the MyoII-dependent biological processes. Many of the serine/threonine kinases that phosphorylate the MyoII RLCs work downstream of members of the Rho family of small GTPases, such as Rac, Rho and Cdc42. Rho GTPases are molecular switches that are active in their GTP-bound form and inactive in their GDP-bound form. Rho GTPases are activated by guanine nucleotide exchange factors (GEFs) that aid in GTP-loading, and are inactivated by GTPase activating proteins (GAPs) that induce GTP hydrolysis (Van Aelst and D'Souza-Schorey, 1997; Hall and Nobes, 2000; Cherfils and Zeghouf, 2013). Rac and Cdc42 are major regulators of actin polymerization and formation of lamellipodia and filopodia, respectively (Nobes and Hall, 1995; Machacek et al., 2009). RhoA regulates MyoII activity through its effectors such as myotonic dystrophy kinase-related Cdc42-binding kinase (MRCK), RhoA-associated kinase (ROCK) and citron kinase (Amano et al., 1996; Conti and Adelstein, 2008). RhoA is also the major regulator of formation of stress fibers, which are bundles of actin-myosin filaments (Chrzanowska-Wodnicka and Burridge, 1996; Tojkander et al., 2012). Dephosphorylation of the MyoII RLC is carried out by the protein phosphatase 1 (PP1) which decreases MyoII activity (Ito et al., 2004). In addition to phosphorylating MyoII RLC Ser19, ROCK has been shown to inactivate PP1 by phosphorylation, thus enhancing MyoII activity.

An important function of MyoII is in cell adhesion and migration. MyoII is required for maturation of newly-formed, small nascent adhesions into more elongated and larger adhesions. Accordingly, cells with higher MyoII-mediated actin contractility exhibit larger adhesions (Balaban et al., 2001). The mechanism by which MyoII mediates adhesion maturation is not well known, however, there are two proposed views: The first posits that MyoII brings together bundles of actin filaments along with adhesion proteins at their end, thereby increasing integrin avidity and the size and complexity of adhesions. The second suggests that MyoII-mediated mechanical force exposes cryptic binding sites in adhesion proteins, such as talin, to enhance the molecular interactions between adhesion proteins (Vicente-Manzanares et al., 2009).

MyoII is an important mediator of mechanical force in and around the cells; it generates forces by contracting actin filaments and responds to external mechanical stimuli. Application of mechanical force to the plasma membrane leads to activation of MyoII and assembly of actomyosin filaments at these sites to counteract the tension (Luo et al., 2012). Cells also sense the stiffness of their environment and respond to increased matrix stiffness by increasing MyoII-mediated contractility (Fouchard et al., 2011). In cancer, increased Rho-dependent cytoskeletal tension and MyoII activity were found to promote the stiffening of the stromal ECM (Paszek et al., 2005; McBeath et al., 2004). In summary, MyoII is critical for generation of and response to forces in and around the cells, thereby playing important roles in the progression of cancer.

Platelet-derived growth factors and their receptors

Platelet-derived growth factors (PDGFs) were first discovered in the 1970s as serum factors released by platelets that stimulate the proliferation of connective tissue cells such as fibroblasts and vascular smooth muscle cells (Kohler and Lipton, 1974; Ross et al., 1974). Later studies found that PDGFs are also secreted by other cell types such as macrophages, epithelial and endothelial cells. PDGFs promote proliferation, migration and differentiation of mesenchymal cells and play important roles in wound healing and epithelial regeneration (Andrae et al., 2008). PDGF signaling through the PDGF receptors (PDGFRs) is required for the normal development of the blood vessels and many organs such as the lungs, intestines and skin (Chen et al., 2013). Dysregulation of PDGF signaling have been reported in fibrosis and different types of cancers, including prostate, lung, ovarian and colorectal cancers and leukemia (Farooqi and Siddik, 2015; Andrae et al., 2008; Bonner, 2004).

There are four types of PDGF ligands (PDGF-A, -B, -C and -D) encoded by four different genes. Two PDGF polypeptide chains come together to make a biologically active PDGF ligand. There are four PDGF homodimers and one heterodimer, PDGF-AB (Figure 7) (Kazlauskas, 2017). PDGFRs are receptor tyrosine kinases (RTKs) composed of five extracellular immunoglobulin (Ig) loops, a single-pass transmembrane domain and an intracellular tyrosine kinase (TK) domain (Gialeli et al., 2014; Appiah-Kubi et al., 2016). There are two PDGFRs, PDGFRα and -β, which dimerize in response to binding of the dimeric ligand. In addition to the PDGFR homodimers, heterodimerization of α and β receptors was also reported. The interactions between different PDGF ligands and receptors are shown in Figure 7. Following receptor dimerization, intrinsic tyrosine kinase is activated and phosphorylates specific residues in the cytoplasmic region, creating a docking site for

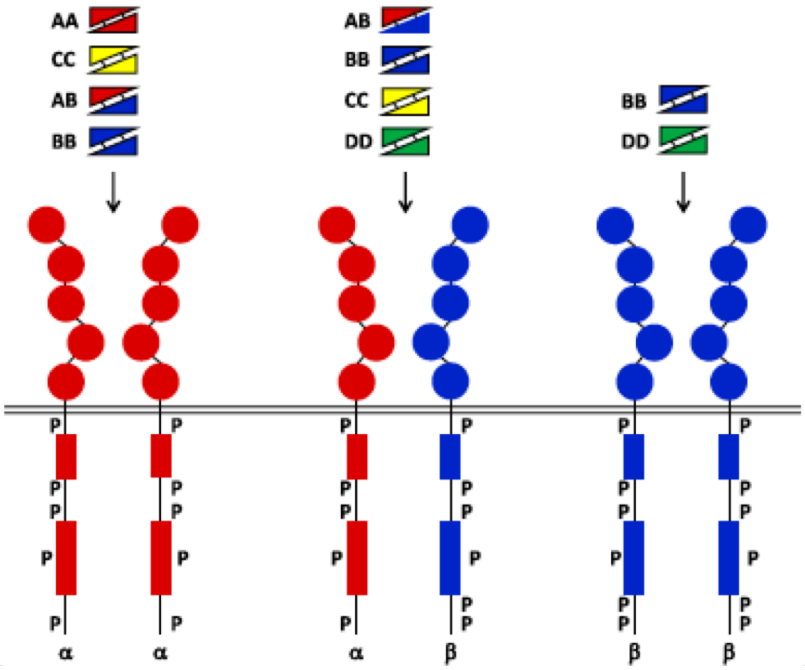

Figure 7. PDGF-PDGFR interactions. Five different PDGF ligand dimers bind to three PDGFR dimers. Each PDGFR has five extracellular immunoglobulin-like domains and two intracellular tyrosine kinase domains. Ligand binding activates receptor tyrosine kinases which autophosphorylate the cytoplasmic tyrosine residues to create docking sites for SH2-domain containing proteins, such as Grb2, SHP2 and PLC-γ.

Reprinted from (Heldin, 2013a)

downstream proteins (Cao, 2013; Wang et al., 2016). Proteins such as phospholipase C-γ (PLC-γ), tyrosine phosphatase SHP-2 and Grb2 recognize the phosphorylated tyrosine residues on PDGFRs through their Src-homology 2 (SH2) domains and activate downstream signaling cascades. PDGFRs activate several well-known signaling pathways such as PI3K and Ras/MAPK to regulate cellular activities such as transcription, growth, differentiation, and migration (Heldin, 2013a). In addition, PDGFRs have been shown to modulate integrin activity. Integrin α5β1 and PDGFRs were found in complex with tissue transglutaminase, an interaction that modulates the activity of both receptors, potentially converging and amplifying their downstream signaling (Akimov and Belkin, 2001; Zemskov et al., 2009a).

Overexpression and genetic alterations of PDGF ligands and receptors were detected in a number of cancers. In cancer cells, PDGF/PDGFR signaling may act in an autocrine fashion to induce tumor growth (Lokker et al., 2002; Jechlinger et al., 2006). Activation of the PDGFR pathway has also been shown to induce EMT in breast and prostate cancer cells (Kong et al., 2008; Jechlinger et al., 2006). In addition to the autocrine effects of PDGF on tumor cells, other cell types in the tumor stroma express PDGF receptors and respond to PDGF ligands in a paracrine fashion (Heldin, 2013a). CAFs express high amounts of both PDGFRs (Gialeli et al., 2014). Secretion of PDGF by cancer cells recruits fibroblasts to tumors in breast and lung cancers (Shao et al., 2000; Tejada et al., 2006). Stromal expression of PDGFRs have been associated with poor prognosis in breast and prostate cancers (Heldin, 2013a). Although activation of the PDGFR pathway in fibroblasts was implicated in wound healing and tissue remodeling, how activation of this pathway affects stromal ECM regulation is not well known.

CHAPTER II

CANCER-ASSOCIATED FIBROBLASTS PROMOTE DIRECTIONAL CANCER CELL MIGRATION BY ALIGNING FIBRONECTIN

Begum Erdogan[1§]*, Mingfang Ao[1§], Lauren M. White[1], Anna L. Means[2,3], Bryson Brewer[4], Lijie Yang[4], M. Kay Washington[5], Chanjuan Shi[5], Omar E. Franco[6,8], Alissa M. Weaver[3,5,7], Simon W. Hayward[6,7,8], Deyu Li[4], Donna J. Webb[1,7†]

[1]Department of Biological Sciences, [2]Department of Surgery, [3]Department of Cell and Developmental Biology, [4]Department of Mechanical Engineering, [5]Department of Pathology, Microbiology and Immunology, [6]Department of Urologic Surgery, [7]Department of Cancer Biology, Vanderbilt University, Nashville, TN 37232, [8]Department of Surgery, NorthShore University HealthSystem, Evanston, IL 60201

[§]*These authors contributed equally*
[†]*Deceased author, May 15, 2017*

[*]Correspondence to Begum Erdogan: email: erdoganbeg@gmail.com; mailing address: VU station B, Box 35-1634, Nashville, TN 37235; phone: 615-947-5325

This article has been published under the same title in the Journal of Cell Biology (2017) November 6; 216 (11): 3799-3816.

Summary

Cancer-associated fibroblasts (CAFs) in the tumor stroma play a key role in tumor progression. Here, Erdogan *et al*. show that CAF-mediated alignment of the fibronectin matrix is a key factor promoting directional cancer cell migration.

Abstract

Cancer-associated fibroblasts (CAFs) are major components of the carcinoma microenvironment that promote tumor progression. However, the mechanisms by which CAFs regulate cancer cell migration are poorly understood. In this study, we show that fibronectin assembled by CAFs mediates CAF-cancer cell association and directional migration. Compared to normal fibroblasts (NFs), CAFs produce a fibronectin (Fn)-rich extracellular matrix (ECM) with anisotropic fiber orientation, which guides the cancer cells to migrate directionally. CAFs align the Fn matrix by increasing MyoII- and PDGFRα-mediated contractility and traction forces which are transduced to Fn through α5β1 integrin. We further show that prostate cancer cells use αv integrin to migrate efficiently and directionally on CAF-derived matrices. We also demonstrate that aligned Fn is a prominent feature of invasion sites in human prostatic and pancreatic carcinoma samples. Collectively, we present a new mechanism by which CAFs organize the Fn matrix and promote directional cancer cell migration.

Introduction

Cancer-associated fibroblasts (CAFs) are one of the most abundant cell types in the tumor microenvironment and have the ability to promote tumor growth (Olumi et al., 1999; Orimo et al., 2005). A key function of normal fibroblasts is to maintain the homeostasis of the extracellular matrix (ECM) (Kalluri and Zeisberg, 2006). In contrast, CAFs and other activated fibroblasts exhibit changes in this critical process. CAFs secrete high levels of ECM proteins such as fibronectin (Fn) and type I and type II collagen, and express oncofetal isoforms of Fn (Barsky et al., 1984; Tuxhorn et al., 2002; Schor et al., 2003; Clarke et al., 2016; Gopal et al., 2017). In addition, CAFs have been shown to alter the architecture and physical properties of the ECM, influencing cell migration, invasion and growth (Kaukonen et al., 2016b; Jolly et al., 2016). Through force-mediated matrix remodeling, CAFs deform collagen I matrices, generating tracks which cancer cells follow (Gaggioli et al., 2007). CAFs also have been shown to generate aligned matrix fibers *in vitro* (Amatangelo et al., 2005; Lee et al., 2011b; Franco-Barraza et al., 2017). Alignment of ECM fibers have also been observed in tumors and found to be associated with poor patient prognosis (Conklin et al., 2011b; Franco-Barraza et al., 2017). However, the mechanisms of ECM alignment and its role in CAF-cancer cell interactions remain poorly understood.

Fn is one of the most abundant ECM proteins and mediates various cellular activities, including adhesion, migration, growth and differentiation (Pankov and Yamada, 2002). Fn binds to ECM proteins such as collagen, periostin, fibrillin, and tenascin-C and facilitates their assembly and organization (Kadler et al., 2008; Kii et al., 2010a). Aberrant expression of Fn has also been associated with tumor progression (Topalovski and Brekken, 2016;

Insua-Rodríguez and Oskarsson, 2016; Wang and Hielscher, 2017). Hence, there is substantial interest in understanding the function of Fn in the tumor microenvironment.

Fn is assembled into fibers through binding to transmembrane integrin adhesion receptors (Mao and Schwarzbauer, 2005; Campbell and Humphries, 2011). Integrin α5β1 is the major Fn integrin and facilitates Fn fibrillogenesis by activating cellular contractility and applying traction forces to Fn (Hinz, 2006; Lemmon et al., 2009; Schwarzbauer and DeSimone, 2011). Although the role of α5β1 integrin in Fn matrix assembly is well known, it is not clear how inside-out signaling in activated fibroblasts is regulated and leads to matrix reorganization.

Growth factor signaling is important in mediating cancer cell-tumor stroma interactions to promote tumor progression. One of the key growth factors connecting cancer and stromal cells is platelet-derived growth factor (PDGF). PDGF is a potent activator of fibroblasts through binding to cell-surface PDGF receptors (PDGFRs). PDGFRs are tyrosine kinase receptors composed of homo- or heterodimers of two PDGFR chains, PDGFRα and PDGFRβ (Donovan et al., 2013). Most cancer cells, including prostate carcinomas, express PDGF ligands but not PDGFRs (Lines et al., 1988; Sitaras, et al., 1988). In contrast, CAFs overexpress both PDGFRs compared to normal fibroblasts (NFs) (Augsten, 2014). PDGF ligands secreted by cancer cells are known to induce proliferation, migration and recruitment of stromal fibroblasts (Östman, 2004). A recent study showed that inactivation of PDGFRα in fibroblasts decreases connective tissue remodeling (Horikawa et al., 2015); however its role in remodeling of other tissues and/or disease states is poorly understood.

In the present study, we demonstrate that Fn fibrillogenesis by CAFs promotes CAF-cancer cell interactions and mediates directional migration of cancer cells in co-culture

assays. Fn-rich cell-derived matrices isolated from CAF but not NF cultures exhibit aligned fiber organization and promote directional cancer cell migration. Compared with NFs, we find that matrix organization by CAFs is mediated by enhanced myosin-II-driven contractility and increased traction forces, transduced to the ECM via α5β1 integrin. Furthermore, we provide evidence that upregulated PDGFRα activity in CAFs plays a role in contractility and parallel Fn organization. We also identify αv integrin as a regulator of cancer cell migration on CAF matrices. Taken together, we demonstrate a new mechanism driving CAF-cancer cell interaction and directional cancer cell migration.

Materials and Methods

Antibodies and reagents

Primary antibodies were diluted 1:300 for immunofluorescence (IF) unless otherwise noted. The primary antibodies used were as follows: mouse anti-fibronectin (#610077, BD Transduction Laboratories, San Jose, CA, diluted 1:300 for IF, 1:1000 for WB), rabbit anti-fibronectin (clone F14, Biogenex, Fremont, CA, 1:1000 for immunohistochemistry and 1:100 for IF), mouse anti-integrin α5 (clone SNAKA51, EMD Millipore, Billerica, MA), rabbit anti-integrin α5 (#AB1949, EMD Millipore, 1:750 for IF), mouse anti-integrin α5 (clone 6F4, a kind gift from R. Horwitz, Allen Institute for Cell Science, Seattle, WA, 1:1000 for WB), mouse anti-integrin β1 (clone 12G10, Abcam, Cambridge, UK), rabbit anti-integrin β1 (#AB1952, EMD Millipore, 1:1000 for WB), rabbit anti-MLC2 (#3672S, Cell Signaling Technology, Beverly, MA), rabbit anti-phospho-S19-MLC2 (#3671S, Cell Signaling Technology), rabbit anti-PDGFRα (clone D1E1E, Cell Signaling Technology), rabbit anti-p-PDGFRα-Y762 (clone D9B1N, Cell Signaling Technology, 1:300 for WB), mouse anti-

vinculin (clone hVIN-1, Sigma-Aldrich, St. Louis, MO, 1:1000 for IF), mouse anti-E-cadherin (clone 36, BD Transduction Laboratories), mouse anti-N-cadherin (clone 8C11, Santa Cruz Biotechnology, Dallas, TX), mouse anti-α tubulin (clone DM1A, Sigma-Aldrich, 1:5000 for WB), mouse anti-β-actin (clone AC15, Sigma-Aldrich, 1:5000 for WB or clone 1A4, Biogenex, 1:1000 for tissue IF). For function blocking experiments, mouse anti-integrin α5 (clone JBS5, Millipore), mouse anti-integrin α5 (clone P1D6, Millipore), mouse anti-integrin αv (clone 272-17E6, Abcam) and goat anti-PDGFRα (clone AF307, R&D Systems, Minneapolis, MN) were used. Mouse IgG (#0107-01) and rabbit IgG (#0111-01) were purchased from SouthernBiotech (Birmingham, AL) and were used as controls in function blocking experiments. For IF staining, Alexa Fluor® 488 goat anti-mouse, Alexa Fluor® 488 donkey anti-rabbit, Alexa Fluor® 488 goat anti-mouse IgG1, Alexa Fluor® 555 goat anti-rabbit and Alexa Fluor® 555 goat anti-mouse IgG2a secondary antibodies were used at 1:600 dilution (Thermo Fisher Scientific, Waltham, MA). For WB, Alexa Fluor® 680 donkey anti-mouse, Alexa Fluor® 680 goat anti-rabbit (Thermo Fisher Scientific), IRDye800® donkey anti-mouse (Rockland, Inc., Limerick, PA) and anti-rabbit HRP-conjugated IgG (Promega, Madison, WI) secondary antibodies were used. siGENOME siRNA SMARTpool for FN1 (#M-009853-01-005) and non-targeting control (#D-001206-14-05) were ordered from Dharmacon (GE Life Sciences, Lafayette, CO) and 50 nM of either siRNA pool was transfected into CAFs using DharmaFECT 1 transfection reagent (GE Life Sciences) following manufacturer's protocols. Cells were kept in Fn-depleted medium which was prepared using gelatin-agarose beads (Sigma, G5384). Fibronectin (F2006) and fluorescein isothiocyanate isomer (F7250) was purchased from Sigma. RGD and RGE peptides were purchased from Bachem (Bubendorf, Switzerland). Rat tail type I collagen

was purchased from BD Biosciences. Blebbistatin was purchased from EMD Bioscience. GFP-vinculin plasmid was a generous gift from Susan Craig (Johns Hopkins University School of Medicine, Baltimore, MD).

Fibroblast isolation and cell maintenance

Human prostatic CAFs were isolated from prostate cancers and NFs from benign prostate hyperplasia tissues. Fibroblasts were isolated from six separate patients' tissue samples (three prostate cancer patients and three BPH patients). CAFs and NFs were prepared as previously described (Olumi et al., 1999). Cells were verified using a tissue recombination bioassay to confirm that CAFs induced tumor formation from BPH1 cells and that NFs did not elicit tumorigenesis. CAFs and NFs were used between passages 4-8 to ensure proper function in ECM production and communication with cancer cells.

Prostatic cancer DU145 cells and fibroblasts were maintained in Roswell Park Memorial Institute medium (RPMI) 1640 with 10% fetal bovine serum (FBS) and penicillin–streptomycin as described previously (Ao et al., 2007). Human head and neck cancer cells SCC61 and JHU012 were maintained in Dulbecco's Modified Eagle's/F12 Medium (Life Technology, Carlsbad, CA) supplemented with 10% FBS and penicillin–streptomycin (Ao et al., 2015).

Fabrication of two-channel co-culture devices

The co-culture microfluidic device was prepared using standard soft-lithography techniques as previously described (Xia and Whitesides, 1998; Jean et al., 2014). First, a master mold was fabricated using photolithography, patterning a layer of photoresist SU8 by

ultraviolet (UV) exposure through a 20,000 dpi photomask. Second, polydimethylsiloxane (PDMS, Ellsworth Adhesives, Germantown, WI) pre-polymer was mixed with a curing agent at a mass ratio of 10:1 and then poured over the mold. After degassing for 30 minutes and curing in a 70°C oven for 2 hours, the PDMS was fully polymerized. The resulting PDMS component was then cut out and peeled from the mold. Inlet and outlet holes were punched through the PDMS layer using a 3.5 mm diameter punch. Third, the PDMS layer was bonded to a 100 μm-thick glass coverslip (No. 1, VWR Vista Vision, Suwanee, GA) after both components were exposed to oxygen plasma. Next, Pyrex cloning cylinders of 8 mm diameter and 8 mm height (Fisher Scientific, Pittsburgh, PA, USA) were attached to the inlet and outlet holes using uncured liquid PDMS for loading and removing cells and media. The liquid PDMS "glues" was subsequently allowed to cure at 70°C for 2 hours. Sterilized water was loaded into the device to keep the walls of the microfluidic channels hydrophilic. Finally, the assembled device was sterilized under UV light for 1 hour.

Microscopy

A Quorum WaveFX spinning disk confocal system equipped with a Nikon Eclipse Ti microscope and a Hamamatsu ImagEM-CCD camera was used for imaging the IF-stained coverslips and for recording cell migration where multiple channel acquisition was required. A Plan Fluor 40X objective (NA 1.3) was used for imaging the IF-stained coverslips. A Nikon 10X Ph1 ADL objective (NA 0.25) and a Plan Fluor 20X objective (NA 0.75) were used to image cell migration. DAPI, Alexa Fluor 488, Alexa Fluor 555 and acti-stain 670 were excited by laser lines at 405 nm, 491 nm, 561 nm and 642 nm, respectively (Semrock, Rochester, NY). Emission filters for these fluorophores were 460/50, 525/50, 593/40 or

620/60 and 700/75, respectively (Semrock). Images were acquired and analyzed using MetaMorph software (Molecular Devices, Sunnyvale, CA).

Total internal reflection fluorescence (TIRF) microscopy and cell migration movies in phase contrast were performed using an inverted Olympus IX71 microscope (Melville, NY) with a Retiga EXi CCD camera (QImaging, Surrey, BC). An Olympus UPlanFl N 10X objective (NA 0.30) was used for cell migration assays. TIRF images were taken using an Olympus PlanApo 60X OTIRFM objective (NA 1.45) with a 488 nm laser line from a HeNe laser (Prairie Technologies, Middleton, WI). MetaMorph was used for image acquisition and analysis.

Co-culture in microfluidic devices

Microfluidic devices were incubated with culture medium at 37°C and sub-confluent fibroblasts and cancer cells were labeled with CellTracker^{TM} Green or CellTracker^{TM} Red ((#C2925 and #C34552, Thermo Fisher Scientific), respectively. After a gentle but thorough wash, cells were detached and mixed at 1:1 ratio in RPMI complete growth medium. A total of 10^4 cells, suspended in 20 μL of medium, were loaded into each inlet reservoir of a microfluidic cell culture chamber. The cell density was kept low to be able to observe interactions between individual cells. After incubating for approximately 2 hours at 37°C to allow cells to attach, 200-300 μl of RPMI full growth medium was added to the inlet reservoir and cells were incubated overnight. The next day, the cell culture medium was replaced with phenol-red free RPMI supplemented with 5% FBS and 50 mM HEPES, and time-lapse imaging was performed at 37˚C in a temperature-controlled chamber (Live Cell Instrument, Seoul, Korea). Areas of interest were chosen where a fibroblast-cancer cell pair can be

identified and their movement with regards to each other can be analyzed. Images were taken every 10 minutes for 12 hours using the spinning disk confocal system described above. To visualize Fn in co-culture experiments, 5 μg/ml FITC-Fn was added to the culture medium. For these experiments, CAFs and DU145 cells were mixed in 1:1 ratio to yield a total of $4x10^4$ cells which were seeded to a 35 mm glass-bottomed dish and incubated overnight. During this incubation, CAFs incorporated FITC-Fn as they assembled Fn fibers which enabled us to visualize Fn matrix. The next day, the cells were imaged using the 40X objective in the spinning disk confocal system. Images were taken every 30 seconds for 1 h. Cell migration association index was determined by calculating the angle (σ) between the axis of migrating cancer cells and fibroblasts. The association index was defined as the cosine of the angle σ; an index of 0 indicates perpendicular migration of cells in relation to each other, while an index of 1 signifies cells migrating parallel to each other. The migration directionality ratio was calculated by dividing the net distance (D) by the actual path length traveled by the cell (T).

Preparation of FITC-labeled Fn

Fn was diluted to 0.5 mg/ml in borate buffer (170 mM $Na_2B_4O_7$ pH 9.3, 40 mM NaCl) and 6 mg of FITC was dissolved in 200 ml borate buffer. 1 ml of 0.5 mg/ml Fn solution was loaded to a dialysis cassette and placed in the FITC-containing borate buffer and dialyzed at room temperature for 1.5 h in the dark. Next, Fn cassette was dialyzed extensively against 1X PBS pH 7.4 for 2 days, changing the PBS buffer 4-5 times. Protein concentration was determined using the following formula: FITC-protein (mg/ml) = [OD280-(0.36 x OD493)] / 1.4. Fn was then dialyzed against 50% glycerol and stored at -20°C.

Generation of three dimensional cell-derived matrices (CDMs) and migration assays

Three dimensional CDMs were generated as previously described (Beacham et al., 2006). Briefly, 35 mm diameter glass bottom dishes or 6-well plates were coated using a 0.2% (w/v) gelatin solution for 1 hour at 37°C. The gelatin-coated dishes were treated with 1% (v/v) glutaraldehyde in PBS for 30 minutes, followed by a 30-minute treatment of 1M ethanolamine at room temperature. The dishes were then washed extensively using PBS. NFs or CAFs were plated on dishes as a confluent layer, and they were cultured for 8 days in complete growth medium (RPMI 1640 with 10% FBS and penicillin–streptomycin). For CDM generation using CAFs transfected with Fn siRNA, RPMI medium with 10% Fn-depleted FBS and antibiotics was used. In all experiments, the cell culture medium was replenished and supplemented with freshly prepared 50 μg/ml of ascorbic acid on alternate days. On day 8, cells were rinsed with PBS, then extracted from the matrix using an alkaline detergent (0.5% (v/v) Triton X-100 and 20 mM NH_4OH in PBS), leaving the 3D matrix intact and attached to the culture dish.

To visualize the matrix, the CDMs were labeled using 2 μg/ml NHS-ester Alexa Fluor® 488 dye (#A20000, Thermo Fisher Scientific), which was dissolved in 50 mM sodium bicarbonate buffer (pH 9), by incubation for 15 minutes in the dark. The matrices were washed with PBS and treated with 200 mM Tris buffer (pH 7.5) for 10 minutes to deactivate the NHS esters. The labeled 3D CDMs were blocked with 1% BSA solution and stored at 4°C until ready to use. This protocol was kindly provided by A. Doyle (National Institutes of Health, Bethesda, MD).

For cell migration assays using the CDMs, cancer cells were labeled with CellTracker™ Red CMTPX dye (#C34552, Thermo Fisher Scientific) following the

manufacturer's protocol. For 2D migration assays, cells were plated 2 hours prior to imaging. For 3D migration assays, cells were plated 24 hours prior to imaging to allow for invasion of the cells into the 3D matrix. The cells were maintained in phenol red-free RPMI 1640 medium supplemented with 5% FBS and 50 mm HEPES in a 37°C temperature-controlled chamber (Live Cell Instrument, Seoul, Korea) during acquisition. Images were acquired every 5-10 minutes for 6 hours using the spinning disk confocal microscope. MetaMorph was used to track migrating cells and to measure the net distance from the first time point to the last time point. The migration directionality ratio was calculated as described above. Migration speed was calculated by dividing the total distance traveled (μm) by total time (h). In experiments testing integrin function in DU145 cell migration on CAF-CDMs, 10 μg/ml of either function blocking antibody (JBS5 or 17E6) or control IgG was added to culture medium 30 minutes prior to imaging. Function-blocking properties of each antibody were confirmed by cell attachment assays using crystal violet staining.

Immunofluorescence

For most experiments, cells were plated onto glass coverslips coated with 5 μg/ml Fn (#F0895, Sigma-Aldrich) and allowed to attach for 3 hours. However, to allow for Fn matrix deposition and formation of fibrillar adhesions, Fn and integrin staining was performed 48 hours after the cells were plated onto uncoated glass coverslips. Cells were fixed using 4% paraformaldehyde supplemented with 0.12M sucrose in PBS for 15 minutes at room temperature. Following fixation, cells were permeabilized with 0.2% (v/v) Triton X-100 for 3 minutes in most experiments. Cells were not permeabilized for Fn staining, in order to observe the extracellular Fn matrix organization. Blocking was performed for 1 h with 20%

goat serum in PBS. Primary and secondary antibodies were diluted in 5% goat serum and were incubated with the cells at 4°C overnight and 45 minutes at room temperature, respectively. Following each antibody step, coverslips were washed with PBS extensively. DAPI (#AS-83210, AnaSpec, Inc., Fremont, CA) and phalloidin (acti-stain 670, #PHDN1, Cytoskeleton, Denver, CO) co-stains were performed simultaneously with the secondary antibodies. Coverslips were mounted on the glass slides using Aqua Poly/Mount (Polysciences, Inc., Warrington, PA).

The average fluorescence intensity was quantified by dividing the background-corrected, integrated fluorescence intensity in individual cells by the cell unit area using MetaMorph. The size and number of vinculin adhesions were calculated by tracing individual adhesions and using the measure tool within MetaMorph.

Calculation of angles between the fibers and FFT analysis

Fn images were opened in MetaMorph and a template of 9 dots, which was formed by selecting three dots 120 degrees apart on three concentric circles, was placed on the image. The angle between a fiber that intersected with one of the reference dots and its closest intersecting fiber was quantified using Image J (NIH, http://rsb.info.nih.gov/ij). A minimum of 50 angles were measured for each experimental condition in each experiment. This procedure was adapted from a previous protocol for quantifying ECM alignment (Yang et al., 2011).

To characterize fiber orientation, Fast Fourier Transform (FFT) was also used as previously reported (Ayres et al., 2006). Briefly, the FFT function was performed on fluorescence images of Fn and CDMs using ImageJ. Then, a 512 pixel diameter circle was

overlaid on the FFT output image (2048×2048 pixels) in the center using the Oval Profile plug-in (William O'Connell, University of California-San Diego, CA). A radial summation of gray value intensities over the circle was conducted and normalized by dividing it by the total intensity. Peak intensities observed 180° apart from each other indicated an aligned fiber orientation, whereas no noticeable peaks were observed when fibers were unorganized.

Traction force microscopy

Traction forces of fibroblasts were measured as described previously (Sabass et al., 2008; Jean et al., 2013). Briefly, rectangular glass coverslips were mounted with polyacrylamide (PAA) gels embedded with 0.2 μm FluoSpheres® crimson (625/645) fluorescent beads (Invitrogen, Eugene, OR). Immediately after gels solidified, the PAA gel surface was activated using 1 mg/ml Sulfo-SANPAH (ProteoChem, Loves Park, IL) solution in ddH_2O under UV light for 5 minutes on ice. The PAA gels were then washed with ddH_2O and incubated with 25 μg/ml Fn overnight at 4˚C. The Young's modulus of the PAA gels was 15.6 kPa as calculated previously (Sabass et al., 2008; Yeung et al., 2005). This PAA gel compliancy was chosen based on previous reports of prostate cancer tissue stiffness (Hoyt et al., 2008; Zhai et al., 2010). A total of 2×10^3 CellTracker™ green-labeled fibroblasts were incubated on top of the coated coverslip for 3 hours at 37°C to allow cells to adhere before being subjected to imaging. For each cell of interest, a DIC and a fluorescent image of the cell and a fluorescence image of the FluoSpheres® beads beneath the attached cell were taken. Then, trypsin was added to dissociate the cells from the PAA gel, and another fluorescence image of the FluoSpheres® beads was acquired from the same field. The spinning disk confocal microscope was utilized to acquire all of the images. The images were

analyzed using the LIBTRC software developed by Micah Dembo (Boston University, Boston, MA) to determine the average traction forces by cells, normalized to the cell area. Traction force maps were then generated using this software (Dembo and Wang, 1999).

Cell contraction assay

CAFs and NFs were suspended in full growth medium at a density of $6X10^5$ cells/mL. Then, rat tail type I collagen was neutralized and diluted to a concentration of 3 mg/mL. The cell suspension and prepared collagen were mixed on ice at 1:2 ratio, to get a final mixture with $2X10^5$ cells/mL and 2 mg/mL of collagen. 600 µl of the above mixture was loaded into each well of a 12-well-plate and incubated at 37˚C until polymerization was complete. Gels were then covered with 1 ml of medium and detached from plates using a pipette tip to circle around the inside wall of each well. The plates were scanned at the beginning of the assay after 24-hour incubation (end of assay) at 37˚C. The gel area was measured at these time points using MetaMorph. Percent contraction of the gels were calculated by dividing the gel area at 24 hours by the gel area at 0 hours, and multiplying by 100.

Western blot

Cells were lysed using RIPA buffer (25mM Tris-HCl, pH 7.6, 150mM NaCl, 1% NP-40, 1% sodium deoxycholate, 0.1% SDS) with protease inhibitor cocktail (Sigma-Aldrich). The protein concentration in the cell lysates were measured by a BCA assay (BioRad Laboratories, Hercules, CA). 30 µg of each cell lysate was run in an SDS-PAGE gel and transferred to a nitrocellulose membrane. Following blocking in 4% non-fat dry milk in TBS-T solution for 1 h, the membrane was first incubated with the primary antibody at 4°C

overnight, then incubated with the secondary antibody for 1 h at room temperature. The membranes were imaged using an Odyssey CLx imaging system (LI-COR Biosciences, Lincoln, NE). For p-PDGFRα WB, CAFs and NFs were starved overnight and the next morning, stimulated with complete culture medium for 2 h. Cell lysates were then prepared as described above with addition of PhosSTOP phosphatase inhibitor cocktail (Sigma). HRP-conjugated secondary antibodies were used and detected using SuperSignal West Femto maximum sensitivity substrate kit (Thermo Scientific) via Amersham Imager 600 (GE Life Sciences, Pittsburgh, PA). The normalized band intensities were measured using Image Studio Lite Software version 4 (LI-COR Biosciences), which were further normalized to loading controls, either β-actin or α-tubulin.

Adhesion turnover assay

Twenty-four hours prior to the assay, fibroblasts were transfected with 1.5 μg of GFP-vinculin using TransIT-X2® dynamic delivery system according to the manufacturer's instructions (Mirus Bio LLC, Madison, WI). Prior to the assay, 35 mm diameter glass bottom dishes were coated with 5 μg/ml Fn overnight at 4°C. The next day, cells were plated on Fn-coated dishes and allowed to adhere for 1 hour at 37°C. Time-lapse images of GFP-vinculin were acquired at 15 second intervals for 20 minutes using the Olympus IX71 microscope with PlanApo 60X OTIRFM objective (NA 1.45) as described above. Rate constants for adhesion assembly and disassembly were determined as described previously (Webb et al., 2004) using MetaMorph.

Histology

De-identified, formalin-fixed, paraffin-embedded tissue was procured from four cases of prostate cancer and ten cases of pancreatic ductal adenocarcinoma through the Comparative Human Tissue Network with approval from the Vanderbilt Institutional Review Board. Five μm sections were processed as described (Shi et al., 2014) and labeled with antibodies to Fn for colorimetric analysis. Detection was performed using Vectastain Elite ABC kit (Vector Laboratories, Burlingame, CA) following a reaction with 3,3′-Diaminobenzidine (Vector Laboratories). For fluorescent analysis, antibodies to αSMA were detected using the Vectastain Elite ABC kit followed by tyramide signal amplification with the TSA Plus Cyanine 3 kit (Perkin Elmer LAS, Boston, MA) followed by heat inactivation. Binding of anti-Fn antibodies was detected with Cy2-anti-rabbit antibodies (Jackson Immunoresearch Laboratories, West Grove, PA). Slides were counterstained with hematoxylin (Sigma Aldrich) or Toto3 (Molecular Probes, Eugene, OR) and Dapi (Sigma Aldrich). Colorimetric images were obtained on an Axioskop 40 microscope (Carl Zeiss Microimaging, Thornwood, NY) and fluorescent images were captured on the Quorum WaveFX spinning disk confocal system with Nikon Eclipse Ti microscope as described above.

Data analysis and statistics

Statistical analysis was performed using SPSS software version 24, and the Shapiro-Wilk test was performed to assess data normality. P-values were determined using either a student's t-test (if data were normally distributed) or Mann-Whitney U test (if data were not normally distributed). In figures, p-values of less than 0.001 were denoted (***), less than

0.01 were denoted (**) and less than 0.05 were denoted (*) and were designated as statistically significant. The bar graphs were generated using Microsoft Excel and presented as mean ± SEM from at least three independent experiments. The box and whisker plots were generated using GraphPad Prism version 7.02 (GraphPad Software, La Jolla, CA), in which the box ranges from 25-75th percentile, with the middle line indicating the median, and the whiskers indicating 5-95th percentile.

Online supplemental videos

Video 1 shows three fields of DU145-NF co-culture migration. Video 2 shows three fields of DU145-CAF co-culture migration. Video 3 shows JHU012-NF (left) and JHU012-CAF (right) co-culture migration. Video 4 shows a DU145 cell migrating along a CAF and interacting with FITC-Fn fiber (green) assembled by the CAF. Video 5 shows co-culture migration of DU145 cells with control (left) or Fn-KD (right) CAFs. Video 6 shows a DU145 cell migrating on NF-CDM. Video 7 shows a DU145 cell migrating on CAF-CDM. Video 8 shows JHU012 cell migrating on NF (left) and CAF (right) CDM. Video 9 shows adhesion turnover of a NF transfected with vinculin-GFP. Video 10 shows adhesion turnover of a CAF transfected with vinculin-GFP. Online supplemental videos can be viewed at: http://jcb.rupress.org/content/216/11/3799

Results

Fibronectin promotes CAF-cancer cell association and directional cancer cell migration

To investigate the effects of CAFs on cancer cell migration, we co-cultured prostatic fibroblasts with DU145 prostate cancer cells. CellTracker green-labeled CAFs or NFs were

mixed with CellTracker red-labeled DU145 prostate cancer cells in a 1:1 ratio and loaded into two separate, side-by-side chambers of a microfluidic device to mimic the close interactions within the tumor microenvironment (Fig. 8A). When DU145 cells were co-cultured with NFs, they exhibited minimal interaction with NFs and migrated randomly (Fig. 10A-E, supplemental video 1). In contrast, in co-cultures with CAFs, DU145 cells migrated towards and along the axis of CAFs resulting in a higher association index with CAFs (Fig. 10A-E, supplemental video 2). Interestingly, no difference in the migration speeds of DU-145 cells was found in either co-culture condition (Fig. 8B). To test whether CAF-promoted directional cancer cell migration is restricted to tissue-matched cancer cells, or whether CAFs can induce similar effects on other cancer cell types, we subjected head and neck squamous cell carcinoma (HNSCC) cell lines JHU012 and SCC61 to co-culture with prostate CAFs and NFs. Intriguingly, although derived from a different tissue, HNSCC cell lines also displayed an increased association with fibroblasts and directional migration when co-cultured with prostate CAFs. However, co-culturing with NFs did not affect the migration directionality of HNSCC cells or induce an association between NFs and HNSCC cells (Fig. 8 C-G, supplemental video 3).

Prostate CAF-induced directional migration in both the prostate cell line DU145 and the HNSCC cell lines JHU012 and SCC61 suggest that the mechanism by which CAFs modulate cancer cell migration is not organ specific. Previous studies identified different ways that CAFs alter the ECM composition and architecture (Gaggioli et al., 2007; Jolly et al., 2016). As ECM is a major factor that regulates cell migration, we hypothesized that increased association and directional cancer cell migration in co-cultures with CAFs are due to changes in the ECM. Fn is a major ECM protein that is secreted and assembled into fibers

by fibroblasts. Aberrant expression of Fn and its fetal isoforms have been reported in many cancers (Topalovski and Brekken, 2016; Wang and Hielscher, 2017; Bae et al., 2013; Gopal et al., 2017). Therefore, we first studied the expression of Fn and its splice variant Fn-EDA in prostate CAFs. We found that CAFs expressed 50% more Fn compared to NFs (Fig. 9 H and I). In addition, there was a 3.5-fold increase in the expression of the isoform of Fn in CAFs relative to NFs (Fig. 9 J and K). Next, we studied if cancer cells interact with Fn in co-cultures. After 24 h of incubation, cells were fixed and stained for Fn and F-actin. In co-cultures with NFs, in the rarer cases where cancer cells made physical contact with fibroblasts, we did not observe detectable Fn in the contact area (Fig. 10F, left). However, when co-cultured with CAFs, cancer cells frequently appeared to be attached to Fn fibers at contact sites with the CAFs (Fig. 10F, right). To visualize the interaction between CAF-assembled Fn fibrils and cancer cells in live imaging co-culture experiments, we added FITC-labeled Fn to the culture medium at the same time that cells were plated. In the 24 h incubation, CAFs incorporated FITC-Fn into Fn fibrils. The next day, time lapse microscopy was performed. We observed that DU145 cells actively pull on the Fn fibers on the periphery of CAFs as they migrate (Fig. 11G and supplemental video 4). Next, we tested if Fn derived from CAFs is critical for directional cancer cell migration and increased association with CAFs. First, Fn expression was knocked down in CAFs using an siRNA pool, which reduced Fn expression by 80% (Fig. 9 L and M). Then, DU145 cells were co-cultured with control or Fn-KD CAFs for 24 h and time-lapse microscopy was performed. Knocking down Fn significantly reduced the association and migration directionality of DU145 cells with CAFs (Fig. 11 H-J, supplemental video 5). Notably, migration speed of DU145 cells was also decreased in co-cultures with Fn-KD CAFs compared to control CAFs (Fig. 9N).

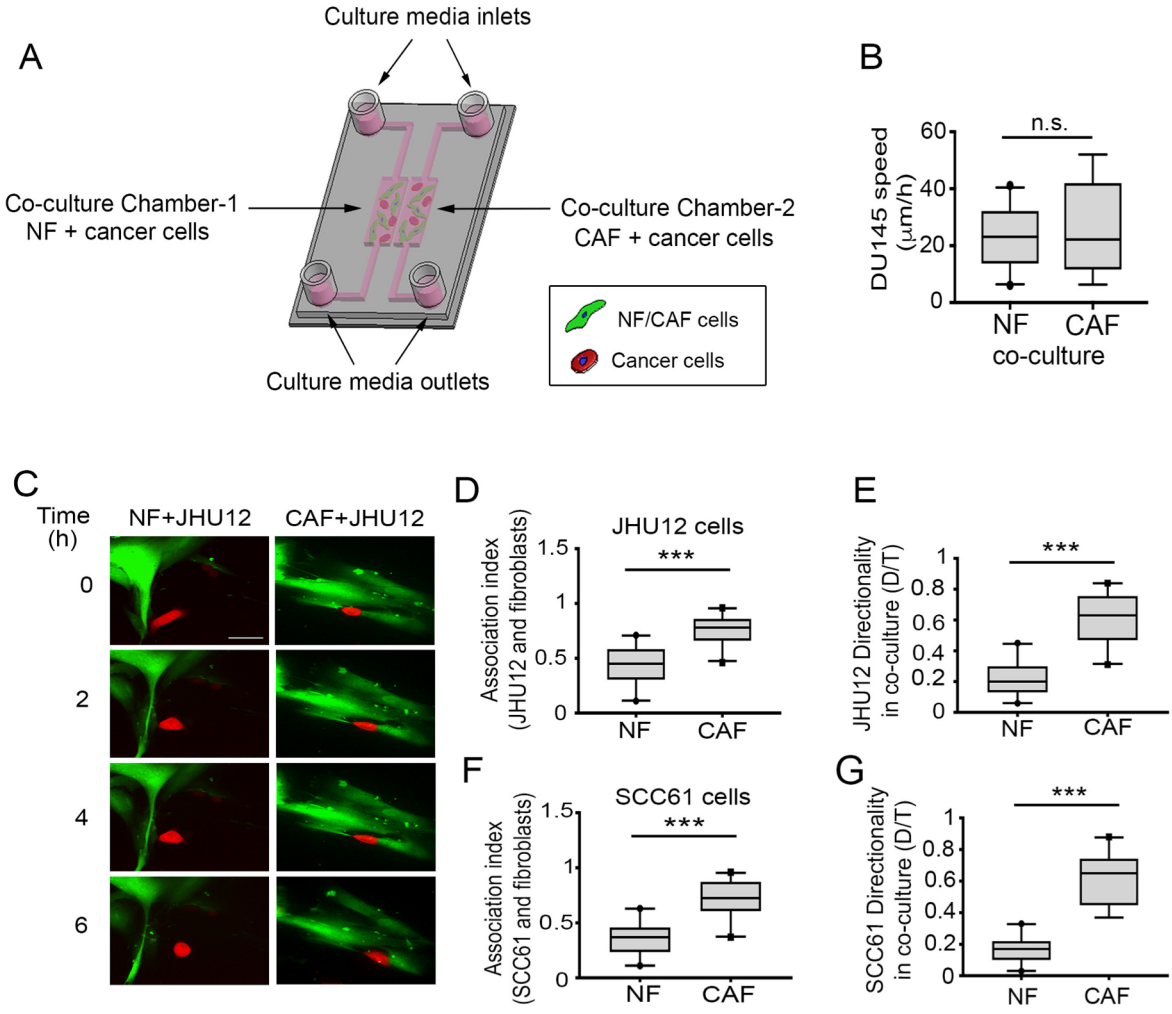

Figure 8. HNSCC cells show high association and directional migration with prostate CAFs. (A) Schematic of the two chamber microfluidic devices used in co-culture experiments. Green labeled fibroblasts and red labeled cancer cells were mixed in a 1:1 ratio and loaded into two separate chambers and subjected to time-lapse microscopy after a 24 h incubation. (B) Migration speed of DU145 cells in co-cultures with NFs or CAFs. (C) Time-lapse images showing co-culture of fibroblasts (green) and JHU12 cells (red). Scale bar = 20 μm. See also video 3. (D) Quantification of the association index of JHU12 cells with NFs and CAFs (E) The directionality ratio of JHU12 cell migration in co-culture with NFs or CAFs (D-E) >22 cells from three experiments were analyzed for each condition (***, P<0.001, determined by Mann-Whitney U test). (F-G) Quantification of the association index (F) of SCC61 cells with NFs and CAFs and the directionality ratio (G) of SCC61 cell migration in co-culture with NFs or CAFs. >22 cells from three experiments were analyzed for each condition (***, P<0.001, determined by Mann-Whitney U test).

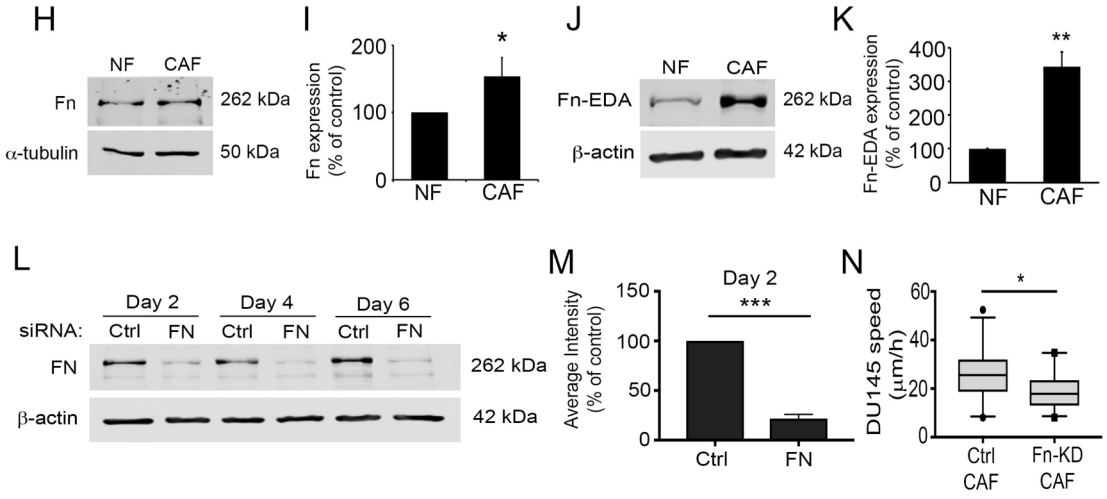

Figure 9. Fn expression in CAFs. (H) Western blot analysis of Fn in NFs and CAFs. α-tubulin is used as a loading control. (I) Quantification of the amount of Fn in CAFs relative to NFs, normalized to α-tubulin. (J) Western blot analysis of Fn-EDA isoform in NFs and CAFs. β-actin is used as a loading control. (K) Quantification of the amount of Fn-EDA in CAFs relative to NFs, normalized to β-actin. (I and K) Error bars represent the SEM for four independent experiments (*, $P<0.05$, determined by Student's t test). (L) Western blot showing knockdown of Fn by siRNAs 2,4 and 6 days after transfection. β-actin is used as a loading control. (M) Quantification of the average intensity of Fn bands on day 2, in 3 independent experiments. (***, $P<0.001$, determined by Student's t test). (N) Migration speed of DU145 cells in co-cultures with control or Fn-KD CAFs. *, $P<0.05$, determined by Mann-Whitney U test.

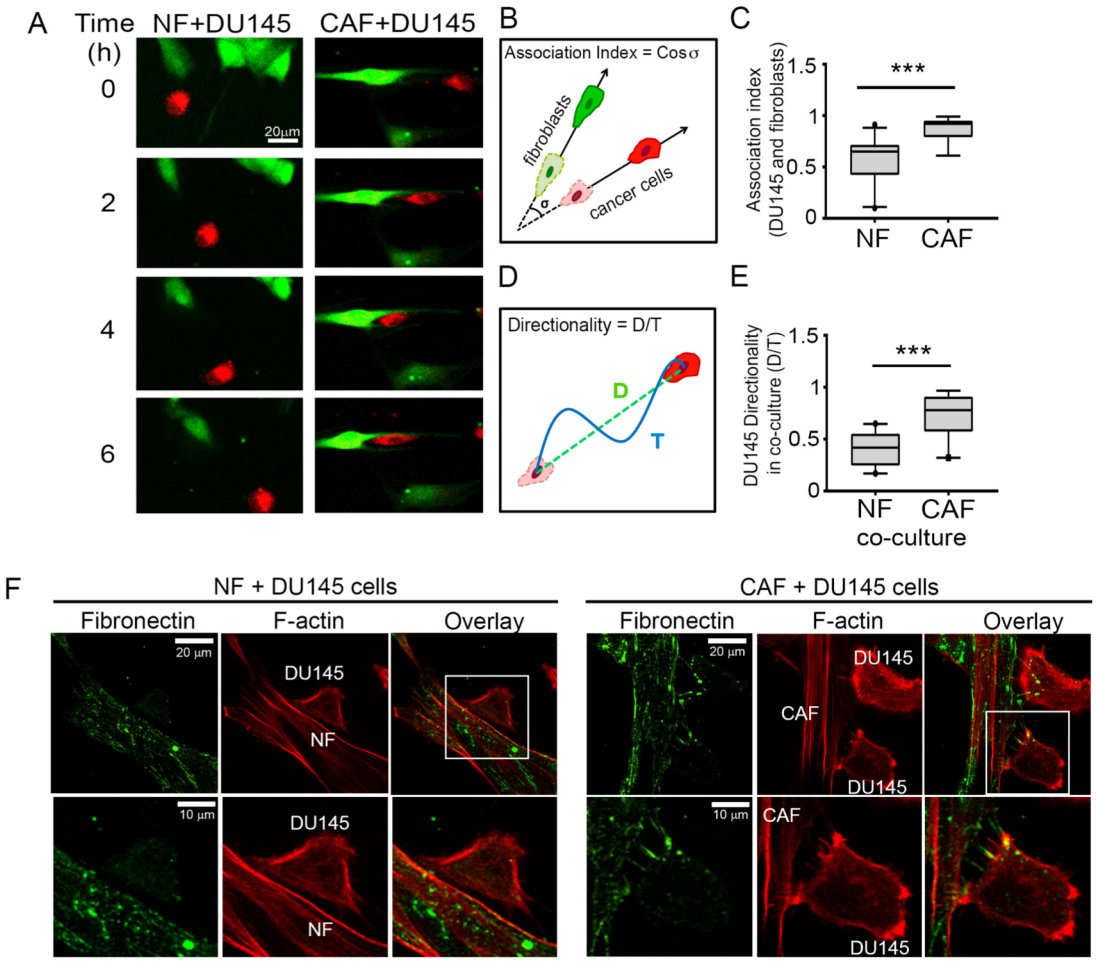

Figure 10. Fibronectin secreted by CAFs promotes CAF-cancer cell association and directional cancer cell migration. (A) Time-lapse images showing co-culture of DU145 prostate cancer cells (red) with NFs (left; green) or CAFs (right; green) in microfluidic devices. Scale bar = 20 μm. See supplementary videos 1 and 2. (B) Schematic representation of calculation of the association index between fibroblasts and cancer cells. (C) Association index of DU145 cells with NFs or CAFs. (D) Schematic representation of calculation of the directionality ratio. (E) Directionality ratio of DU145 cells in co-cultures with NFs or CAFs. (C and E) The data represent at least 30 cells per condition in four individual experiments. (F) Fibronectin staining of NF+DU145 cells (left) and CAF+DU145 cell co-cultures (right). Fibronectin (green), F-actin (phalloidin, red). Scale bar for upper panels = 20 μm, lower panels = 10 μm. White boxes in overlay images indicate the areas that are zoomed in on the lower panels.

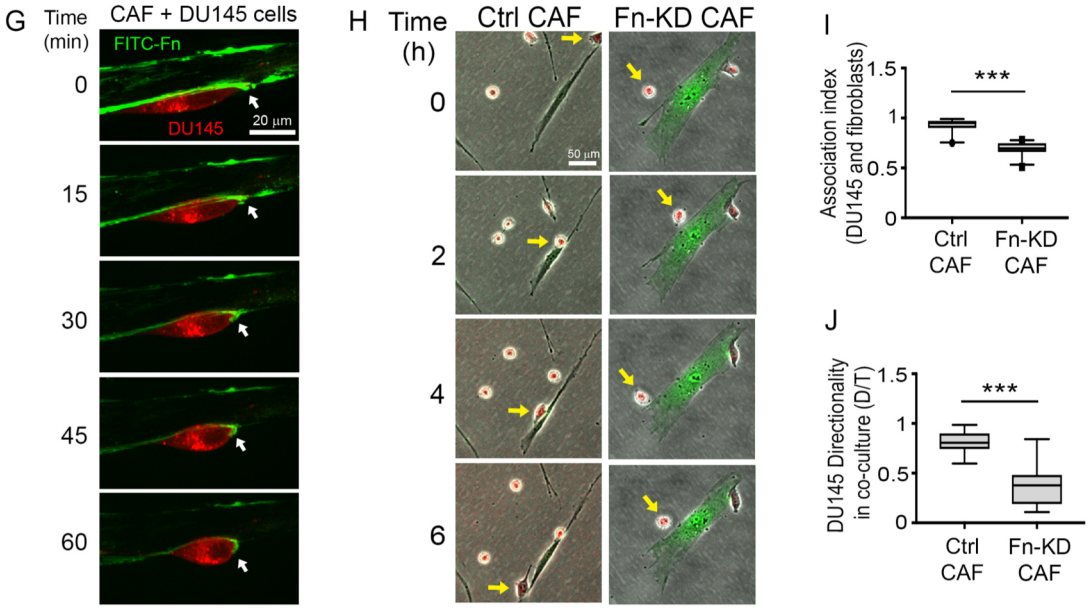

Figure 11. Fn mediates CAF-cancer cell association and migration. (G) Co-culture of CAFs (unlabeled) with DU145 cells (red) cultured in culture medium supplemented with 5ug/ml FITC-Fn (green). Scale bar = 20 µm. White arrow points to the leading edge of the cancer cell where it binds to the Fn fibers assembled by CAFs. See also video 3. (H) Time-lapse images showing co-culture of DU145 cells (red) with CAFs (green) transfected with non-targeting siRNA control (Ctrl CAF, left) or Fn siRNA (Fn-KD CAF, right). Arrows point to the cells of interest. Scale bar: 50 µm. See also video 4. (I) Association index of DU145 cells with control or Fn-KD CAFs. (J) Directionality ratio of DU145 cells in co-cultures with control or Fn-KD CAFs. (I and J) The data represent at least 30 cells per condition in three individual experiments (C, E, I and J) ***, $P<0.001$, determined by Mann-Whitney U test. All box plots range from 25-75th percentile, the central line indicates the median, and the whiskers range from 5-95th percentile.

The close interaction between the cancer cells and CAFs in our co-culture experiments gave rise to the question whether cancer cells and CAFs make heterotypic E-cadherin/N-cadherin adhesions as recently reported (Labernadie et al., 2017). Immunofluorescence staining of DU145-CAF co-cultures for N- and E-cadherins revealed that DU145 cells make E-cadherin junctions with other DU145 cancer cells (Fig. 12 A, upper panel). In contrast, CAFs exhibited N-cadherin junctions when contacting other CAFs (Fig. 12 A, lower panel). However, we did not observe any N-cadherin/E-cadherin connections at sites where DU145 cancer cells made contact with CAFs (Fig. 12 A, lower panel).

Fibronectin is an essential component of the CAF CDM and promotes directional migration of cancer cells

Our results indicated that Fn, secreted by CAFs, is important for regulation of cancer cell migration. In addition to Fn expression, changes in Fn organization can play a role in mediating cancer cell migration. Therefore, we studied the architecture of Fn matrix in NFs and CAFs. After 48 h incubation, NFs assembled Fn into an intricate network of fibers resembling a mesh; in contrast, CAFs organized Fn into parallel fibers (Fig. 12B). The angles between the Fn fibers in CAF matrix were significantly smaller compared to the NF matrix, indicating a more aligned fiber organization (Fig. 12C). Similarly, the peaks that were observed in Fast Fourier Transform (FFT) analysis indicated that Fn was arranged in a specific direction by CAFs, compared to the unorganized fiber network assembled by NFs (Fig. 12D).

To better understand the role of CAF-derived Fn in regulating cancer cell migration, we generated cell-derived matrices (CDMs). The CDMs are produced by the CAFs and NFs,

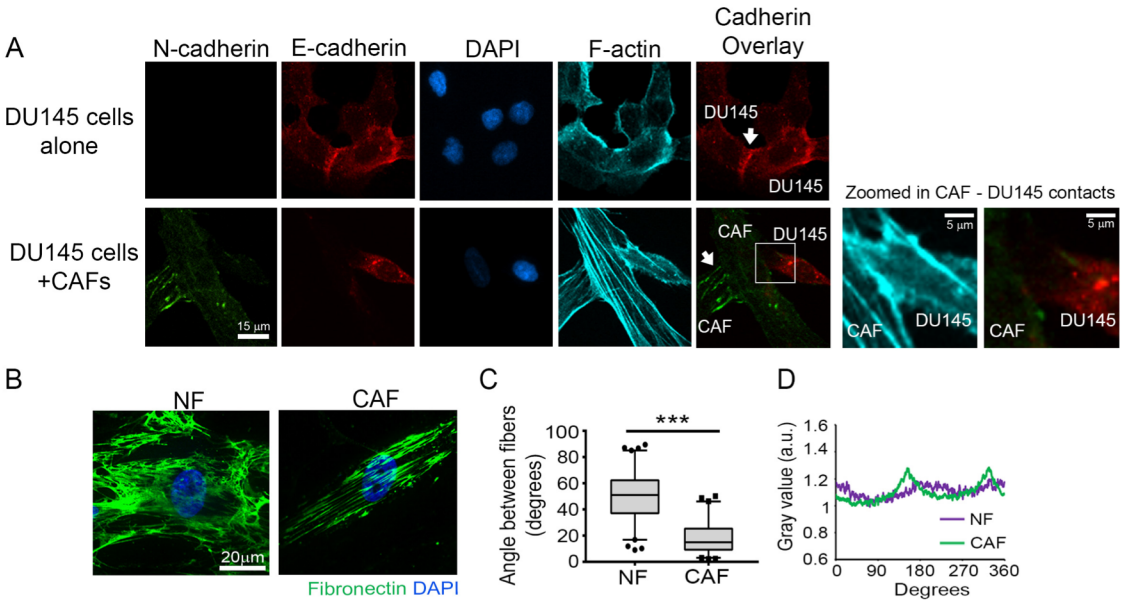

Figure 12. CAFs and DU145 cells do not form cadherin junctions. (A) N-cadherin and E-cadherin co-staining of DU145 cells and CU145-CAF co-cultures. N-cadherin (green), E-cadherin (red), nucleus (DAPI, blue), F-actin (phalloidin, cyan). White arrows point to E-cadherin junctions in the upper panel, N-cadherin junctions in the lower panel. Scale bar = 15 µm. White box indicates the area that is zoomed in to show CAF-cancer cell contact. Scale bar = 5 µm. (B) Fn organization by NFs and CAFs; Fn (green), nuclei (DAPI, blue). Scale bar = 20 µm. (C) Measurements of angles between Fn fibers in NFs and CAFs. > 150 angles per condition from at least 16 images from three independent experiments. (D) FFT analysis of Fn images shown in B.

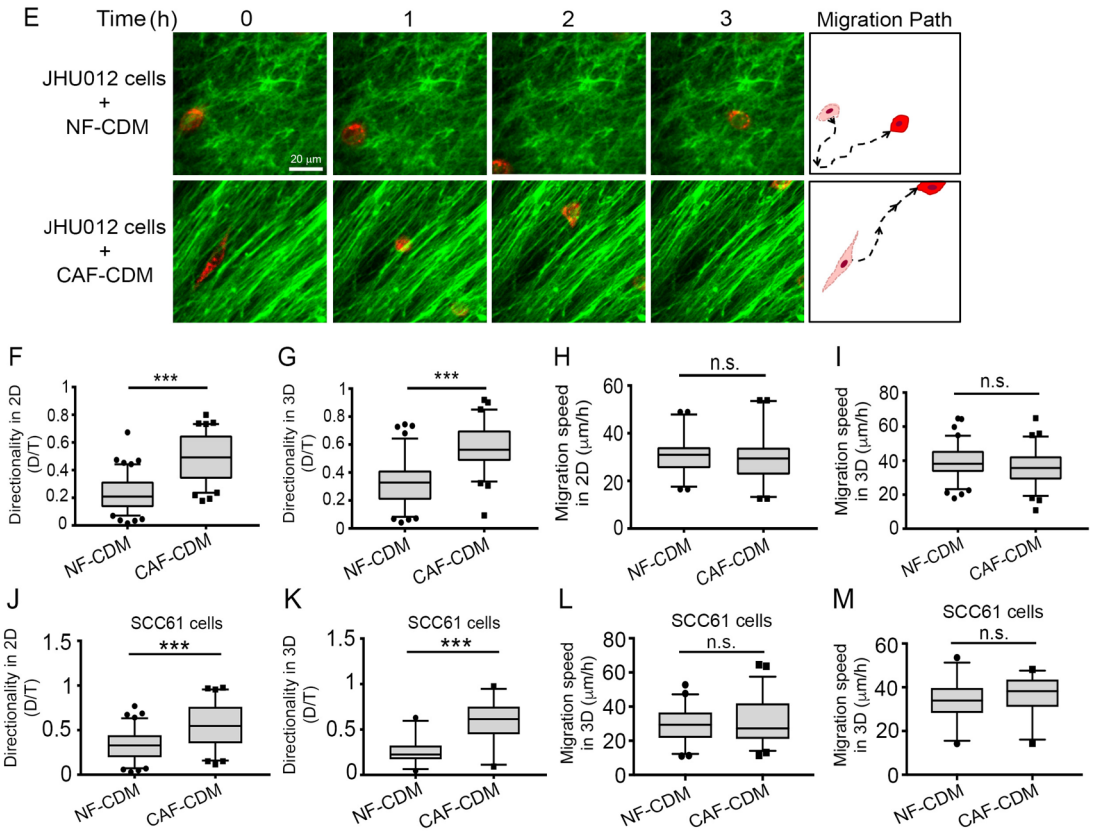

Figure 13. JHU12 and SCC61 HNSCC cells migrate directionally on CAF matrix. (E) Time-lapse images showing JHU12 cells (red) migrating on NF and CAF-derived matrices (labeled with NHS-ester 488 dye, green). Scale bar = 20 µm. See also video 8. (F-I) Box plots showing JHU12 cell migration directionality ratio on NF and CAF CDMs in 2D (F) or in 3D (G), and migration speed in 2D (H) and in 3D (I). >75 cells were analyzed per condition from three independent experiments. (***, P<0.001, n.s. not significant, analyzed by Mann-Whitney U test). (J-M) Box plots showing SCC61 cell migration directionality ratio on NF and CAF CDMs in 2D (J) or in 3D (K), and migration speed in 2D (L) and 3D (M). (J and L) >60 cells were analyzed per condition from four independent experiments. (K and M) >30 cells were analyzed per condition from three independent experiments (***, P<0.001, determined by Mann-Whitney U test). The box plots range from 25-75th percentile, the middle line indicates the median, and the whiskers range from 5-95th percentile.

which were removed from the matrix on day 8, leaving the matrix intact (Franco-Barraza et al., 2016). The matrix was then visualized by labeling with NHS-ester-488. The CDMs produced by NFs displayed a random network of fibers; however, ECM fibers in the CAF-derived CDMs presented an anisotropic fiber orientation with prominent peaks 180˚ apart by FFT analysis (Fig. 14 A-C). The majority of the fibers in both NF and CAF CDMs co-localized with Fn, indicating that Fn is an abundant component of these matrices (Fig. 14 A).

To study cancer cell migration on the CDMs, cells were plated either on top of the CDMs in a 2D format or allowed to invade into the matrix following an overnight incubation (3D). In both 2D and 3D conditions, directional migration of DU145 cells was enhanced on CAF CDMs compared to NF-CDMs (Fig. 14 D, E and G, supplemental videos 6 and 7). Of note, we did not observe a difference in migration speed of DU145 cells on either NF or CAF CDMs (Fig. 14 F and H). Similar to DU145 cells, JHU012 and SCC61 cells also migrated more directionally in CAF CDMs, as opposed to random migration observed in NF-generated CDMs (Fig. 13 E-G and supplemental video 8 for JHU012 cells; Fig. 13 J-K, SCC61 cells). There was also no difference in migration speed of JHU012 and SCC61 cells on NF or CAF CDMs in 2D or 3D conditions (Fig. 13 H-I, JHU012 cells, L-M, SCC61 cells).

Since our data suggested that CAF-secreted Fn mediates migration of cancer cells in co-culture experiments, we sought to determine the role of Fn on cell migration in CDMs. Knocking down Fn in CAFs completely abrogated Fn fibrillogenesis; at 48 h, we observed a minimal number of short Fn fibers in KD cells with most Fn appearing as spots (Fig. 15I). Knockdown of Fn in CAFs lasted at least up to 6 days (Fig. 9 L), therefore, we used the control and Fn-KD CAFs to generate CDMs. While the CDM by control CAFs was abundant and exhibited aligned organization (Fig. 15 J, upper panel), CDM assembled by Fn-KD CAFs

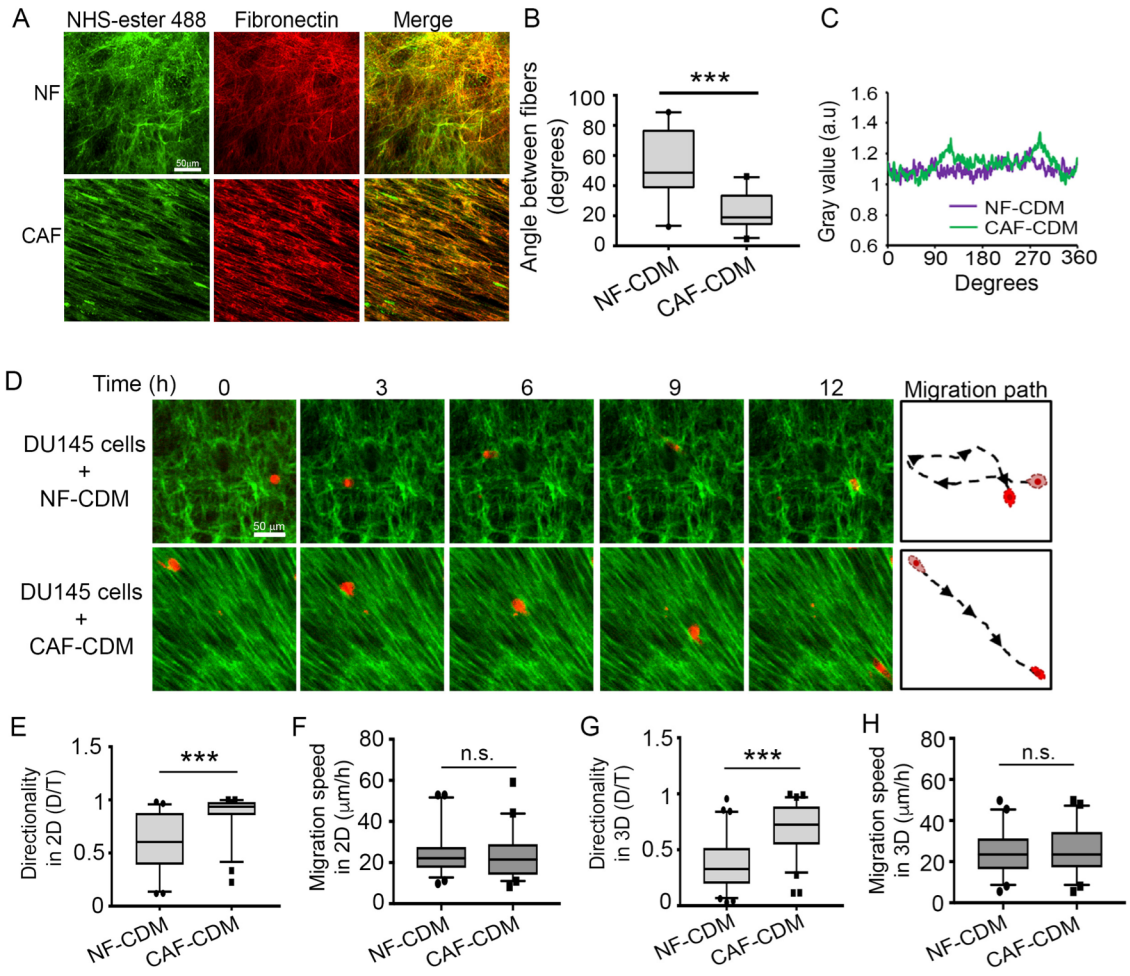

Figure 14. Aligned Fn organization by CAFs mediates directional cancer cell migration (A) Representative images of NHS-ester 488 (green) and anti-Fn (red) staining in CDMs generated by NFs and CAFs. Scale bar = 50 μm. (B) Measurements of angles between Fn fibers in NF and CAF CDMs. >100 angles per condition was measured from at least 12 images from three independent experiments. (***, P<0.001, Mann-Whitney U test). (C) FFT analysis of CDMs stained with Fn antibody shown in (A). (D) Time-lapse images showing DU145 cells (red) migrating on NF and CAF-derived matrices (labeled with NHS-ester 488 dye, green). Scale bar = 50 μm. See also videos 5 and 6. (E-H) Box plots showing DU145 cell migration directionality ratio on NF and CAF CDMs in 2D (E) or in 3D (G), and migration speed in 2D (F) and in 3D (H). >70 cells were analyzed per condition from three independent experiments. (***, P<0.001, analyzed by Mann-Whitney U test). Box plots range from 25-75th percentile, the central line indicates the median, and the whiskers range from 5-95th percentile.

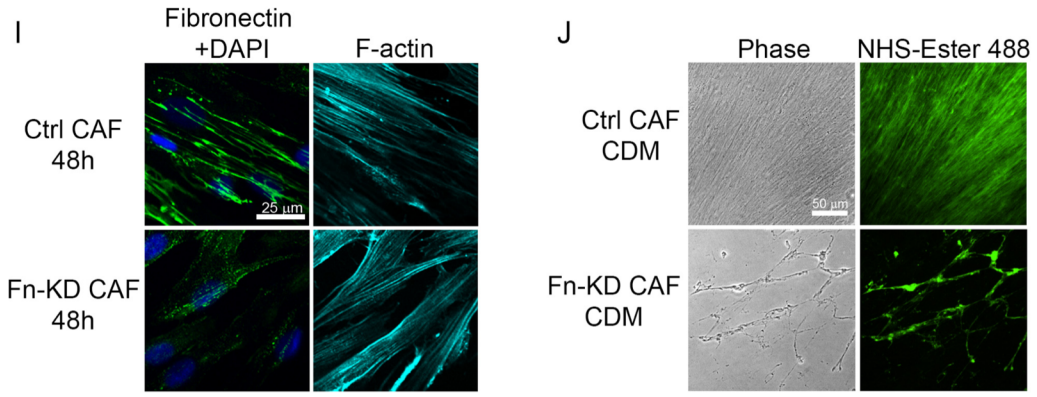

Figure 15. Knocking down Fn disrupts matrix assembly. (I) Fn staining of control or Fn-KD CAFs at 48 h. Nucleus (DAPI, blue), F-actin (phalloidin, cyan). Scale bar = 25 µm. (J) Representative images of CDMs generated by control or Fn-KD CAFs. Scale bar = 50 µm.

exhibited sparse fibers and bare areas of culture dish (Fig. 15J, lower panel). Due to the defective matrix assembly by Fn-KD CAFs, we could not test cancer cell migration on these CDMs. Nevertheless, these results emphasize the previously reported importance of Fn in matrix assembly and organization including incorporation of other ECM proteins into the matrix (Singh et al., 2010). Collectively, our data demonstrate that CAFs assemble a Fn-rich, highly organized matrix that promotes directional migration of both prostate cancer and HNSCC cells.

CAFs organize Fn as parallel fibers through increased traction forces and contractility

Our data indicate that anisotropic organization of the ECM by CAFs promotes the directional migration of cancer cells, which prompted us to investigate how CAFs mediate Fn organization. Cellular traction forces and MyoII-mediated contractility are critical factors in Fn matrix assembly (Lemmon et al., 2009). In addition, actomyosin contractility has been associated with matrix remodeling in 3D organotypic assays (Calvo et al., 2013). Therefore, we hypothesized that changes in mechanical force by CAFs lead to alignment of Fn fibers. We first compared traction stresses generated by CAFs and NFs using traction force microscopy and observed that CAFs exert approximately 50% higher traction force on Fn compared to NFs (Fig. 16, A and B). Next, we performed collagen gel contraction assays to assess contractility of CAFs and NFs. In these assays, CAFs contracted the collagen-I gel to 40% of its original area; however, NFs contracted the gels to 58%, indicating that CAFs are significantly more contractile than NFs (Fig. 18, A and B). Moreover, immunofluorescent staining of pS19-MLC2 revealed that CAFs have 60% more active MyoII than NFs (Fig 16, C and D). However, we did not observe a difference in the total amounts of MLC2 expression

between NFs and CAFs (Fig. 16, C and E). To further investigate whether MyoII-mediated contractility plays a role in alignment of Fn by CAFs, we treated CAFs and NFs with 20 μM blebbistatin, a MyoII-specific inhibitor, for 48 h and then stained them for Fn. Indeed, blebbistatin treatment disrupted the linear organization of Fn by CAFs and led to a more random network of fibers compared to vehicle-treated control CAFs (Fig. 17, F and G). No changes were observed in matrix organization when NFs were treated with 20 μM blebbistatin (Fig. 18, C). As actomyosin contractility is necessary for Fn fibrillogenesis, we treated CAFs with higher concentrations of blebbistatin (50 μM and 100 μM). These increased blebbistatin concentrations almost completely abolished Fn fiber formation by CAFs (Fig. 18 D). We also treated CAFs with 20 μM blebbistatin during CDM generation. NHS-ester 488 staining of these matrices showed that the anisotropic fiber orientation by CAFs was reverted into a NF-like CDM organization (Fig. 17, H and I). To test whether CAF CDMs generated during blebbistatin treatment affects directional cell migration, DU145 cells were plated onto these CDMs and time-lapse microscopy was performed. DU145 cells migrated directionally on control CAF CDMs with a directionality ratio of 0.75. In contrast, CAF CDMs treated with blebbistatin did not support the directional migration of cancer cells, decreasing the directionality ratio to 0.42 (Fig. 17 J). We did not observe a significant difference in DU145 migration speed on either of the CDMs (Fig. 17 K).

CAFs form larger adhesions that turnover more slowly compared to NFs

Adhesions are attachment points in cells that link the actin cytoskeleton and transmit MyoII-mediated mechanical force to the ECM (Burridge and Fath, 1989). The adhesion

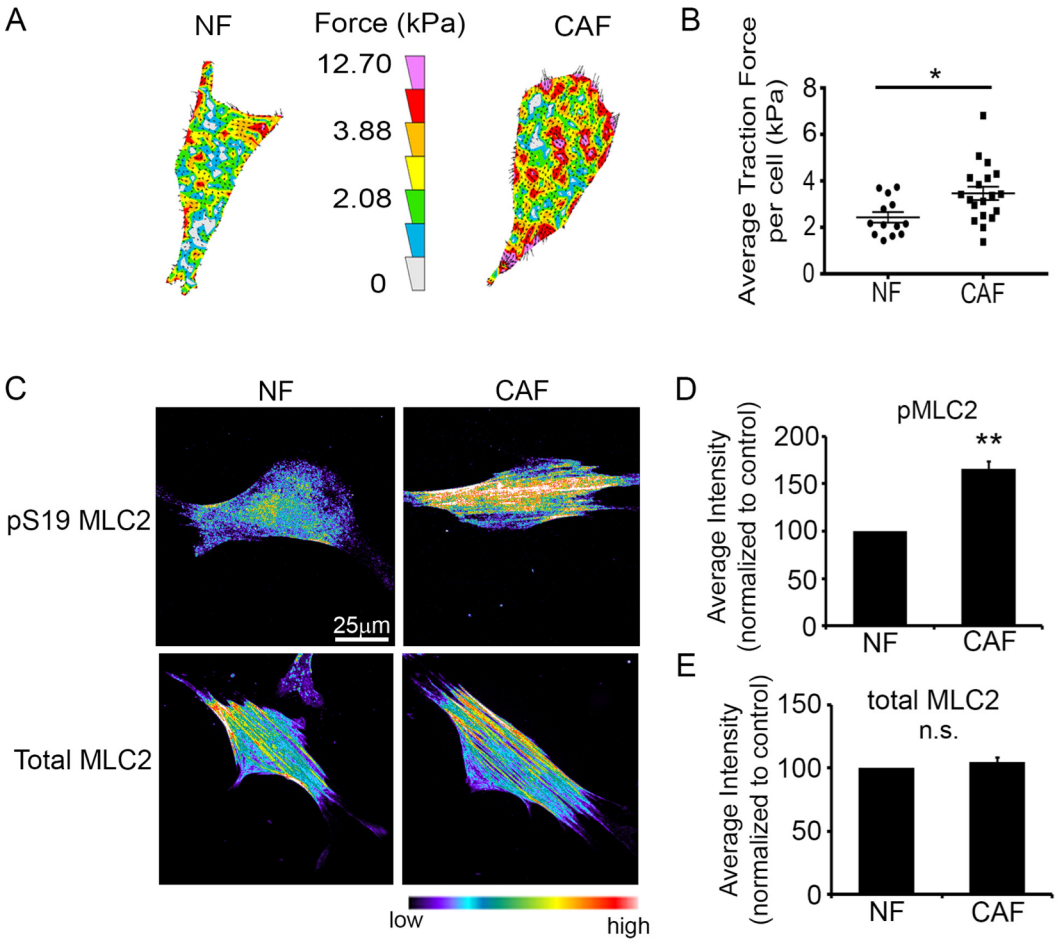

Figure 16. Myosin-II-driven traction force and contractility mediate parallel Fn organization by CAFs. (A) Representative traction force vector maps of a NF and a CAF. Warmer colors indicate areas with high traction forces. (B) Dot plot shows average traction forces in NFs and CAFs. Line indicates mean, error bars indicate SEM. A total of 13 NFs and 19 CAFs were analyzed in three independent experiments (*, $P<0.02$, determined by Student's t test) (C) Immunostaining for pS19 MLC2 or total MLC2 in NFs and CAFs. Images are shown in pseudo-color, warmer colors indicating high intensity, cooler colors indicating low intensity. (D-E) Quantification of average fluorescent intensity of pS19-MLC2 (D) and total MLC2 (E) in NFs and CAFs, normalized to NFs. Error bars indicate SEM from three individual experiments, >77 cells were analyzed per condition. (**, $P<0.01$, n.s., not significant, determined by Student's t test).

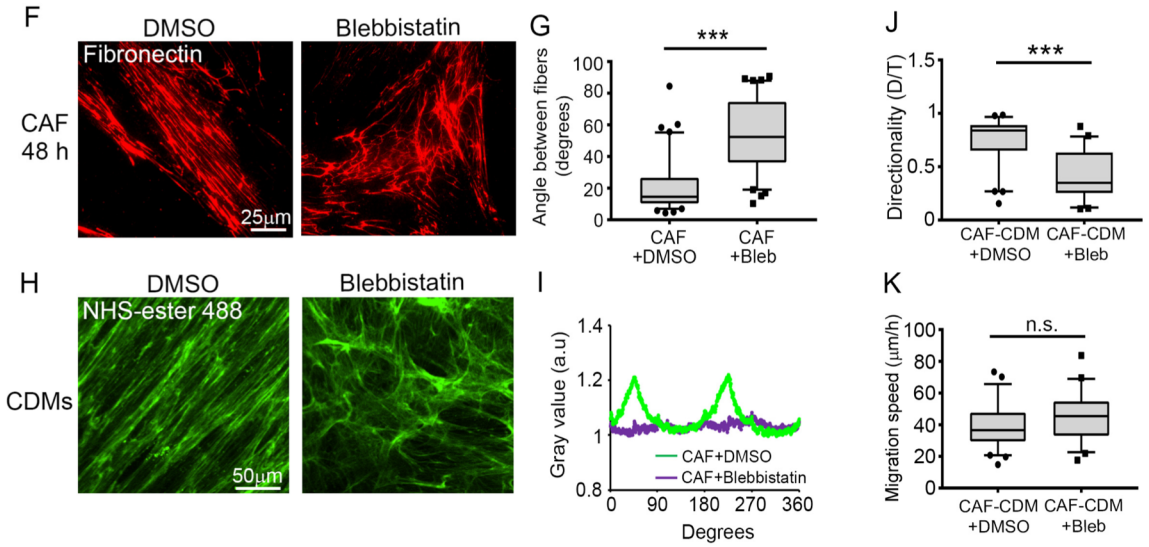

Figure 17. Inhibiting MyoII disrupts matrix alignment by CAFs. (F) Fn staining of CAFs after 48 h treatment with DMSO (left) or 20 μM blebbistatin (right). Scale bar = 25 μm. (G) Measurements of angles between Fn fibers in CAFs treated with DMSO or blebbistatin. > 80 angles measured per condition from at least 12 images from three independent experiments. (***, P<0.001, analyzed by Mann-Whitney U test). (H) NHS-ester 488 staining of CAF CDMs generated during DMSO (left) or blebbistatin (right) treatment. Scale bar = 50 μm. (I) FFT analysis of CDM images shown in H. (J-K) Box plots showing directionality ratio (J) and migration speed (K) of DU145 cell migration on CAF CDMs generated during DMSO or blebbistatin treatment. (***, P<0.001, n.s., not significant, analyzed by Mann-Whitney U test). >50 cells per condition from three independent experiments were analyzed. The box plots range from 25-75th percentile, the central line indicates the median, and the whiskers range from 5-95th percentile.

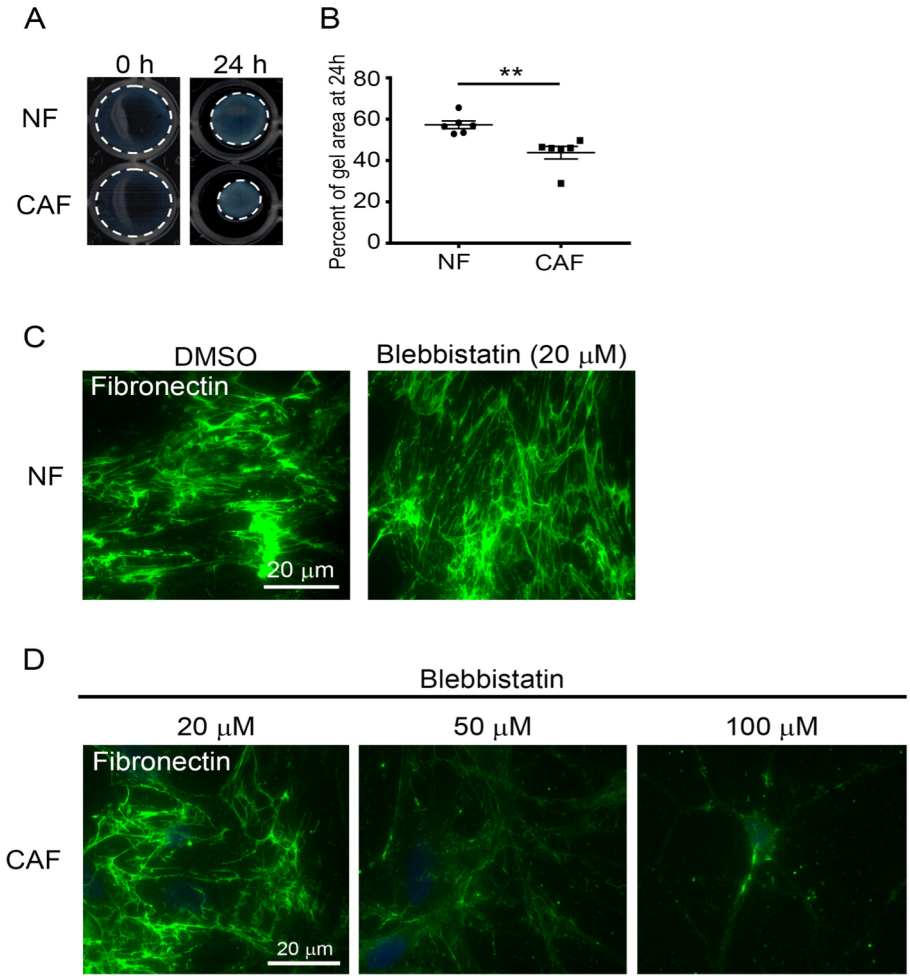

Figure 18. Myosin-II driven contractility mediates CAF Fn organization. (A) Representative images of collagen gel contraction assay at 0 h (left) and 24 h (right). White dotted lines encircle the gel at 24 h. (B) Dot plot shows the quantification of collagen gel contraction assays. Six gels from three independent experiments were analyzed. (**, $P<0.01$, determined by Student's t test). (C) Blebbistatin (20 μM) treatment of NFs does not affect Fn matrix assembly or organization by NFs. Scale bar = 20 μm. (D) Fn staining of CAFs treated with 20 μM (left), 50 μM (middle) and 100 μM (right) of blebbistatin. Scale bar = 20 μm.

protein vinculin is mechanosensitive and increased size of the vinculin-containing adhesions has been correlated with increased mechanical force (Galbraith et al., 2002; Grashoff et al., 2010). As we observed significant changes in the traction forces and contractility of CAFs, we investigated the size and number of vinculin-positive adhesions in CAFs and NFs. CAFs displayed significantly larger adhesions relative to NFs (Fig. 19, A and B). Moreover, vinculin adhesions were more abundant in CAFs in comparison to NFs (Fig. 19 C).

Larger adhesions in CAFs could be due to altered adhesion dynamics in these cells. Therefore, we assessed adhesion turnover in CAFs and NFs by live-cell imaging. Vinculin-GFP-transfected fibroblasts were plated onto Fn-coated glass bottom dishes and imaged for 20 minutes using TIRF microscopy. Analysis of individual adhesions revealed that CAFs assemble and disassemble adhesions at approximately half the speed of NFs (Fig. 20 D-F, supplemental videos 9 and 10).

Increased α5β1 integrin activity in CAFs transduce mechanical forces to Fn, leading to its alignment

α5β1 integrin is the major Fn-binding integrin that is responsible for Fn matrix assembly in fibroblasts. To test whether changes in Fn organization by CAFs might be mediated by α5β1 activity, we assessed active and total α5 integrin levels in CAFs and NFs. Immunofluorescent analysis of active α5 integrin using SNAKA51 antibody, which recognizes the active form of α5 integrin in fibrillar adhesions (Clark et al., 2005), revealed that CAFs display an ~30% increase in active α5 integrin relative to NFs (Fig. 21, A and B). However, no difference was observed in the average fluorescent intensities of total α5

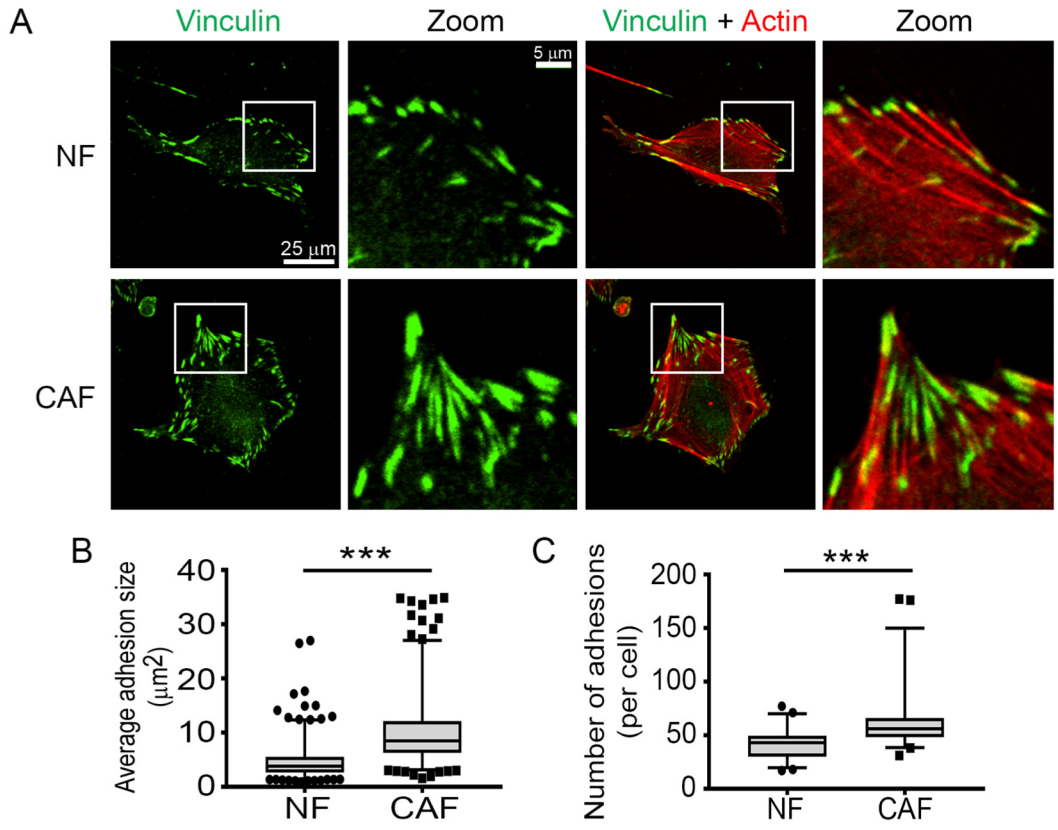

Figure 19. CAFs form larger adhesions that turnover more slowly compared to NFs. (A) Immunofluorescence staining of vinculin (green) and actin (red) in NFs and CAFs. White boxes indicate selected areas of interest in zoom. Scale bar in original images is 25 µm, and 5 µm in zoomed images. (B-C) Box plots show average adhesion size (µm²) (B) and adhesion number (C) in NFs and CAFs. > 600 adhesions per condition (B) >50 cells per condition (C) were analyzed from three independent experiments (***, P<0.001, determined by Mann Whitney U test)

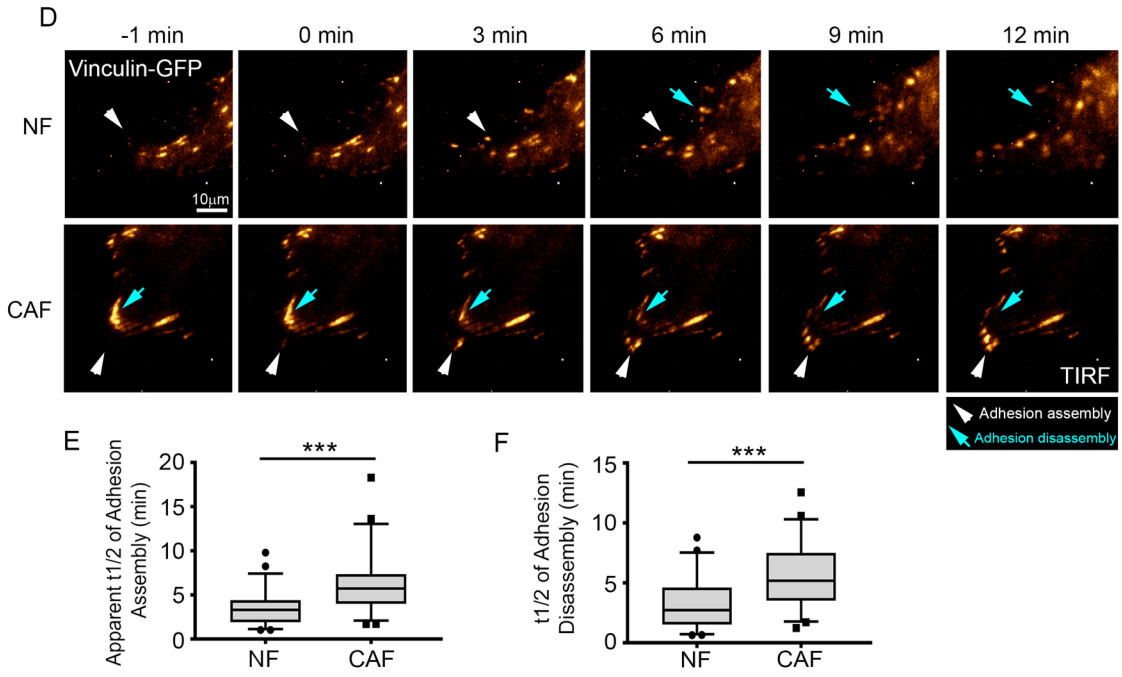

Figure 20. Adhesions turnover rates are slower in CAFs. (D) Time-lapse images show adhesion assembly and disassembly. NFs and CAFs were transfected with vinculin-GFP (pseudo-colored in gold) (white arrowheads, adhesion assembly; blue arrows, adhesion disassembly). See also videos 9 and 10. Scale bar = 10 μm. (E-F) Quantification of the apparent $t_{1/2}$ of adhesion assembly (E) and disassembly (F) for NFs and CAFs. 50-60 adhesions were analyzed per condition from four independent experiments. (***, P<0.001, determined by Mann Whitney U test). All box plots range from 25-75th percentile, the middle line indicates the median, and the whiskers range from 5-95th percentile.

integrin staining between CAFs and NFs (Fig. 21, A and C). Western blot analysis of α5 integrin protein levels also did not show a difference between CAFs and NFs (Fig. 23, A and B). Assessment of active and total β1 integrin levels similarly showed a higher level of active β1 integrin in CAFs compared to NFs without a change in total β1 levels (Fig. 23 C-F).

Mechanical force can lead to activation of integrins, and integrins act as transducers of the force generated within the cell to the ECM (Ross et al., 2013). Since we observed that CAFs exert higher traction stresses on Fn, we tested whether this force is transmitted via α5β1 integrin to Fn. CAFs were plated on Fn-coated polyacrylamide gels and treated with 5 μg/ml of either anti-integrin α5 function-blocking antibody (clone JBS5) or control IgG and subjected to traction force microscopy. Treatment with JBS5 led to a significant decrease in the average traction forces of CAFs, which was similar to the average traction forces observed with NFs (Fig. 22, D and E), indicating that α5β1 integrin plays a central role in force transmission to Fn in CAFs. We then tested whether blocking α5β1 integrin affects Fn organization by CAFs. A synthetic RGD peptide was used at 10 μM concentration to block α5β1 integrin in CAFs during matrix formation, and an equal concentration of the RGE peptide was used as a control due to its decreased affinity for integrins. RGE peptide-treated CAFs displayed aligned Fn fiber organization; however, treatment with the RGD peptide disrupted fiber assembly and alignment by CAFs, resulting in a more NF-like fiber organization, which was quantified by measuring the angles between Fn fibers (Fig. 24, G and H). Notably, the RGD peptide does not only block α5β1 integrin, but it also affects other integrins that bind to the RGD sequence. Thus, we also evaluated Fn matrix organization while treating the CAFs with an anti-α5 integrin blocking antibody (clone P1D6) or control

IgG. Control IgG-treated CAFs aligned Fn fibers, similar to our previous observations, while treatment with 5 μg/ml of P1D6 antibody perturbed the fiber assembly and alignment, resulting in a decreased number of fibers that were randomly organized (Fig. 22, F and G).

Next, we investigated whether changes in Fn organization by RGD treatment of CAFs affected cancer cell migration by treating the CAFs with RGD or RGE peptides during CDM generation. RGD treatment of CAFs resulted in CDMs with a meshwork-like fiber organization in the CDMs, compared to anisotropic fiber orientation in control CDMs generated by RGE-treated CAFs (Fig. 22 H and I). DU145 cells were plated onto these CDMs and subjected to time-lapse microscopy. DU145 cells exhibited enhanced directional migration on control CAF-CDMs; however, the directionality ratio was significantly reduced on CAF CDMs that were generated during RGD treatment (Fig. 24 I). Interestingly, we observed a slight, but discernible increase in the migration speed of DU145 cells on RGD-treated CAF CDMs in comparison to control (Fig. 24 J).

Aligned matrix organization by CAFs is mediated by PDGFRα

Fn-α5β1 integrin binding has been shown to activate PDGFRα in mesenchymal stem cells (Veevers-Lowe et al., 2011). Furthermore, PDGFRα has been associated with connective tissue remodeling by fibroblasts (Horikawa et al., 2015) and overexpression of PDGFRs in tumor stroma is correlated with poor prognosis in several cancers (Heldin, 2013a). To dissect the role of PDGFRα in CAF-mediated ECM organization, we studied PDGFRα expression and function in prostate CAFs and NFs. Immunofluorescence staining and western blot analysis both showed that CAFs express ~3 fold higher amounts of PDGFRα compared to NFs (Fig 25 A-D). In addition, CAFs exhibited a 60% increase in

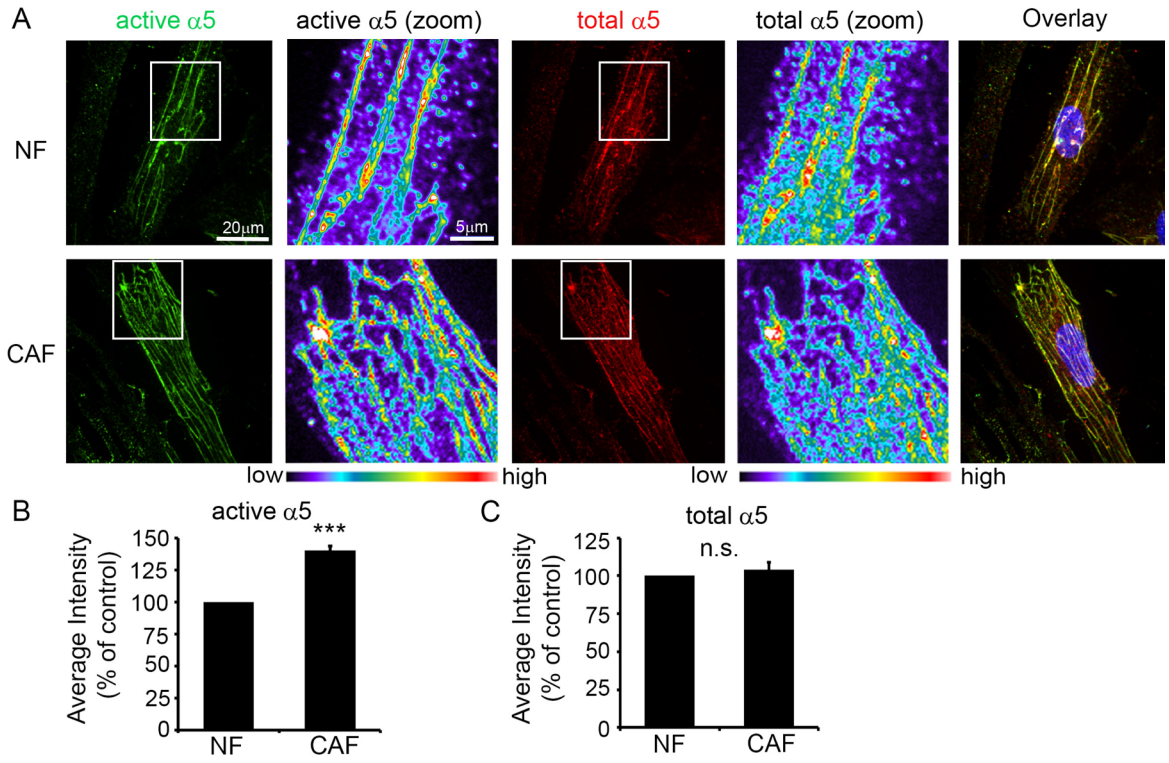

Figure 21. CAFs have higher active α5 integrin activity than NFs. (A) Immunofluorescence staining of NFs and CAFs for active α5 integrin (green, left) and total α5 integrin (red, middle). Scale bar = 20 μm. Zoomed images have been pseudo-colored, to show differences in fluorescence intensity, warmer colors indicating higher intensity. Scale bar = 5 μm. (B-C) Quantification of average fluorescent intensity of active (B) and total (C) α5 integrin. 80-95 cells per condition from five independent experiments were analyzed. Error bars indicate SEM for five experiments. (***, $P<0.001$, n.s., not significant, determined by Student's t test).

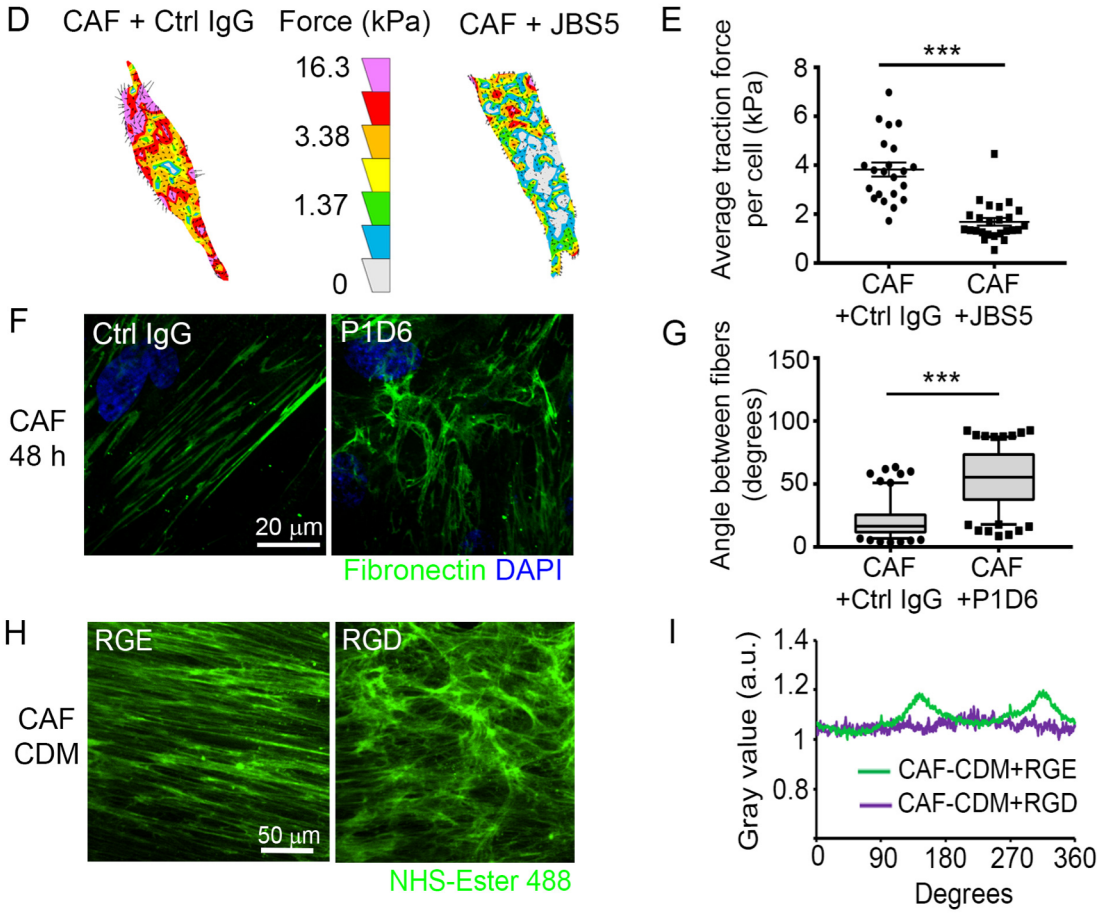

Figure 22. α5β1 integrin in CAFs transduce mechanical forces to Fn. (D) Representative traction force vector maps of CAFs treated with 5 µg/ml control IgG (left) or α5 integrin function blocking antibody JBS5 (right). Warmer colors indicate areas with high traction forces. (E) The dot plot shows average traction forces in control and JBS5-treated CAFs. Line indicates mean, error bars indicate SEM. 22 control CAFs and 25 JBS5-treated CAFs were analyzed in four independent experiments (***, P<0.001, determined by Mann Whitney U test). (F) Fn staining of CAFs following 48 h treatment with 5 µg/ml control IgG or α5 integrin function blocking antibody P1D6. Scale bar = 20 µm. (G) Measurements of angles between Fn fibers in CAFs treated with IgG or JBS5. >160 angles measured per condition from at least 16 images from three independent experiments. (***, P<0.001, determined by Mann-Whitney U test). (H) NHS-ester 488 staining of CAF CDMs generated during 10 µM RGE or RGD treatment. Scale bar = 50 µm. (I) FFT analysis of CAF CDMs shown in H.

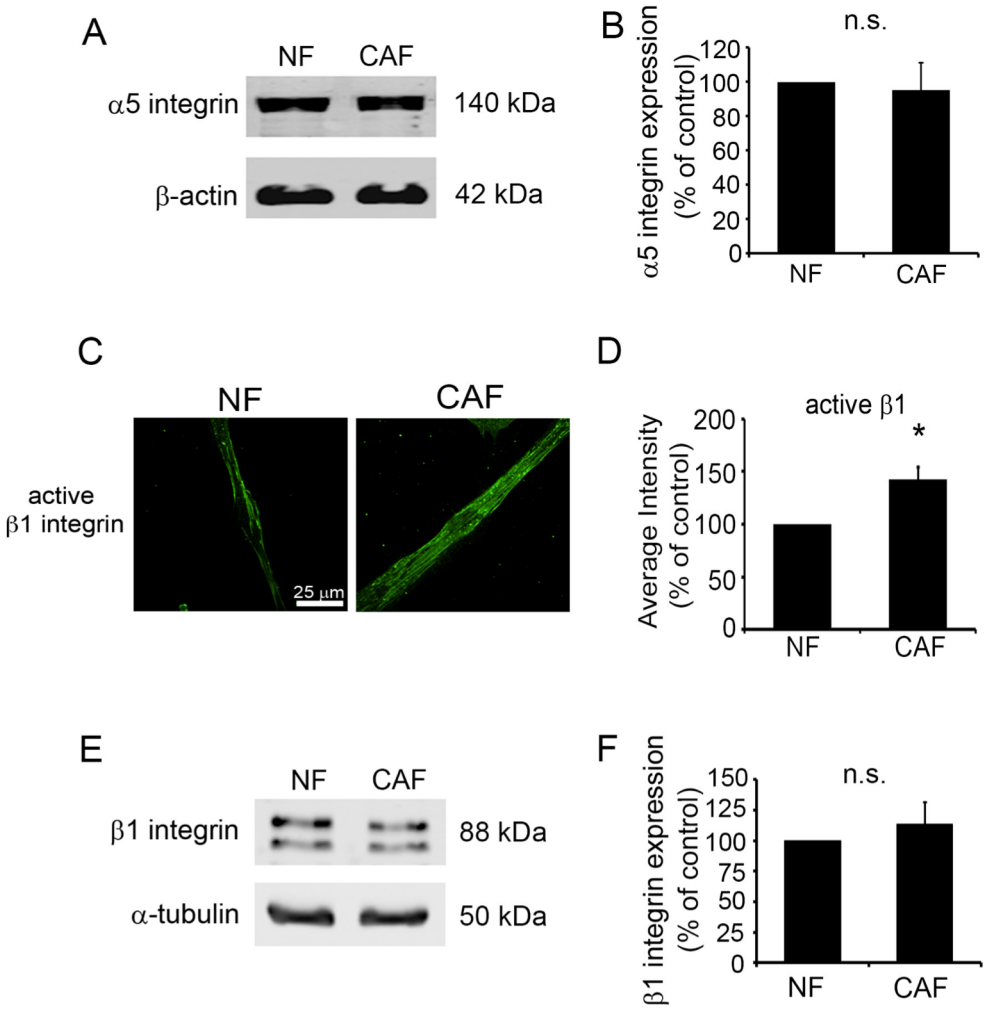

Figure 23. CAFs express similar levels of α5β1 integrin relative to NFs. (A) Western blot analysis of α5 integrin in NFs and CAFs. β-actin is used as a loading control. (B) Quantification of the amount of α5 integrin in CAFs relative to NFs, normalized to β-actin. Error bars represent the SEM from three independent experiments (n.s., not significant, determined by Student's t test). (C) Immunofluorescence staining of NFs and CAFs for active β1 integrin clone 12G10. Scale bar = 25 μm. (D) Quantification of average fluorescent intensity of active β1 integrin. >50 cells per condition from three independent experiments were analyzed. Error bars indicate SEM of three experiments. (*, $P<0.05$, determined by Student's t test). (E) Western blot analysis of β1 integrin in NFs and CAFs. α-tubulin is used as a loading control. (F) Quantification of the amount of β1 integrin in CAFs relative to NFs, normalized to α-tubulin. Error bars represent the SEM from three independent experiments (n.s., not significant, determined by Student's t test).

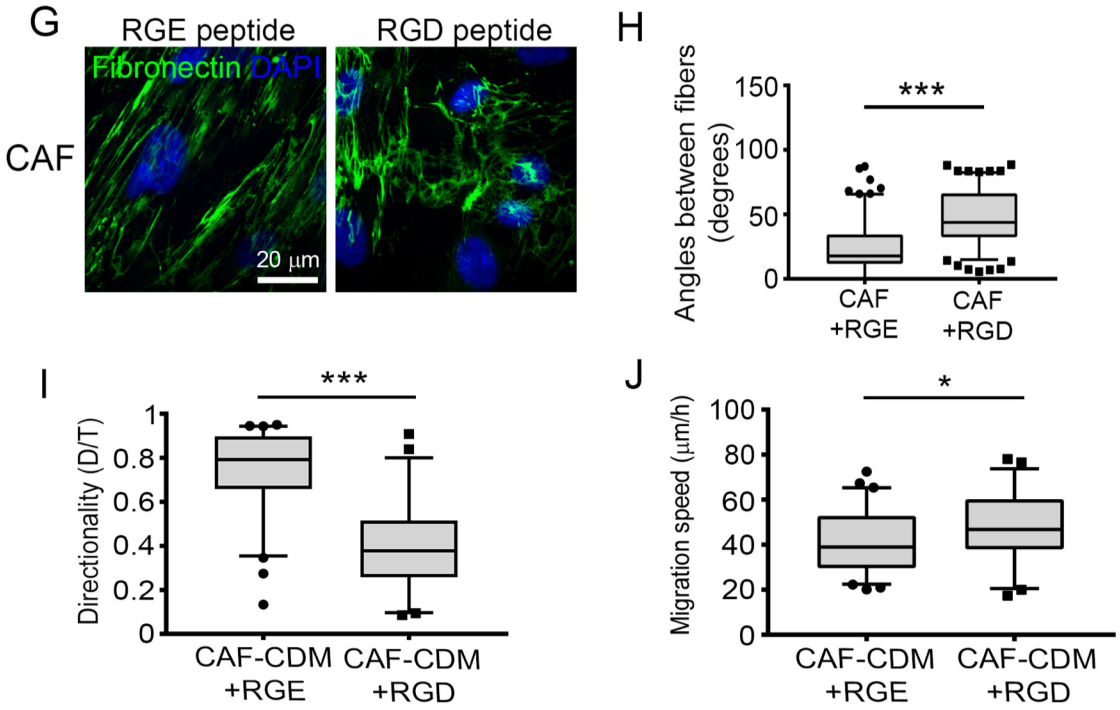

Figure 24. Blocking α5β1 integrin disrupts Fn organization. (G) Fn staining of CAFs following 48 h treatment with 10 μM RGE or RGD peptides. Scale bar = 20 μm. (H) Measurements of angles between Fn fibers in CAFs treated with RGE or RGD peptides. >150 angles measured per condition from at least 16 images from three independent experiments. (***, P<0.001, analyzed by Mann-Whitney U test). (I-J) Box plot showing the directionality ratio (I) and migration speed (J) of DU145 cell migration on CAF CDMs generated during RGE or RGD peptide treatment. (***, P<0.001, *, P<0.05, analyzed by Mann-Whitney U test). >55 cells per condition from three independent experiments were analyzed. The box plots range from 25-75th percentile, the middle line indicates the median, and the whiskers range from 5-95th percentile.

PDGFRα activity, as assessed by tyrosine 762 phosphorylation, upon stimulation with growth medium containing serum (an abundant source of PDGFs) (Fig. 25, E and F).

To determine if upregulated PDGFRα expression and activity in CAFs affects contractility, we performed collagen gel contraction assays. Blocking PDGFRα activity with a neutralizing antibody, AF307, significantly reduced the contractility of CAFs (Fig. 25, G and H). Furthermore, we found that inhibiting PDGFRα in CAFs decreased the traction forces applied to Fn (Fig. 26, I and J). Likewise, addition of PDGFRα blocking antibody, AF307 significantly changed the matrix organization by CAFs, from aligned fibers to a more random organization (Fig. 26, K and L). Since previous studies have reported that α5β1 integrin and PDGF receptors can crosstalk on the cell membrane and modulate each other's activity (Zemskov et al., 2009b; Eliceiri, 2001), we also tested whether PDGFRα has a similar function in our system. Indeed, we observed a decrease in active α5β1 levels when CAFs were treated with AF307 (Fig. 26, M and N). These data suggest that PDGFRα collaborates with α5β1 integrin to promote cellular contractility and organize extracellular matrix.

Fn fibers are aligned at sites of invasion in human prostate cancer tissues

To determine if Fn alignment *in vivo* is regulated differently by CAFs and NFs, we examined Fn in four prostate cancer cases (Figures 27-29), comparing regions of normal adjacent prostate tissue to regions of invasive carcinoma. Regions of normal adjacent prostate tissue contained low levels of Fn (Fig. 27, A-C). In regions of benign prostatic hyperplasia, Fn was more abundant than in normal prostate but was largely disorganized (Fig. 29, A-C). However, in regions of invasion, Fn was present at high levels and formed

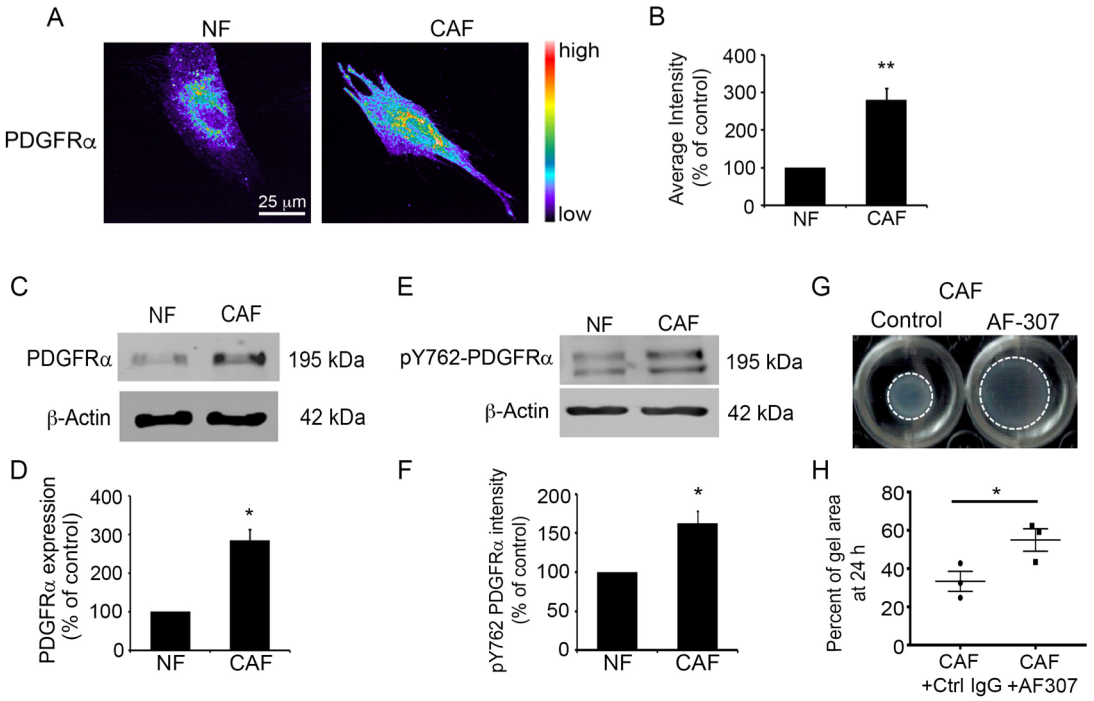

Figure 25. CAFs overexpress PDGFRα. (A) Immunofluorescence staining of PDGFRα in NFs and CAFs. Images are shown pseudo-color, warmer colors indicating high intensity, cooler colors indicating low intensity. Scale bar = 25 μm. (B) Quantification of average fluorescent intensity of PDGFRα. >60 cells per condition from three independent experiments were analyzed. Error bars indicate SEM for three experiments. (**, P<0.01, determined by Student's t test) (C and E) Western blot analysis of PDGFRα (C) and pY762-PDGFRα (E) in NFs and CAFs. β-actin is used as a loading control. (D and F) Quantification of PDGFRα (D) pY762-PDGFRα (E) average intensity in NFs and CAFs, normalized to β-actin. Error bars represent the SEM from three independent experiments (*, P<0.05, determined by Student's t test). (G) Collagen gel contraction of CAFs treated with either 10 μg/ml of control antibody or PDGFRα neutralizing antibody (AF-307). Dashed lines circle the gels following 24 h treatment. (H) Quantification of collagen gel contraction at 24 h. Three gels from three independent experiments were analyzed. Error bars indicate SEM for three experiments. (*, P<0.05, determined by Student's t test).

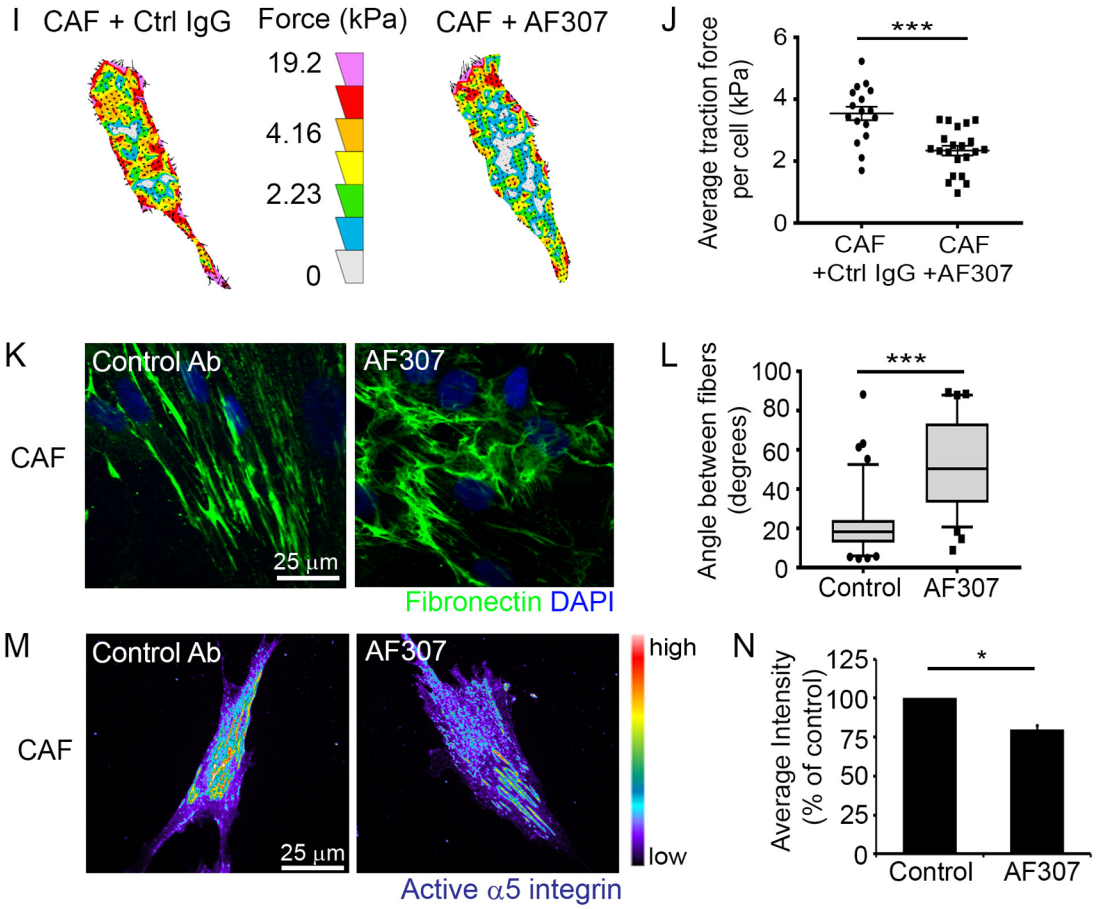

Figure 26. Aligned matrix organization by CAFs is mediated by PDGFRα. (I) Representative traction force vector maps of CAFs treated with 10 µg/ml control IgG (left) or AF307 (right). Warmer colors indicate areas with high traction forces. (J) Scatter dot plot shows average traction forces in control and AF307-treated CAFs. Line indicates mean, error bars indicate SEM. 17 control CAFs and 21 AF307-treated CAFs were analyzed in three independent experiments (***, P<0.001, determined by Mann Whitney U test). (K) Fn staining of CAFs following 48 h treatment with 10 µg/ml control IgG or AF307. Scale bar = 25 µm. (L) Measurements of angles between Fn fibers in CAFs treated with control IgG or AF307. >100 angles measured per condition from at least 12 images from three independent experiments. (***, P<0.001, analyzed by Mann-Whitney U test). Box plots range from 25-75th percentile, whiskers range from 5-95th percentile and the line indicates the median. (M) Active α5 integrin staining of CAFs following 48 h treatment with 10 µg/ml control IgG or AF307. Scale bar = 25 µm. (N) Quantification of average fluorescent intensity of active α5 integrin in control IgG or AF307-treated CAFs. >70 cells per condition were analyzed in three independent experiments (*, P<0.05, determined by Student's t test).

well-organized, parallel fibers contacting many invading cancer cells (Fig. 27 D-I and Fig. 29 D-I). By double immunofluorescence, alpha smooth muscle actin-positive (αSMA+) fibroblasts adjacent to normal prostatic epithelium (NFs) were surrounded by disorganized Fn (Fig. 28 J), while αSMA+ fibroblasts around cancer cells (CAFs) were surrounded by well-organized, linear Fn fascicles (Fig. 28 K and L). Within the tumor, expansive regions of confluent epithelial growth with minimal stroma exhibited little to no Fn (data not shown), supporting the idea that Fn fibers are produced by surrounding CAFs. Consistent with the prostate cancer results, pancreatic cancer samples showed a similar rearrangement of Fn around benign and malignant lesions. Fn was largely disorganized surrounding acinar-to-ductal metaplasia and pancreatic intraepithelial neoplasms (PanIN; benign precursors) areas within pancreatic ductal adenocarcinoma samples (Fig. 30, J and K). However, invading clusters of cancer cells were arranged in parallel with numerous, well-organized Fn fibers in pancreatic ductal adenocarcinoma (PDAC) (Fig. 30, L and M).

Prostate cancer cells use αv integrin to migrate on CAF CDMs

Our data shows that the alignment of matrix fibers by CAFs promotes directional cancer cell migration. Interestingly, a recent study identified integrins αvβ6 and α9β1 as responsible for efficient and directional cell migration on HNSCC CAF CDMs (Gopal et al., 2017). Therefore, we tested integrins known to be expressed by prostate cancer cells to determine which class of integrins are responsible for directional cancer cell migration on prostatic CAF CDMs. The expression of α5 and αv integrins are deregulated in prostate cancers and changes in their expression and activity have been linked to cancer migration and invasion (Sutherland et al., 2012a). Therefore, we assessed DU145 cell migration in 2D

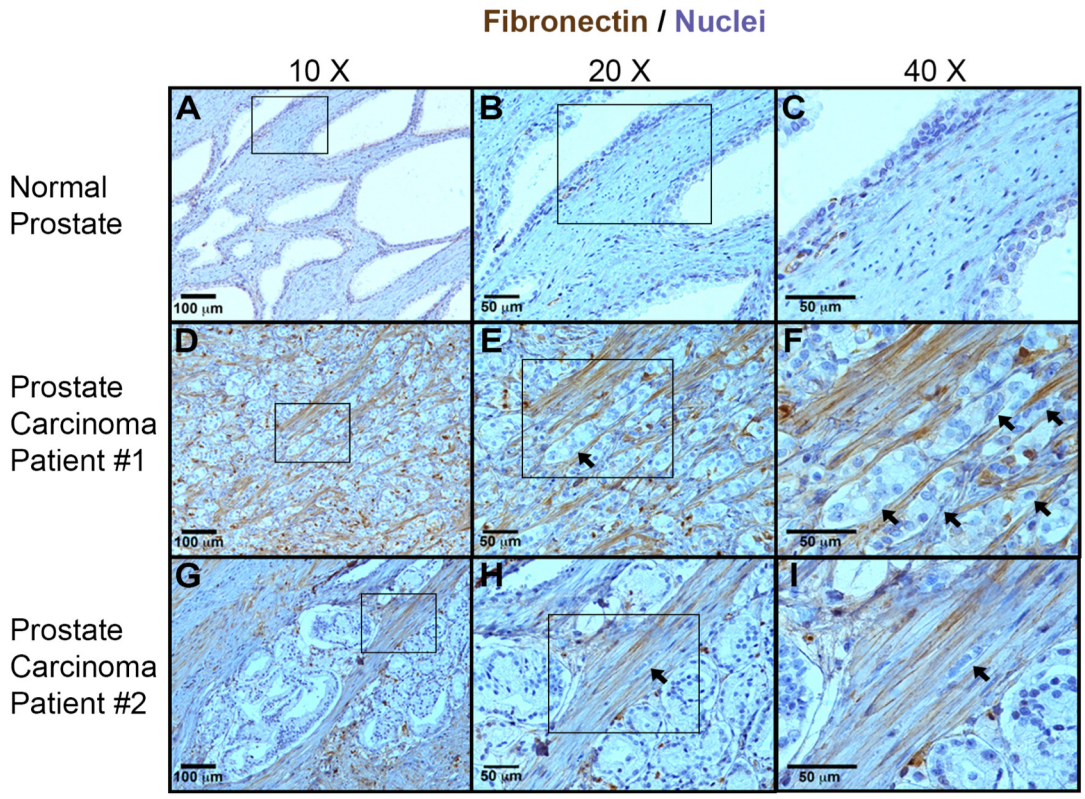

Figure 27. Fn structure differs around normal versus malignant prostate epithelium. (A-C) A minimal staining for Fn (brown) is observed around normal prostate epithelium adjacent to cancer. Cells were counterstained with hematoxylin (blue). (D-I) Fn forms long parallel fascicles in invasive regions of two different cancer cases (D-F and G-I). E is an enlargement of D and F is an enlargement of E. Similarly, H is an enlargement of G and I is and enlargement of H. (D-I) Arrows indicate invading tumor cells.

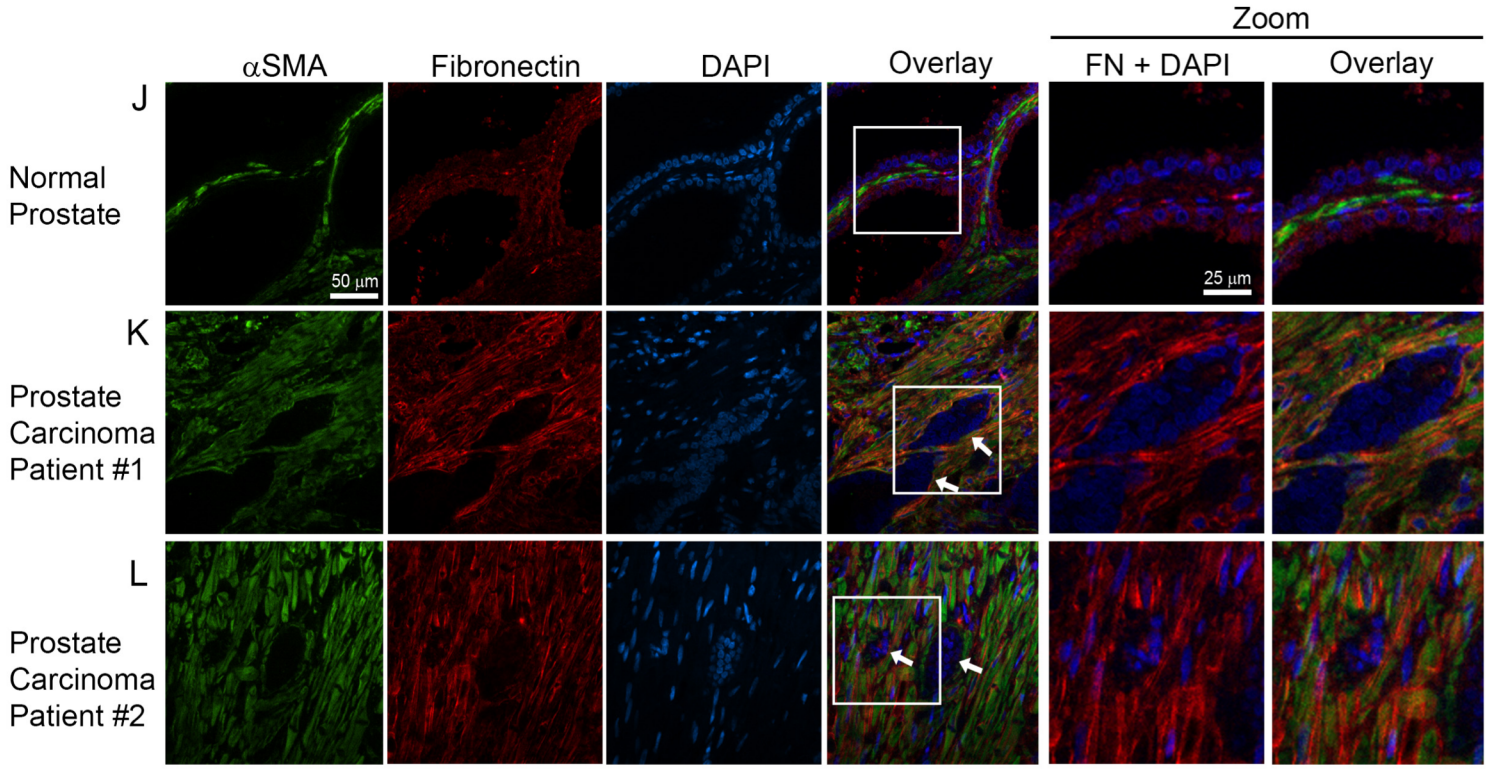

Figure 28. Aligned Fn and αSMA colocalize in cancer tissues. (J-L) Immunofluorescent labeling of αSMA (green; left panels), Fn (red; second panels) and nuclear counterstain DAPI (blue; third panels) indicate that myofibroblasts surround both benign (J) and malignant prostate (K, L) epithelium but only form long parallel Fn fascicles around invading cells. Scale bar for four left panels = 50 μm, scale bar for zoomed in images = 25 μm.

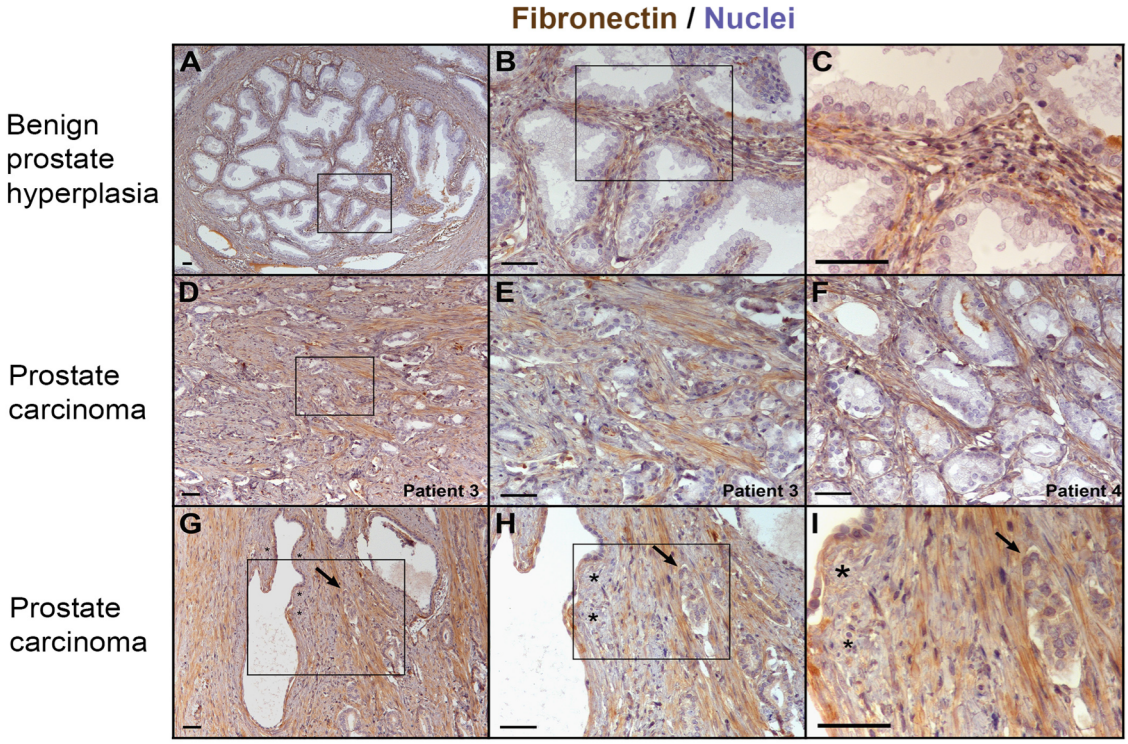

Figure 29. Aligned Fn fibers surround invasive prostate cells in patient tumors. (A-C) In a region of benign prostatic hyperplasia adjacent to tumor, Fn (brown) is abundant but disorganized. Box in A indicates frame for panel B; box in B indicates frame for panel C. (D-F) Invading cells are surrounded by parallel, linear Fn fascicles. Box in D indicates frame for panel E. (G-I). In a region of mixed normal adjacent and cancer epithelium cancer cells (arrows) are surrounded by long Fn fascicles while normal (asterisks) is not. Box in G indicates frame for panel H; box in H indicates frame for panel I.

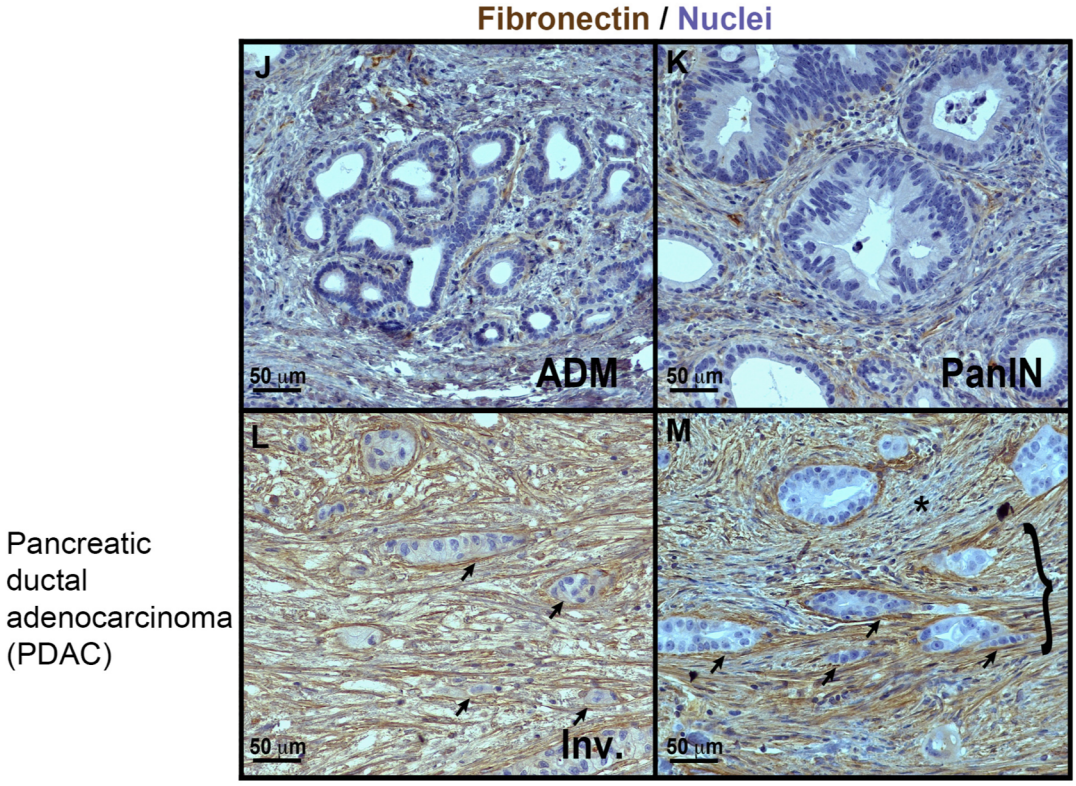

Figure 30. Pancreatic cancers exhibit aligned Fn fibers. (J and K) Surrounding benign regions such as acinar-to-ductal metaplasia (ADM) and PanINs, Fn (brown) was disorganized. (L) A region of invasion shows well-organized, parallel Fn fascicles adjacent to the invading cells which can invade as individual cells or as clusters of cells (arrows). (M) Regions of invasion along Fn tracks are juxtaposed to regions of disorganized Fn (asterisk) where cells are not invading. Scale bars = 50 μm.

cell migration assays on CAF CDMs using respective α5 and αv function blocking antibodies JBS5 and 17E6. When α5 integrin was blocked, DU145 cells migrated with decreased directionality but increased migration speed compared to control IgG treated cells (Fig. 31 A-C). By contrast, when αv integrins were inhibited, both migration directionality and speed was significantly impaired compared to control cells (Fig. 31 A-C). These results suggest that αv integrin mediates both directional and efficient cell migration on CAF CDMs.

Discussion

Evidence has accumulated to show that changes in the tumor microenvironment support cancer progression (Miles and Sikes, 2014). CAFs are a key component of the tumor microenvironment with tumor-supportive roles (Mezawa and Orimo, 2016). Cancer cell migration and invasion are critical initial steps in metastasis; however, the mechanisms by which tumor-stroma interactions regulate these processes are not well understood. In this study, we identified a new mechanism by which CAFs promote cancer cell migration (Fig. 32). Using a co-culture system, we demonstrate that cancer cells associate with primary human prostate CAFs and migrate directionally along them. We provide evidence that CAF-cancer cell association is promoted by the Fn fibrils assembled by CAFs and cancer cells pull on the CAF-assembled Fn to migrate along CAFs. Furthermore, we show that the CAF-cancer cell association is blocked when Fn is knocked down in CAFs. Interestingly, prostate CAFs were also able to promote an increased association with HNSCC cells and induce their directional migration. This finding suggests a ubiquitous mechanism by which CAFs from different tumor microenvironments can modulate cancer cell migration, which was not previously known.

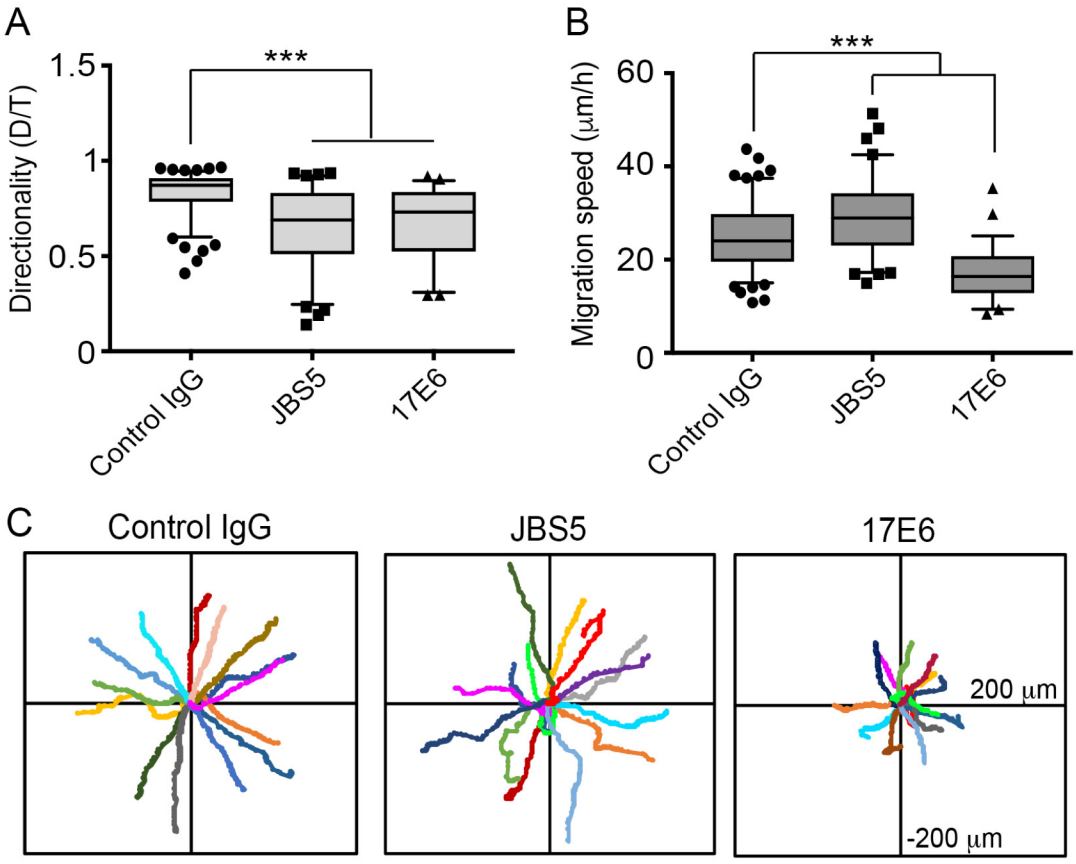

Figure 31. αv integrins are critical for cancer cell migration on CAF CDMs (A-B) Quantifications of migration directionality (A) and speed (B) of DU145 cells on CAF CDMs when treated with control IgG, α5 integrin function blocking antibody JBS5 or αv function blocking antibody 17E6. >80 cells per condition was analyzed in four independent experiments. (***, P<0.001, determined by one-way ANOVA and Tukey post hoc test). (C) Rose plots showing migration trajectories of 14 representative cells treated with control IgG, JBS5 or 17E6 antibodies.

D

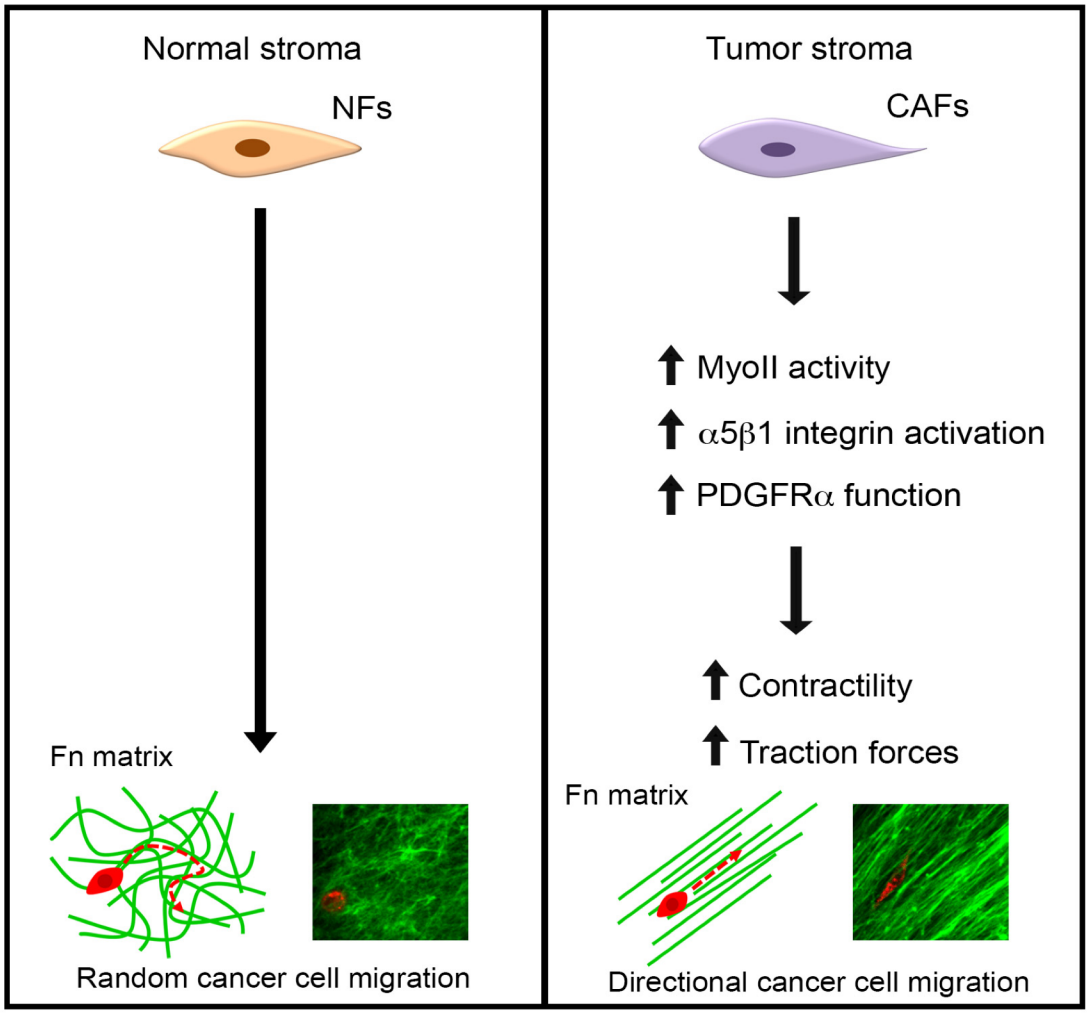

Figure 32. Proposed model of CAF-mediated directional cancer cell migration. (D) The normal fibroblastic matrix resembles a random meshwork of fibers, which do not induce migration directionality. However, CAFs organize the Fn matrix into aligned fibers through increased MyoII, α5β1 integrin and PDGFRα-mediated contractility and traction forces. Anisotropic organization of matrix fibers by CAFs promotes directional migration of cancer cells.

In addition to its influence on CAF-cancer cell association, we show that Fn is critical for ECM synthesis and organization by CAFs. Fn is a major component of the CDMs generated by CAFs and NFs and knocking down Fn expression in CAFs completely disrupts ECM synthesis and organization. Moreover, CAFs organize Fn into parallel fibers, whereas Fn matrix assembled by NFs resembles a mesh. ECM architecture can guide directional migration of cells through physical cues, as migrating cells utilize the ECM as attachment points during migration (Petrie et al., 2009). CAF-mediated parallel organization of CAF CDMs promotes directional migration of both prostate cancer and HNSCC cells, where cell migration is in the same direction as the orientation of the fibers. In clinical prostate carcinoma samples, we observed aligned Fn fibers at the sites of invasion, which were adjacent to invading cancer cells. Interestingly, parallel-organized Fn was also present in pancreatic ductal adenocarcinomas, indicating that alignment of Fn fibers is a clinical feature of both carcinomas and may contribute to cancer cell dissemination.

Although overexpression of Fn and its EDA isoform was reported to be a feature of CAFs more than a decade ago (Kalluri and Zeisberg, 2006), the impact of changes in Fn matrix on cancer cell migration are just now emerging. A recent article by Gopal *et al.* studied the CAF matrisome and identified Fn-EDA as a marker of poor survival in HNSCC patients (Gopal et al., 2017). Interestingly, this study reports directional migration of HNSCC cells on CAF CDMs, in a collective manner. We did not observe collective cell migration of either prostate cancer or HNSCC cells on CAF CDMs; however, this could be due to differences in epithelial properties of the cancer cell lines that were selected or differences in cell density between the two studies. Nevertheless, both studies identify Fn as a critical component of CAF CDMs that regulates directional cell migration.

A few studies have identified factors that can lead to ECM alignment, including the serine proteinase fibroblast activation protein (FAP) (Lee et al., 2011a), and the transcription factors Snail1 and Twist1, which may act downstream of TGFβ to induce the CAF phenotype (Stanisavljevic et al., 2015; Garcia-Palmero et al., 2016). However, the mechanism by which CAFs organize the ECM still remains largely unclear. Here, we demonstrate that mechanical force is an important factor that enables CAFs to generate an aligned ECM. MyoII-mediated contractility is a prominent feature of CAFs (Calvo et al., 2013). We found that prostate CAFs have elevated MyoII activity, are highly contractile, and apply high traction stresses on Fn. Remarkably, treatment with low doses of MyoII inhibitor perturbed the aligned Fn organization by CAFs, giving rise to a more random network of fibers similar to that assembled by NFs. Since DU145 cells did not migrate directionally when plated onto CAF CDMs generated during blebbistatin treatment, these results suggest that matrix organization is a major driver of cancer cell migration directionality and is mediated by MyoII-driven contractility and high traction force generated by CAFs.

α5β1 integrin plays a major role in Fn fibrillogenesis and can be activated by mechanical force from within the cell, through actomyosin contractility (Friedland et al., 2009). Consistent with previous studies identifying α5β1 integrin as a mechanotransducer (Roca-Cusachs et al., 2012; Schwartz and DeSimone, 2008), we found that high traction forces produced by CAFs were transduced by α5β1 integrin to Fn. Although there were no differences in the expression of α5 and β1 integrin subunits between CAFs and NFs, we found increased activation of α5 and β1 integrins in CAFs in comparison to NFs. The increased Fn expression and contractility of CAFs explains the enhancement observed in α5β1 integrin activation (Lin et al., 2013). The overexpression and activation of PDGFRα

may also enhance α5β1 integrin activity, as indicated by our blocking antibody results. As many signals converge on integrins to induce inside-out signaling, it seems likely that there are additional mechanisms that could lead to enhanced activation of α5β1 integrin in CAFs, such as any deregulations in the cell metabolism sensor AMP-activated protein kinase (AMPK), which was recently reported to be a negative regulator of β1 integrin activity and Fn fibrillogenesis in fibroblasts (Georgiadou et al., 2017) or deregulation of the integrin inhibitor Sharpin protein which was shown to control collagen remodeling and traction forces (Peuhu et al., 2017). We should note that other integrins can also contribute to changes in CDM organization, including αvβ5, as recently reported by Franco-Barraza et al. (Franco-Barraza et al., 2017).

As part of the mechanism by which CAFs promote ECM organization, we found that prostate CAFs overexpress PDGFRα and exhibit increased Y762 phosphorylation. Inhibition of PDGFRα significantly abrogated collagen gel contraction and traction stresses generated by CAFs, as well as α5β1 integrin activity and FN organization. These data are consistent with previous demonstrations of crosstalk between α5β1 integrin and PDGFRα in mesenchymal stem cells (Veevers-Lowe et al., 2011). Interestingly, α5β1 integrin and PDGFRs have been shown to be in complex with tissue transglutaminase which modulates the activity of both receptors, and potentially converging and amplifying their downstream signaling (Akimov and Belkin, 2001; Zemskov et al., 2009b). However, it is also possible that PDGFRα signaling can activate contractility directly, which would lead to indirect activation of α5β1 integrin. For example, PDGFRα signaling can activate RhoA-ROCK pathway in mesenchymal stem cells, leading to increased polymerization of αSMA in actin

filaments (Ball et al., 2007), which is also a characteristic feature of CAFs. Therefore, integrin α5β1 and PDGFRα signaling may converge on activation of RhoA-mediated contractility (Danen et al., 2002). PDGFR signaling is a promising target in many cancers (Heldin, 2013b), thus, understanding the regulation of CAFs and stromal ECM by PDGFRs may provide valuable information for targeting the tumor stroma in carcinomas.

In response to the profound changes in the tumor microenvironment, cancer cells express and activate different integrins to regulate processes such as cell attachment and migration. Gopal et al. (2017) reported that HNSCC cells upregulate α5β1, αvβ5 and αvβ6 integrins when cultured on Fn-EDA rich CAF CDMs. They further identified that the collective migration of HNSCC cells on CAF CDMs was mediated by αvβ6 and Fn EDA-binding α9β1 integrins (Gopal et al., 2017). These findings prompted us to investigate the integrins involved in directional migration of prostate cancer cells on CAF CDMs. Similar to Gopal et al., we found that blocking α5β1 integrin in prostate cancer cells induced faster migration with decreased directionality and blocking αv integrin activity decreased both directionality and speed. These results suggest that α5β1 integrins may be responsible for forming stronger attachments to matrix as previously reported (Roca-Cusachs et al., 2009), whereas αv integrins are critical for cell migration. Aberrant expression of RGD-binding integrins α5 and αv have been reported in prostate cancers and are being explored as potential targets for therapy (Sutherland et al., 2012b; Goel et al., 2008). Gopal et al. also showed that EDA-binding integrin α9β1 regulates cell migration on CAF CDMs (Gopal et al., 2017). Although, CAFs in our study also express high levels of EDA-Fn (shown in Fig. S1J and K), we did not find any studies that report α9 integrin expression in prostate cancers. ITGA9 expression was not detected in 11 prostate cancer tissues examined in The Human

Protein Atlas, therefore, we did not study this integrin. Other EDA-binding integrins, α4β1 and α4β7, were also not investigated as there are multiple reports showing that α4 integrin is not expressed in prostate cancer and DU145 cells (Rokhlin and Cohen, 1995; Barthel et al., 2013; Chen et al., 2015). Taken together, our results indicate differing roles for integrins in CAFs and cancer cells in mediating matrix assembly and cell migration, thus, highlighting the complexity of integrin signaling in tumors.

Collectively, our study shows that CAFs organize Fn matrix through increased contractility and traction forces, which are mediated by MyoII, α5β1 integrin and PDGFRα. This matrix organization leads cancer cells to migrate directionally using αv integrins (Fig. 8 D). Alignment of the Fn fibers is a prominent feature of both prostatic and pancreatic cancer stromas both *in vivo* and *in vitro* and is likely to guide the invasion of cancer cells. Surprisingly, our data suggest that CAFs in the tumor microenvironment are not tissue type specific in their ability to regulate cancer cell migration. For example, CAFs from prostate can regulate the migration of HNSCC cells. This indicates a commonly-used mechanism for modulating the migration of cancer cells, which has far reaching implications in the development of tumor metastases. Furthermore, biochemical targeting of this pathway could prove beneficial in limiting stromal support during the metastasis of cancer cells.

CHAPTER III

CONCLUSIONS AND FUTURE DIRECTIONS

The leading cause of cancer morbidity and mortality is metastasis, which is the process in which cancer cells spread from the primary tumor to distant sites in the body and form tumors at these sites. An early step in the metastatic process is the cancer cell invasion into the tumor stroma where the cancer cells come in contact with stromal cells. Research from the last two decades revealed the importance of the stromal cells in the regulation of cancer progression and metastasis. One of the cell types in the stroma is the fibroblasts, which are critical for tissue maintenance and repair. In tumors, fibroblasts can become activated by cancer cells and present a myofibroblast-like phenotype. These fibroblasts are called cancer-associated fibroblasts (CAFs) and their origin, activation and function in the tumor microenvironment and influence on tumor progression has been an ongoing subject of interest.

In this project, we aimed to identify the effects of CAFs on cancer cell migration. To do this, we started by co-culturing CAFs and NFs with prostate cancer and HNSCC cells in two-chamber microfluidic devices. These devices provided a platform where close cellular interactions between cells of the tumor microenvironment can be mimicked and imaged via live-cell microscopy. We found that cancer cells interact with CAFs more than they do with NFs, and migrate directionally along the CAFs. Interestingly, HNSCC cells also interacted more with prostate CAFs, indicating that CAFs mediate cancer cell interaction and migration through a ubiquitous mechanism that is not tissue specific.

Fibroblasts are known to secrete and assemble matrix fibers, and remodel the ECM through cellular contractility and secretion of MMPs. Previous studies have shown that CAFs reorganize the 3D collagen matrix to facilitate cancer cell migration (Calvo et al., 2013; Gaggioli et al., 2007). However, these studies did not investigate the role of matrix proteins directly secreted by CAFs. In our co-culture experiments, the microfluidic devices were not coated with ECM; only matrix proteins secreted by CAFs during the overnight incubation were present, which enabled us to see the interaction of the cancer cells with CAF-derived ECM molecules. Staining fibroblast-cancer cell co-cultures for the ECM protein Fn showed that the cancer cells are binding to Fn, assembled into fibers by CAFs. Conversely, we did not observe Fn in the areas where cancer cells were near NFs. Live imaging of cancer cell-CAF-Fn interaction showed that cancer cells are using Fn to migrate along CAFs. Knocking down Fn in CAFs by siRNA, diminished cancer cell-CAF association and cancer cell directional migration. Previously, CAF-secreted biochemical factors and ECM remodeling were shown to mediate cancer cell migration and invasion. These seminal studies identified major communication mechanisms between CAFs and cancer cells (Gaggioli et al., 2007; Calvo et al., 2013). However, the role of Fn as a mediator of CAF-cancer cell interactions is recently emerging. A recent study identified CAF-mediated Fn fibrillogenesis in 3D collagen matrices as an inducer of cancer cell invasion (Attieh et al., 2017). In another recent study, EDA isoform of Fn (Fn-EDA) which was secreted and assembled to matrix by CAFs was found to stimulate collective migration of HNSCC cells through EDA-binding integrins (Gopal et al., 2017).

We found that prostate CAFs, used in our study, also overexpressed Fn and the Fn-EDA isoform compared to NFs. TGFβ is a potent activator of fibroblasts and stimulation by

TGFβ was previously shown to upregulate Fn expression (Hinz et al., 2007). Therefore, it is tempting to speculate that CAFs were activated *in vivo* by TGFβ signaling. However, other signaling pathways and mechanical stimulus have also been shown to generate CAFs (Rasanen and Vaheri, 2010; Ao et al., 2015). Therefore, it would be interesting to investigate the regulation of Fn expression in CAFs. In addition, changes in translational machinery in CAFs, such as elevated expression of initiator tRNA, was shown to play a role in upregulation of synthesis and secretion of ECM proteins such as collagen-II (Clarke et al., 2016). Deregulation of tRNA expression and ribosome function has been reported in cancers as an inducer of cell migration and metastasis (Birch et al., 2016). Therefore, it is possible that translational machinery in CAFs is programmed to produce increased amounts of Fn. However, more studies are needed to determine the translational regulation of Fn synthesis and secretion in CAFs.

The close interaction that we observed in the co-culture of CAFs and cancer cells raised the question whether these two different types of cells form cell-cell junctions as recently reported (Labernadie et al., 2017). In this study, authors showed that CAFs and cancer cells form heterotypic N-cadherin/E-cadherin connections, which enables CAFs to exert pulling forces on the cancer cells to direct their invasion into the 3D matrix. When we stained co-cultures for N- and E-cadherins, we found that CAFs and cancer cells express N- and E-cadherins, respectively. However, they did not associate with each other through forming heterotypic N-cadherin/E-cadherin adhesions. We must note that these results do not rule out the possibility that CAFs and cancer cell may interact via other cell-cell junction proteins, such as P-cadherin. Furthermore, localization of cell-cell junction proteins may be different in the 3D spheroid assay used in the Labernadie study compared to the 2D co-

culture system used in our study. Still, knocking down Fn in CAFs significantly decreased the CAF-cancer cell association in our co-culture assays, suggesting that CAF-cancer cell association is mediated by Fn.

Aside from the overexpression of matrix proteins, CAFs have been shown to regulate cancer cell migration through altering the organization of matrix fibers (Beacham and Cukierman, 2005; Amatangelo et al., 2005; Provenzano et al., 2008). Alignment of matrix fibers can provide the cells with directional cues through a process known as the contact guidance (Doyle et al., 2009). Since we found that cancer cells migrate more directionally when co-cultured with CAFs, we next tested whether there are changes in the matrix organization by CAFs. When CAFs and NFs were allowed to generate their own matrices (CDMs), we found a striking difference in matrix organization. The ECM assembled by NFs was highly disorganized, resembling a meshwork, however, CAFs organized ECM in aligned fibers. The aligned matrix organization by CAFs promoted directionally persistent migration of both prostate and HNSCC cells. A few proteins overexpressed by CAFs, such as fibroblast activation protein (FAP) and Caveolin-1 (Cav1) were implicated in matrix alignment (Lee et al., 2011b; Goetz et al., 2011). Both FAP and Cav1 seem to affect the cellular contractility to align the matrix fibers. FAP is a serine protease with dipeptidyl peptidase and gelatinase/collagenase activities that is frequently overexpressed in CAFs. Lee *at al*. found that overexpression of FAP by CAFs upregulates the expression of collagen, Fn and αSMA, and leads to an aligned matrix. Interestingly, although FAP enzymatic activity was found to be important for matrix alignment and collagen expression, it was not required for Fn and αSMA expression. Cav1 is the principal structural component of the specialized plasma membrane domains called caveolae (Grande-Garcia et al., 2007). Goetz *et al*. found that

Cav1 is overexpressed in CAFs and showed that Cav1 blocked the Rho GTPase inhibitor, p190, by partitioning it to the plasma membrane. Thus, Cav1-expressing CAFs presented an increase in Rho-mediated contractility which resulted in alignment of the matrix. It is interesting that an earlier study identified Cav1 as a critical regulator of α5β1 integrin and Fn turnover (Shi and Sottile, 2008; Sottile, J. and Chandler, 2004). However, this function of Cav1 with regards to matrix alignment has not been investigated. It is plausible that in addition to regulating Rho GTPase activity, Cav1 regulates α5β1 integrin and Fn turnover in CAFs. In summary, changes in matrix organization by CAFs were previously reported and linked to the increased contractility of CAFs, however, it was not clear how mechanistically this contractility mediates matrix alignment.

In our study, we found that CAFs from prostate cancer are also highly contractile and present elevated phosphorylation of MyoII RLC, compared to NFs. These contractile forces are transduced to Fn as increased traction forces, as measured by traction force microscopy. Blocking MyoII activity in CAFs perturbed the matrix organization by CAFs, giving rise to disorganized NF-like matrix arrangement. These results suggest that CAF contractility and traction forces drive matrix alignment. Focal adhesions are sites of force transmission between the cytoskeleton and the ECM. As MyoII regulates adhesion maturation, increases in MyoII activity and actomyosin contractility could mediate adhesion structure and dynamics (Vicente-Manzanares et al., 2009). Thus, we investigated vinculin-positive adhesions in CAFs. Focal adhesion protein vinculin is a mechanosensitive component of adhesions (Hinz and Gabbiani, 2003; Grashoff et al., 2010). Focal adhesions respond to force by elongation and recruitment of vinculin and the amount of vinculin aggregates have been correlated with the amount of force generated at focal adhesions (Balaban et al., 2001;

Galbraith et al., 2002). We found that CAFs have larger vinculin-positive adhesions that turn over more slowly in comparison to NFs. In addition to MyoII activity, ECM stiffness have also been shown to impact focal adhesion size and maturation (Katz et al., 2000). For example, cells on softer substrates demonstrate smaller and more dynamic adhesions whereas cells on stiffer substrates exhibit larger and more stable adhesions (Parsons et al., 2010). In myofibroblasts, increases in the substrate rigidity were found to yield to larger adhesions that can exert higher forces. These adhesions drove the recruitment of αSMA to stress fibers, which is also a characteristic of CAFs (Hinz, 2006). Although we did not investigate ECM stiffness in this study, prior studies showed that matrix fibers are stiffened by CAFs (Goetz et al., 2011; Garcia-Palmero et al., 2016). Therefore, it is possible that CAFs in our study also generate stiffer ECM fibers.

Mechanical forces generated in cells by MyoII-mediated contractility can be transduced to the ECM via integrins. α5β1 integrin is a Fn-specific adhesion receptor that is largely responsible for Fn fibrillogenesis. Using conformation-specific antibodies, we found that there is more active α5β1 integrin in CAFs compared to NFs. Increased activation of α5β1 integrin in CAFs could be a result of increased Fn expression by CAFs and/or increased actomyosin contractility, as integrins can become activated through an "inside-out" mechanism. Another mechanism of α5β1 integrin activation may be regulation by PDGFRs, as we found that blocking PDGFRα decreases active α5β1 integrin levels.

Integrins are considered mechanosensitive proteins as they can respond to both intracellular and extracellular forces across the plasma membrane (Ross et al., 2013). By traction force microscopy, we found that α5β1 integrin mediates transmission of cellular forces to Fn. In addition, blocking α5β1 integrin function alters Fn and CDM organization

by CAFs, indicating that aligned Fn organization by CAFs is α5β1 integrin-dependent. It is important to note that blocking α5β1 integrin did not completely abolish Fn fibrillogenesis or matrix formation to the degree that we observed with Fn knockdown. This result indicates that other integrins, such as αvβ3, may also be involved in matrix assembly by CAFs, corroborating the findings of a recent report (Attieh et al., 2017). However, our results indicate that the traction forces and matrix alignment is mediated by α5β1 integrin activity in CAFs. Furthermore, blocking α5β1 integrin activity altered overall ECM organization, which is composed of many ECM molecules, suggesting that Fn fibrillogenesis acts as a template for matrix, influencing organization of other ECM proteins.

Another group of adhesion receptors that plays a role in integrin-mediated Fn fibrillogenesis is the syndecan family (Woods, 2001). Syndecans (Sdcs) are transmembrane heparan sulfate proteoglycans with four known members (Sdc1-4). Sdc2 and Sdc4 were found to be involved in Fn matrix assembly (Wierzbicka-Patynowski and Schwarzbauer, 2003). Interestingly, Sdc1 is overexpressed in CAFs from breast cancer and was shown to contribute to the arrangement of Fn in parallel fibers (Yang et al., 2011). The authors of this study speculate that Sdc1 may cooperate with integrins to promote alignment of Fn fibers. However, more research is needed to elucidate the role of syndecan-integrin interplay in CAF-mediated matrix assembly and organization.

Integrin activity can be mediated by growth factor receptors (GFRs). Cellular responses to the ECM and soluble growth factors have been found to be regulated by the physical association and functional collaboration between integrins and GFRs (Eliceiri, 2001; Yamada and Even-Ram, 2002). Binding to Fn was shown to induce tyrosine phosphorylation of both PDGFRα and -β in an α5β1 integrin-dependent manner (Veevers-

Lowe et al., 2011). The fact that both PDGFRs are frequently overexpressed by CAFs and even used as a CAF marker, prompted us to investigate their role in α5β1-mediated matrix alignment by CAFs. We found that CAFs express approximately 3-fold more PDGFRα compared to NFs. In addition, we observed higher amounts of active PDGFRα in CAFs relative to NFs. PDGF signaling in fibroblasts was shown to be important for fibroblast proliferation and recruitment (Donovan et al., 2013a). However, its role in fibroblast activation and CAF-mediated matrix organization has remained unclear. We found that blocking PDGFRα decreases active α5β1 integrin, contractility and traction forces in CAFs. Furthermore, inhibiting PDGFRα disrupts matrix alignment by CAFs. These results could be due to the crosstalk between PDGFRα and α5β1 integrin, which were shown to be in close interaction on the plasma membrane, with cell surface tissue transglutaminase (tTG) bridging the two receptors. tTG is a Ca^{2+}-dependent enzyme that covalently crosslinks several ECM proteins, including Fn (Akimov and Belkin, 2001). tTG was shown to enhance Fn matrix formation mediated by α5β1 integrin, however this function did not require its enzymatic activity (Akimov and Belkin, 2001). Therefore, it is possible that tTG expression and/or activity is deregulated in CAFs, and contributes to the PDGFRα and α5β1 integrin crosstalk and matrix alignment by CAFs. It is also possible that PDGFRα modulates α5β1 integrin activity via downstream signaling. PDGFRα can activate RhoA-ROCK pathway in mesenchymal stem cells, leading to increased polymerization of αSMA in actin filaments (Ball et al., 2007), leading to increased cellular contractility, which can, in turn, activate α5β1 integrin. Further research is required for elucidating the mechanisms of PDGFRα-α5β1 integrin interaction in CAFs and its role in matrix organization.

Overexpression of PDGFRβ is common in CAFs and we also found higher levels of PDGFRβ in CAFs used in our study (data not shown). PDGFRα and –β transduce distinct signals in cells and mediate diverse functions (Cao, 2013). Therefore, it would be interesting to discern the function of PDGFRβ in CAFs with regards to ECM organization.

A critical regulator of cell migration is the integrin-based cell-matrix adhesions. In response to different extracellular environments, cells can change the expression of cell surface integrins and use different classes of integrins for various cellular functions. Gopal *et al*. found that HNSCC cells upregulate expressions of integrins α5β1, αvβ5 and αvβ6 when cultured on CAF CDMs and use integrins αvβ6 and Fn-EDA-binding α9β1 to migrate on CAF CDMs (Gopal et al., 2017). Similarly, we also investigated integrins that may be involved in prostate cancer cell migration on CAF CDMs. We found that blocking α5β1 in prostate cancer cells decreases directionality but increases migration speed. Conversely, blocking αv integrin activity decreased both directionality and speed. These results suggest α5β1 that may be responsible for forming stronger attachments to matrix as previously reported (Roca-Cusachs et al., 2009), whereas αv integrins are critical for cell migration. Gopal *et al*. also showed that EDA-binding integrin α9β1 regulates cell migration on CAF CDMs (Gopal et al., 2017). CAFs in our study also express high levels of Fn-EDA, but we did not find any studies that report α9 integrin expression in prostate cancers. ITGA9 gene expression was not detected in 11 prostate cancer tissues examined in The Human Protein Atlas, therefore, we did not study this integrin. Other EDA-binding integrins, α4β1 and α4β7, were also not investigated as there are multiple reports showing that α4 integrin is not expressed in prostate cancer and DU145 cells (Rokhlin and Cohen, 1995; Barthel et al., 2013; Chen et al., 2015).

It is intriguing that α5β1 integrin plays opposing roles in malignant cells versus tumor stroma. α5β1 integrin mediates ECM alignment by CAFs, which promotes directional migration of cancer cells, but blocking α5β1 integrin in cancer cells increases cell migration speed. Most studies that investigated α5β1 integrin in cancer, focused on its role in cancer cells or endothelial cells (Schaffner et al., 2013). Some of these studies suggest that α5β1 integrin increases cancer cell survival, EMT and invasion and induce angiogenesis via endothelial cells. A monoclonal antibody against α5β1 integrin, volociximab, has been developed and tested in renal cell carcinoma, pancreatic cancer, malignant melanoma and lung cancer and has shown promising results (Almokadem and Belani, 2012). Further investigation of α5β1 integrin in tumor stroma can advance our understanding of its role in tumors and improve treatment outcomes of patients.

Our data show that parallel arrangement of ECM fibers by CAFs promotes directional cancer cell migration *in vitro*. Thus, we next investigated Fn in human cancer tissues. Fn staining of prostatic and pancreatic cancer tissue sections revealed high levels of Fn as well-organized, parallel fibers at sites of invasion, and invading cancer cells lined up alongside the Fn fibers. We also found that aligned Fn was rich in areas with high αSMA expression, suggesting that CAFs are responsible for Fn alignment *in vivo*. ECM can provide cancer cells with directional cues in tumor microenvironment, which may expedite their invasion into the stroma and facilitate metastasis. To follow up on our findings, it would be interesting to use mouse models of cancer to investigate how targeting MyoII, α5β1 integrin and PDGFRα in tumor stroma affects Fn alignment and cancer cell invasion.

In summary, our study shows that CAFs organize Fn matrix through increased contractility and traction forces, which are mediated by MyoII, α5β1 integrin and PDGFRα.

This matrix organization leads cancer cells to migrate directionally using αv integrins. Increasing number of studies, including this study, highlight the role of CAFs in mediating stromal changes in tumors and regulating cancer cell migration. Therefore, targeting CAFs in the tumor microenvironment may be a feasible therapeutic strategy that needs to be explored further.

REFERENCES

Van Aelst, L., and C. D'Souza-Schorey. 1997. Rho GTPases and signaling networks. *Genes Dev.* 11:2295–2322.

Akimov, S.S., and a M. Belkin. 2001. Cell-surface transglutaminase promotes fibronectin assembly via interaction with the gelatin-binding domain of fibronectin: a role in TGFbeta-dependent matrix deposition. *J. Cell Sci.* 114:2989–3000.

Alahari, S.K., J.W. Lee, and R.L. Juliano. 2000. Nischarin, a novel protein that interacts with the integrin α5 subunit and inhibits cell migration. *J. Cell Biol.* 151:1141–1154.

Alexander, J., and E. Cukierman. 2016. Stromal dynamic reciprocity in cancer: intricacies of fibroblastic-ECM interactions. *Curr. Opin. Cell Biol.* 42:80–93.

Almokadem, S., and C.P. Belani. 2012. Volociximab in cancer. *Expert Opin. Biol. Ther.* 12:251–257.

Amano, M., M. Ito, K. Kimura, Y. Fukata, K. Chihara, T. Nakano, Y. Matsuura, and K. Kaibuchi. 1996. Phosphorylation and activation of myosin by Rho-associated kinase (Rho- kinase). *J. Biol. Chem.* 271:20246–20249.

Amatangelo, M.D., D.E. Bassi, A.J.P. Klein-Szanto, and E. Cukierman. 2005. Stroma-derived three-dimensional matrices are necessary and sufficient to promote desmoplastic differentiation of normal fibroblasts. *Am. J. Pathol.* 167:475–488.

Andrae, J., R. Gallini, and C. Betsholtz. 2008. Role of platelet-derived growth factors in physiology and medicine. *Genes Dev.* 22:1276–1312.

Ao, M., B.M. Brewer, L. Yang, O.E. Franco Coronel, S.W. Hayward, D.J. Webb, and D. Li.

2015. Stretching fibroblasts remodels fibronectin and alters cancer cell migration. *Sci. Rep.* 5:8334.

Ao, M., O.E. Franco, D. Park, D. Raman, K. Williams, and S.W. Hayward. 2007. Cross-talk between paracrine-acting cytokine and chemokine pathways promotes malignancy in benign human prostatic epithelium. *Cancer Res.* 67:4244–4253.

Appiah-Kubi, K., Y. Wang, H. Qian, M. Wu, X. Yao, Y. Wu, and Y. Chen. 2016. Platelet-derived growth factor receptor/platelet-derived growth factor (PDGFR/PDGF) system is a prognostic and treatment response biomarker with multifarious therapeutic targets in cancers. *Tumor Biol.* 37:10053–10066.

Arnaout, M.A., S.L. Goodman, and J.P. Xiong. 2007. Structure and mechanics of integrin-based cell adhesion. *Curr. Opin. Cell Biol.* 19:495–507. doi:10.1016/j.ceb.2007.08.002.

Arthur, W.T., L.A. Petch, and K. Burridge. 2000. Integrin engagement suppresses RhoA activity via a c-Src-dependent mechanism. *Curr. Biol.* 10:719–722.

Askari, J.A., P.A. Buckley, A.P. Mould, and M.J. Humphries. 2009. Linking integrin conformation to function. *J. Cell Sci.* 122:165–170.

Attieh, Y., A.G. Clark, C. Grass, S. Richon, M. Pocard, P. Mariani, N. Elkhatib, T. Betz, B. Gurchenkov, and D.M. Vignjevic. 2017. Cancer-associated fibroblasts lead tumor invasion through integrin-beta3-dependent fibronectin assembly. *J. Cell Biol.* 1–12.

Augsten, M. 2014. Cancer-associated fibroblasts as another polarized cell type of the tumor microenvironment. *Front. Oncol.* 4:62.

Ayres, C., G.L. Bowlin, S.C. Henderson, L. Taylor, J. Shultz, J. Alexander, T.A. Telemeco, and D.G. Simpson. 2006. Modulation of anisotropy in electrospun tissue-engineering scaffolds: Analysis of fiber alignment by the fast Fourier transform. *Biomaterials*.

27:5524–5534.

Bae, Y.K., A. Kim, M.K. Kim, J.E. Choi, S.H. Kang, and S.J. Lee. 2013. Fibronectin expression in carcinoma cells correlates with tumor aggressiveness and poor clinical outcome in patients with invasive breast cancer. *Hum. Pathol.* 44:2028–2037.

Balaban, N.Q., U.S. Schwarz, D. Riveline, P. Goichberg, G. Tzur, I. Sabanay, D. Mahalu, S. Safran, A. Bershadsky, L. Addadi, and B. Geiger. 2001. Force and focal adhesion assembly: a close relationship studied using elastic micropatterned substrates. *Nat. Cell Biol.* 3:466–472.

Ball, S.G., C.A. Shuttleworth, and C.M. Kielty. 2007. Platelet-derived growth factor receptor-alpha is a key determinant of smooth muscle alpha-actin filaments in bone marrow-derived mesenchymal stem cells. *Int. J. Biochem. Cell Biol.* 39:379–391.

Barsky, S.H., W.R. Green, G.R. Grotendorst, and L.A. Liotta. 1984. Desmoplastic breast carcinoma as a source of human myofibroblasts. *Am. J. Pathol.* 115:329–333.

Barthel, S.R., D.L. Hays, E.M. Yazawa, M. Opperman, K.C. Walley, L. Nimrichter, M.M. Burdick, B.M. Gillard, M.T. Moser, K. Pantel, B.A. Foster, K.J. Pienta, and C.J. Dimitroff. 2013. Definition of molecular determinants of prostate cancer cell bone extravasation. *Cancer Res.* 73:942–952.

Beacham, D.A., and E. Cukierman. 2005. Stromagenesis: The changing face of fibroblastic microenvironments during tumor progression. *Semin. Cancer Biol.* 15:329–341.

Beacham, D., M. Amatangelo, and E. Cukierman. 2006. Preparation of Extracellular Matrices. *Curr. Protoc. Cell Biol.* 1–21.

Birch, J., C.J. Clarke, A.D. Campbell, K. Campbell, L. Mitchell, D. Liko, G. Kalna, D. Strathdee, O.J. Sansom, M. Neilson, K. Blyth, and J.C. Norman. 2016. The initiator

methionine tRNA drives cell migration and invasion leading to increased metastatic potential in melanoma. *Biol. Open*. 5:1371–1379.

Bonner, J.C. 2004. Regulation of PDGF and its receptors in fibrotic diseases. *Cytokine Growth Factor Rev.* 15:255–273.

Bouvard, D., J. Pouwels, N. De Franceschi, and J. Ivaska. 2013. Integrin inactivators: balancing cellular functions in vitro and in vivo. *Nat. Rev. Mol. Cell Biol.* 14:430–42.

Brentnall, T.A., L.A. Lai, J. Coleman, M.P. Bronner, S. Pan, and R. Chen. 2012. Arousal of cancer-associated stroma: Overexpression of palladin activates fibroblasts to promote tumor invasion. *PLoS One*. 7:1–14.

Brinckmann, J. 2005. Collagens at a glance. *Top. Curr. Chem.* 247:1–6.

Burridge, K., and K. Fath. 1989. Focal contacts: Transmembrane links between the extracellular matrix and the cytoskeleton. *BioEssays*. 10:104–108.

Byron, A., M.R. Morgan, and M.J. Humphries. 2010. Adhesion signalling complexes. *Curr. Biol.* 20:R1063–R1067.

Calvo, F., N. Ege, A. Grande-Garcia, S. Hooper, R.P. Jenkins, S.I. Chaudhry, K. Harrington, P. Williamson, E. Moeendarbary, G. Charras, and E. Sahai. 2013. Mechanotransduction and YAP-dependent matrix remodelling is required for the generation and maintenance of cancer-associated fibroblasts. *Nat Cell Biol*. 15:637–646.

Campbell, I.D., and M.J. Humphries. 2011. Integrin structure, activation, and interactions. *Cold Spring Harb. Perspect. Biol.* 3:1–14.

Cao, Y. 2013. Multifarious functions of PDGFs and PDGFRs in tumor growth and metastasis. *Trends Mol. Med.* 19:460–473.

Cao, Z., K. Huang, and A.F. Horwitz. 1999. Identification of a domain on the integrin α5

subunit implicated in cell spreading and signaling. *J. Biol. Chem.* 273:31670–31679.

Carapuça, E.F., E. Gemenetzidis, C. Feig, T.E. Bapiro, M.D. Williams, A.S. Wilson, F.R. Delvecchio, P. Arumugam, R.P. Grose, N.R. Lemoine, F.M. Richards, and H.M. Kocher. 2016. Anti-stromal treatment together with chemotherapy targets multiple signalling pathways in pancreatic adenocarcinoma. *J. Pathol.* 286–296.

Caswell, P.T., H.J. Spence, M. Parsons, D.P. White, K. Clark, K.W. Cheng, G.B. Mills, M.J. Humphries, A.J. Messent, K.I. Anderson, M.W. McCaffrey, B.W. Ozanne, and J.C. Norman. 2007. Rab25 Associates with α5β1 Integrin to Promote Invasive Migration in 3D Microenvironments. *Dev. Cell*. 13:496–510.

Chen, C., Q. Zhang, S. Liu, K.R. Parajuli, Y. Qu, J. Mei, Z. Chen, H. Zhang, D.B. Khismatullin, and Z. You. 2015. IL-17 and insulin/IGF1 enhance adhesion of prostate cancer cells to vascular endothelial cells through CD44-VCAM-1 interaction. *Prostate*. 75:883–895.

Chen, P.-H., X. Chen, and X. He. 2013. Platelet-derived growth factors and their receptors: Structural and functional perspectives. *Biochim. Biophys. Acta - Proteins Proteomics*. 1834:2176–2186.

Cheng, N., a. Chytil, Y. Shyr, a. Joly, and H.L. Moses. 2008. Transforming Growth Factor- Signaling-Deficient Fibroblasts Enhance Hepatocyte Growth Factor Signaling in Mammary Carcinoma Cells to Promote Scattering and Invasion. *Mol. Cancer Res.* 6:1521–1533.

Cherfils, J., and M. Zeghouf. 2013. Regulation of small GTPases by GEFs, GAPs, and GDIs. *Physiol. Rev.* 93:269–309.

Chrzanowska-Wodnicka, M., and K. Burridge. 1996. Rho-stimulated Contractiliry Drives

the Formation of Stress Fibers and Focal Adhesions. *J. Cell Biol.* 133:1403–1415.

Clark, K., M. Langeslag, C.G. Figdor, and F.N. van Leeuwen. 2007. Myosin II and mechanotransduction: a balancing act. *Trends Cell Biol.* 17:178–186.

Clark, K., R. Pankov, M. a Travis, J. a Askari, a P. Mould, S.E. Craig, P. Newham, K.M. Yamada, and M.J. Humphries. 2005. A specific alpha5beta1-integrin conformation promotes directional integrin translocation and fibronectin matrix formation. *J. Cell Sci.* 118:291–300.

Clarke, C.J., T.J. Berg, J. Birch, D. Ennis, L. Mitchell, C. Cloix, A. Campbell, D. Sumpton, C. Nixon, K. Campbell, V.L. Bridgeman, P.B. Vermeulen, S. Foo, E. Kostaras, J.L. Jones, L. Haywood, E. Pulleine, H. Yin, D. Strathdee, O. Sansom, K. Blyth, I. McNeish, S. Zanivan, A.R. Reynolds, and J.C. Norman. 2016. The initiator methionine trna drives secretion of type II collagen from stromal fibroblasts to promote tumor growth and angiogenesis. *Curr. Biol.* 26:755–765.

Conklin, M.W., J.C. Eickhoff, K.M. Riching, C.A. Pehlke, K.W. Eliceiri, P.P. Provenzano, A. Friedl, and P.J. Keely. 2011a. Aligned collagen is a prognostic signature for survival in human breast carcinoma. *Am. J. Pathol.* 178:1221–1232.

Conklin, M.W., J.C. Eickhoff, K.M. Riching, C.A. Pehlke, K.W. Eliceiri, P.P. Provenzano, A. Friedl, and P.J. Keely. 2011b. Aligned collagen is a prognostic signature for survival in human breast carcinoma. *Am. J. Pathol.* 178:1221–1232.

Conti, M.A., and R.S. Adelstein. 2008. Nonmuscle myosin II moves in new directions. *J. Cell Sci.* 121:11–18.

Costa, P., T.M.E. Scales, J. Ivaska, and M. Parsons. 2013. Integrin-Specific Control of Focal Adhesion Kinase and RhoA Regulates Membrane Protrusion and Invasion. *PLoS One*.

8.

Cunha, G.R., S.W. Hayward, Y.Z. Wang, and W.A. Ricke. 2003. Role of the stromal microenvironment in carcinogenesis of the prostate. *Int. J. Cancer*. 107:1–10.

Danen, E.H.J., P. Sonneveld, C. Brakebusch, R. Fässler, and A. Sonnenberg. 2002. The fibronectin-binding integrins α5β1 and αvβ3 differentially modulate RhoA-GTP loading, organization of cell matrix adhesions, and fibronectin fibrillogenesis. *J. Cell Biol.* 159:1071–1086.

Dembo, M., and Y.L. Wang. 1999. Stresses at the cell-to-substrate interface during locomotion of fibroblasts. *Biophys. J.* 76:2307–16.

Desgrosellier, J.S., and D. Cheresh. 2010. Integrins in cancer: biological implications and therapeutic opportunities. *Nat. Rev. Cancer*. 10:9–22.

Donovan, J., D. Abraham, and J. Norman. 2013a. Platelet-derived growth factor signaling in mesenchymal cells. *Front. Biosci.* 18:106–119.

Donovan, J., X. Shiwen, J. Norman, and D. Abraham. 2013b. Platelet-derived growth factor alpha and beta receptors have overlapping functional activities towards fibroblasts. *Fibrogenesis Tissue Repair*. 6:10.

Doyle, A.D., F.W. Wang, K. Matsumoto, and K.M. Yamada. 2009. One-dimensional topography underlies three-dimensional fi brillar cell migration. *J. Cell Biol.* 184:481–490.

Eliceiri, B.P. 2001. Integrin and growth factor receptor crosstalk. *Circ. Res.* 89:1104–1110.

Erdogan, B., and D.J. Webb. 2017. Cancer-associated fibroblasts modulate growth factor signaling and extracellular matrix remodeling to regulate tumor metastasis. *Biochem. Soc. Trans.* 45:229–236.

Farooqi, A.A., and Z.H. Siddik. 2015. Platelet-derived growth factor (PDGF) signalling in cancer: Rapidly emerging signalling landscape. *Cell Biochem. Funct.* 33:257–265.

Fouchard, J., D. Mitrossilis, and A. Asnacios. 2011. Acto-myosin based response to stiffness and rigidity sensing. *Cell Adhes. Migr.* 5:16–19.

Franco-Barraza, J., D. Beacham, A. MD, and C. E. 2016. Preparation of Extracellular Matrices Produced by Cultured and Primary Fibroblasts. *Curr. Protoc. cell Biol.* 71:10.9.1-10.9.34.

Franco-Barraza, J., R. Francescone, T. Luong, N. Shah, R. Madhani, G. Cukierman, E. Dulaimi, K. Devarajan, B.L. Egleston, E. Nicolas, R.K. Alpaugh, R. Malik, R.G. Uzzo, J.P. Hoffman, E.A. Golemis, and E. Cukierman. 2017. Matrix-regulated integrin αvβ5 maintains α5 β1 -dependent desmoplastic traits prognostic of neoplastic recurrence. *Elife*. 6.

Frantz, C., K.M. Stewart, and V.M. Weaver. 2010. The extracellular matrix at a glance. *J. Cell Sci.* 123:4195–4200.

Friedl, P., E. Sahai, S. Weiss, and K.M. Yamada. 2012. New dimensions in cell migration. *Nat. Rev. Mol. Cell Biol.* 13:743–747.

Friedland, J.C., M.H. Lee, and D. Boettiger. 2009. Mechanically activated integrin switch controls alpha5beta1 function. *Science*. 323:642–644.

Fuyuhiro, Y., M. Yashiro, S. Noda, J. Matsuoka, T. Hasegawa, Y. Kato, T. Sawada, and K. Hirakawa. 2012. Cancer-associated orthotopic myofibroblasts stimulates the motility of gastric carcinoma cells. *Cancer Sci.* 103:797–805.

Gaggioli, C., S. Hooper, C. Hidalgo-Carcedo, R. Grosse, J.F. Marshall, K. Harrington, and E. Sahai. 2007. Fibroblast-led collective invasion of carcinoma cells with differing roles

for RhoGTPases in leading and following cells. *Nat. Cell Biol.* 9:1392–1400.

Galbraith, C.G., K.M. Yamada, and M.P. Sheetz. 2002. The relationship between force and focal complex development. *J. Cell Biol.* 159:695–705.

Garcia-Palmero, I., S. Torres, R.A. Bartolome, A. Pelaez-Garcia, M.J. Larriba, M. Lopez-Lucendo, C. Pena, B. Escudero-Paniagua, A. Munoz, and J.I. Casal. 2016. Twist1-induced activation of human fibroblasts promotes matrix stiffness by upregulating palladin and collagen [alpha]1(VI). *Oncogene*.

García-Palmero, I., S. Torres, R.A. Bartolomé, A. Peláez-García, M.J. Larriba, M. Lopez-Lucendo, C. Peña, B. Escudero-Paniagua, A. Muñoz, and J.I. Casal. 2016. Twist1-induced activation of human fibroblasts promotes matrix stiffness by upregulating palladin and collagen α1(VI). *Oncogene*. 1–13.

George, E.L., E.N. Georges-Labouesse, R.S. Patel-King, H. Rayburn, and R.O. Hynes. 1993. Defects in mesoderm, neural tube and vascular development in mouse embryos lacking fibronectin. *Development*. 119:1079–1091.

Georgiadou, M., J. Lilja, G. Jacquemet, C. Guzmán, M. Rafaeva, C. Alibert, Y. Yan, P. Sahgal, M. Lerche, J.-B. Manneville, T.P. Mäkelä, and J. Ivaska. 2017. AMPK negatively regulates tensin-dependent integrin activity. *J. Cell Biol.* jcb.201609066.

Gialeli, C., D. Nikitovic, D. Kletsas, a. D. Theocharis, G.N. Tzanakakis, and N.K. Karamanos. 2014. PDGF/PDGFR signaling and targeting in cancer growth and progression: Focus on tumor microenvironment and cancer-associated fibroblasts. *Curr Pharm Des*. 20:2843–8.

Glentis, A., P. Oertle, P. Mariani, A. Chikina, F. El Marjou, Y. Attieh, F. Zaccarini, M. Lae, D. Loew, F. Dingli, P. Sirven, M. Schoumacher, B.G. Gurchenkov, M. Plodinec, and

D.M. Vignjevic. 2017. Cancer-associated fibroblasts induce metalloprotease-independent cancer cell invasion of the basement membrane. *Nat. Commun.* 8.

Goel, H.L., J. Li, S. Kogan, and L.R. Languino. 2008. Integrins in prostate cancer progression. *Endocr. Relat. Cancer*. 15:657–664.

Goetz, J.G., S. Minguet, I. Navarro-Lérida, J.J. Lazcano, R. Samaniego, E. Calvo, M. Tello, T. Osteso-Ibáñez, T. Pellinen, A. Echarri, A. Cerezo, A.J.P. Klein-Szanto, R. Garcia, P.J. Keely, P. Sánchez-Mateos, E. Cukierman, and M.A. Del Pozo. 2011. Biomechanical Remodeling of the Microenvironment by Stromal Caveolin-1 Favors Tumor Invasion and Metastasis. *Cell*. 146:148–163.

Goicoechea, S.M., R. García-Mata, J. Staub, A. Valdivia, L. Sharek, C.G. McCulloch, R.F. Hwang, R. Urrutia, J.J. Yeh, H.J. Kim, and C.A. Otey. 2014. Palladin promotes invasion of pancreatic cancer cells by enhancing invadopodia formation in cancer-associated fibroblasts. *Oncogene*. 33:1265–73.

Gopal, S., L. Veracini, D. Grall, C. Butori, S. Schaub, S. Audebert, L. Camoin, E. Baudelet, A. Radwanska, S. Beghelli-de la Forest Divonne, S.M. Violette, P.H. Weinreb, S. Rekima, M. Ilie, A. Sudaka, P. Hofman, and E. Van Obberghen-Schilling. 2017. Fibronectin-guided migration of carcinoma collectives. *Nat. Commun.* 8:14105.

Grande-Garcia, A., A. Echarri, J. De Rooij, N.B. Alderson, C.M. Waterman-Storer, J.M. Valdivielso, and M.A. Del Pozo. 2007. Caveolin-1 regulates cell polarization and directional migration through Src kinase and Rho GTPases. *J. Cell Biol.* 177:683–694.

Grashoff, C., B.D. Hoffman, M.D. Brenner, R. Zhou, M. Parsons, M.T. Yang, M.A. McLean, S.G. Sligar, C.S. Chen, T. Ha, and M.A. Schwartz. 2010. Measuring mechanical tension across vinculin reveals regulation of focal adhesion dynamics. *Nature*. 466:263–6.

Grugan, K.D., C.G. Miller, Y. Yao, C.Z. Michaylira, S. Ohashi, A.J. Klein-Szanto, J.A. Diehl, M. Herlyn, M. Han, H. Nakagawa, and A.K. Rustgi. 2010. Fibroblast-secreted hepatocyte growth factor plays a functional role in esophageal squamous cell carcinoma invasion. *Proc. Natl. Acad. Sci. U. S. A.* 107:11026–31.

Guan, J., H. Zhang, Z. Wen, Y. Gu, Y. Cheng, Y. Sun, T. Zhang, C. Jia, Z. Lu, and J. Chen. 2014. Retinoic acid inhibits pancreatic cancer cell migration and EMT through the downregulation of IL-6 in cancer associated fibroblast cells. *Cancer Lett.* 345:132–139.

Gurung, R., R. Yadav, J.G. Brungardt, A. Orlova, E.H. Egelman, and M.R. Beck. 2016. Actin polymerization is stimulated by actin cross-linking protein palladin. *Biochem. J.* 473:383–96.

Hall, A., and C.D. Nobes. 2000. Rho GTPases: molecular switches that control the organization and dynamics of the actin cytoskeleton. *Philos. Trans. R. Soc. Lond. B. Biol. Sci.* 355:965–70.

Harburger, D.S., M. Bouaouina, and D.A. Calderwood. 2009. Kindlin-1 and -2 directly bind the C-terminal region of ?? integrin cytoplasmic tails and exert integrin-specific activation effects. *J. Biol. Chem.* 284:11485–11497.

Harburger, D.S., and D.A. Calderwood. 2009. Integrin signalling at a glance. *J. Cell Sci.* 122:159–163.

Heldin, C.-H. 2013a. Targeting the PDGF signaling pathway in tumor treatment. *Cell Commun. Signal.* 11:97.

Heldin, C.-H. 2013b. Targeting the PDGF signaling pathway in tumor treatment. *Cell Commun. Signal.* 11:97.

Henriksson, M.L., S. Edin, A.M. Dahlin, P.A. Oldenborg, ??ke ??berg, B. Van Guelpen, J.

Rutegard, R. Stenling, and R. Palmqvist. 2011. Colorectal cancer cells activate adjacent fibroblasts resulting in FGF1/FGFR3 signaling and increased invasion. *Am. J. Pathol.* 178:1387–1394.

Hinz, B. 2006. Masters and servants of the force: The role of matrix adhesions in myofibroblast force perception and transmission. *Eur. J. Cell Biol.* 85:175–181.

Hinz, B., and G. Gabbiani. 2003. Mechanisms of force generation and transmission by myofibroblasts. *Curr. Opin. Biotechnol.* 14:538–546.

Hinz, B., S.H. Phan, V.J. Thannickal, A. Galli, M.-L. Bochaton-Piallat, and G. Gabbiani. 2007. The Myofibroblast. *Am. J. Pathol.* 170:1807–1816.

Horikawa, S., Y. Ishii, T. Hamashima, S. Yamamoto, H. Mori, T. Fujimori, J. Shen, R. Inoue, H. Nishizono, and H. Itoh. 2015. PDGFR α plays a crucial role in connective tissue remodeling. *Sci. Rep.* 5:1–14.

Hoyt, K., B. Castaneda, M. Zhang, P. Nigwekar, P.A. di Sant'Agnese, J. V Joseph, J. Strang, D.J. Rubens, and K.J. Parker. 2008. Tissue elasticity properties as biomarkers for prostate cancer. *Cancer Biomark.* 4:213–225.

Hynes, R.O. 1987. Integrins: A family of cell surface receptors. *Cell*. 48:549–554.

Hynes, R.O. 2002. Integrins: Bidirectional, allosteric signaling machines. *Cell*. 110:673–687.

Hynes, R.O. 2009. The Extracellular Matrix: Not Just Pretty Fibrils. *Science (80-.).* 326:1216–1219.

Ilić, D., B. Kovacic, K. Johkura, D.D. Schlaepfer, N. Tomasević, Q. Han, J.-B. Kim, K. Howerton, C. Baumbusch, N. Ogiwara, D.N. Streblow, J. a Nelson, P. Dazin, Y. Shino, K. Sasaki, and C.H. Damsky. 2004. FAK promotes organization of fibronectin matrix and fibrillar adhesions. *J. Cell Sci.* 117:177–187.

Insua-Rodríguez, J., and T. Oskarsson. 2016. The extracellular matrix in breast cancer. *Adv. Drug Deliv. Rev.* 97:41–55.

Ito, M., T. Nakano, F. Erdodi, and D.J. Hartshorne. 2004. Myosin phosphatase: Structure, regulation and function. *Mol. Cell. Biochem.* 259:197–209.

Jakowlew, S.B. 2006. Transforming growth factor-beta in cancer and metastasis. *Cancer Metastasis Rev.* 25:435–57.

Jean, L., D. Majumdar, M. Shi, L.E. Hinkle, N.L. Diggins, M. Ao, J. a Broussard, J.C. Evans, D.P. Choma, and D.J. Webb. 2013. Activation of Rac by Asef2 promotes myosin II-dependent contractility to inhibit cell migration on type I collagen. *J. Cell Sci.* 126:5585–97.

Jean, L., L. Yang, D. Majumdar, Y. Gao, M. Shi, B.M. Brewer, D. Li, and D.J. Webb. 2014. The Rho family GEF Asef2 regulates cell migration in three dimensional (3D) collagen matrices through myosin II. *Cell Adhes. Migr.* 8:460–467.

Jechlinger, M., A. Sommer, R. Moriggl, P. Seither, N. Kraut, P. Capodiecci, M. Donovan, C. Cordon-Cardo, H. Beug, and S. Grünert. 2006. Autocrine PDGFR signaling promotes mammary cancer metastasis. *J. Clin. Invest.* 116:1561–1570.

Jobe, N.P., D. Rosel, B. Dvorankova, O. Kodet, L. Lacina, R. Mateu, K. Smetana, and J. Brabek. 2016. Simultaneous blocking of IL-6 and IL-8 is sufficient to fully inhibit CAF-induced human melanoma cell invasiveness. *Histochem. Cell Biol.* 146:205–217.

Jolly, L.A., S. Novitskiy, P. Owens, N. Massoll, N. Cheng, W. Fang, H.L. Moses, and A.T. Franco. 2016. Fibroblast-mediated collagen remodeling within the tumor microenvironment facilitates progression of thyroid cancers driven by brafv600e and pten loss. *Cancer Res.* 76:1804–1813.

Kadler, K.E., A. Hill, and E.G. Canty-Laird. 2008. Collagen fibrillogenesis: fibronectin, integrins, and minor collagens as organizers and nucleators. *Curr. Opin. Cell Biol.* 20:495–501.

Kalluri, R., and M. Zeisberg. 2006. Fibroblasts in cancer. *Nat. Rev. Cancer*. 6:392–401.

Katsumi, A., T. Naoe, T. Matsushita, K. Kaibuchi, and M.A. Schwartz. 2005. Integrin activation and matrix binding mediate cellular responses to mechanical stretch. *J. Biol. Chem.* 280:16546–16549.

Katz, B.Z., E. Zamir, A. Bershadsky, Z. Kam, K.M. Yamada, and B. Geiger. 2000. Physical state of the extracellular matrix regulates the structure and molecular composition of cell-matrix adhesions. *Mol. Biol. Cell*. 11:1047–1060.

Kaukonen, R., A. Mai, M. Georgiadou, M. Saari, N. De Franceschi, T. Betz, H. Sihto, L. Elo, E. Jokitalo, J. Westermarck, P.-L. Kellokumpu-Lehtinen, H. Joensuu, R. Grenman, and J. Ivaska. 2016a. Normal stroma suppresses cancer cell proliferation via mechanosensitive regulation of JMJD1a-mediated transcription. *Nat. Commun.* 7.

Kaukonen, R., A. Mai, M. Georgiadou, M. Saari, N. De Franceschi, T. Betz, H. Sihto, S. Ventelä, L. Elo, E. Jokitalo, J. Westermarck, P.-L. Kellokumpu-Lehtinen, H. Joensuu, R. Grenman, and J. Ivaska. 2016b. Normal stroma suppresses cancer cell proliferation via mechanosensitive regulation of JMJD1a-mediated transcription. *Nat. Commun.* 7:12237.

Kazlauskas, A. 2017. PDGFs and their receptors. *Gene*. 614:1–7.

Kii, I., T. Nishiyama, M. Li, K. Matsumoto, M. Saito, N. Amizuka, and A. Kudo. 2010a. Incorporation of Tenascin-C into the Extracellular Matrix by Periostin Underlies an Extracellular Meshwork Architecture. *J. Biol. Chem.* 285:2028–2039.

Kii, I., T. Nishiyama, M. Li, K.I. Matsumoto, M. Saito, N. Amizuka, and A. Kudo. 2010b. Incorporation of tenascin-C into the extracellular matrix by periostin underlies an extracellular meshwork architecture. *J. Biol. Chem.* 285:2028–2039.

Kim, S.A., E.K. Lee, and H.J. Kuh. 2015. Co-culture of 3D tumor spheroids with fibroblasts as a model for epithelial-mesenchymal transition in vitro. *Exp. Cell Res.* 335:187–196.

Knuchel, S., P. Anderle, P. Werfelli, E. Diamantis, and C. Rüegg. 2015. Fibroblast surface-associated FGF-2 promotes contact-dependent colorectal cancer cell migration and invasion through FGFR-SRC signaling and integrin αvβ5-mediated adhesion. *Oncotarget*. 6:14300–17.

Kohler, N., and A. Lipton. 1974. Platelets as a source of fibroblast growth-promoting activity. *Exp. Cell Res.* 87:297–301.

Kong, D., Z. Wang, S.H. Sarkar, Y. Li, S. Banerjee, A. Saliganan, H.-R.C. Kim, M.L. Cher, and F.H. Sarkar. 2008. Platelet-derived growth factor-D overexpression contributes to epithelial-mesenchymal transition of PC3 prostate cancer cells. *Stem Cells*. 26:1425–1435.

Kumar, D., C. Kandl, C.D. Hamilton, Y. Shnayder, T.T. Tsue, K. Kakarala, L. Ledgerwood, X.S. Sun, H. (John) Huang, D. Girod, and S.M. Thomas. 2015. Mitigation of Tumor-Associated Fibroblast-Facilitated Head and Neck Cancer Progression With Anti–Hepatocyte Growth Factor Antibody Ficlatuzumab. *JAMA Otolaryngol. Neck Surg.* 66160:1133.

Labernadie, A., T. Kato, A. Brugués, X. Serra-Picamal, S. Derzsi, E. Arwert, A. Weston, V. González-Tarragó, A. Elosegui-Artola, L. Albertazzi, J. Alcaraz, P. Roca-Cusachs, E. Sahai, and X. Trepat. 2017. A mechanically active heterotypic E-cadherin/N-cadherin

adhesion enables fibroblasts to drive cancer cell invasion. *Nat. Cell Biol.* 19:224–237.

Larsen, M., V. V. Artym, J.A. Green, and K.M. Yamada. 2006. The matrix reorganized: extracellular matrix remodeling and integrin signaling. *Curr. Opin. Cell Biol.* 18:463–471.

Lee, H.-O., S.R. Mullins, J. Franco-Barraza, M. Valianou, E. Cukierman, and J.D. Cheng. 2011a. FAP-overexpressing fibroblasts produce an extracellular matrix that enhances invasive velocity and directionality of pancreatic cancer cells. *BMC Cancer*. 11:245.

Lee, H.-O., S.R. Mullins, J. Franco-Barraza, M. Valianou, E. Cukierman, and J.D. Cheng. 2011b. FAP-overexpressing fibroblasts produce an extracellular matrix that enhances invasive velocity and directionality of pancreatic cancer cells. *BMC Cancer*. 11:245.

Legate, K.R., S.A. Wickström, and R. Fässler. 2009. Genetic and cell biological analysis of integrin outside-in signaling. *Genes Dev.* 23:397–418.

Leiss, M., K. Beckmann, A. Gir??s, M. Costell, and R. Fassler. 2008. The role of integrin binding sites in fibronectin matrix assembly in vivo. *Curr. Opin. Cell Biol.* 20:502–507.

Lemmon, C.A., C.S. Chen, and L.H. Romer. 2009. Cell traction forces direct fibronectin matrix assembly. *Biophys. J.* 96:729–738.

Lenselink, E.A. 2015. Role of fibronectin in normal wound healing. *Int. Wound J.* 12:313–316.

Levental, K.R., H. Yu, L. Kass, J.N. Lakins, M. Egeblad, J.T. Erler, S.F.T. Fong, K. Csiszar, A. Giaccia, W. Weninger, M. Yamauchi, D.L. Gasser, and V.M. Weaver. 2009. Matrix Crosslinking Forces Tumor Progression by Enhancing Integrin Signaling. *Cell*. 139:891–906.

Li, B., and J.H.C. Wang. 2011. Fibroblasts and myofibroblasts in wound healing: Force

generation and measurement. *J. Tissue Viability*. 20:108–120.

Li, H., X. Fan, and J. Houghton. 2007. Tumor microenvironment: The role of the tumor stroma in cancer. *J. Cell. Biochem.* 101:805–815.

Li, J., Z. Jia, J. Kong, F. Zhang, S. Fang, X. Li, W. Li, X. Yang, Y. Luo, B. Lin, and T. Liu. 2016. Carcinoma-Associated Fibroblasts Lead the Invasion of Salivary Gland Adenoid Cystic Carcinoma Cells by Creating an Invasive Track. *PLoS One*. 11:e0150247.

Lin, G.L., D.M. Cohen, R.A. Desai, M.T. Breckenridge, L. Gao, M.J. Humphries, and C.S. Chen. 2013. Activation of beta 1 but not beta 3 integrin increases cell traction forces. *FEBS Lett.* 587:763–769.

Lines, E.C., E. Sariban, N.M. Sitaras, H.N. Antoniades, D.W. Kufe, and P. Pantazist. 1988. Expression of platelet-derived growth factor (PDGF)-related transcripts and synthesis of biologically active PDGF-like proteins by human malignant epithelial cell lines. *J. Clin. Invest.* 82:1157–1164.

Liu, J., S. Chen, W. Wang, B.-F. Ning, F. Chen, W. Shen, J. Ding, W. Chen, W.-F. Xie, and X. Zhang. 2016. Cancer-associated fibroblasts promote hepatocellular carcinoma metastasis through chemokine-activated hedgehog and TGF-β pathways. *Cancer Lett.* 379:49–59.

Lokker, N.A., C.M. Sullivan, S.J. Hollenbach, M.A. Israel, and N.A. Giese. 2002. Platelet-derived growth factor (PDGF) autocrine signaling regulates survival and mitogenic pathways in glioblastoma cells: Evidence that the novel PDGF-C and PDGF-D ligands may play a role in the development of brain tumors. *Cancer Res.* 62:3729–3735.

Longtin, R. 2004. Birthday of a breakthrough: fibronectin research proves important, but not as originally expected. *J. Natl. Cancer Inst.* 96:6–8.

Luo, T., K. Mohan, V. Srivastava, Y. Ren, P.A. Iglesias, and D.N. Robinson. 2012. Understanding the cooperative interaction between myosin II and actin cross-linkers mediated by actin filaments during mechanosensation. *Biophys. J.* 102:238–247.

Machacek, M., L. Hodgson, C. Welch, H. Elliott, O. Pertz, P. Nalbant, A. Abell, G.L. Johnson, K.M. Hahn, and G. Danuser. 2009. Coordination of Rho GTPase activities during cell protrusion. *Nature*. 461:99–103.

Madar, S., I. Goldstein, and V. Rotter. 2013. "Cancer associated fibroblasts" - more than meets the eye. *Trends Mol. Med.* 19:447–453. doi:10.1016/j.molmed.2013.05.004.

Magnusson, M.K., and D.F. Mosher. 1998. Fibronectin: structure, assembly, and cardiovascular implications. *Arterioscler. Thromb. Vasc. Biol.* 18:1363–1370.

Mao, Y., and J.E. Schwarzbauer. 2005. Fibronectin fibrillogenesis, a cell-mediated matrix assembly process. *Matrix Biol.* 24:389–399.

Margadant, C., H.N. Monsuur, J.C. Norman, and A. Sonnenberg. 2011. Mechanisms of integrin activation and trafficking. *Curr. Opin. Cell Biol.* 23:607–614.

McBeath, R., D.M. Pirone, C.M. Nelson, K. Bhadriraju, and C.S. Chen. 2004. Cell shape, cytoskeletal tension, and RhoA regulate stem cell lineage commitment. *Dev. Cell*. 6:483–495.

Mezawa, Y., and A. Orimo. 2016. The roles of tumor- and metastasis-promoting carcinoma-associated fibroblasts in human carcinomas. *Cell Tissue Res.* 365:675–689.

Mierke, C.T., B. Frey, M. Fellner, M. Herrmann, and B. Fabry. 2011. Integrin α5β1 facilitates cancer cell invasion through enhanced contractile forces. *J. Cell Sci.* 124:369–383.

Miles, F.L., and R.A. Sikes. 2014. Insidious changes in stromal matrix fuel cancer progression. *Mol. Cancer Res.* 12:297–312.

Min, A., C. Zhu, J. Wang, S. Peng, C. Shuai, S. Gao, Z. Tang, and T. Su. 2015. Focal adhesion kinase knockdown in carcinoma-associated fibroblasts inhibits oral squamous cell carcinoma metastasis via downregulating MCP-1/CCL2 expression. *J. Biochem. Mol. Toxicol.* 29:70–76.

Moser, M., K.R. Legate, R. Zent, and R. Fassler. 2009. The tail of integrins, talin, and kindlins. *Science (80-.).* 324:895–899.

Muro, A.F., F.A. Moretti, B.B. Moore, M. Yan, R.G. Atrasz, C.A. Wilke, K.R. Flaherty, F.J. Martinez, J.L. Tsui, D. Sheppard, F.E. Baralle, G.B. Toews, and E.S. White. 2008. An essential role for fibronectin extra type III domain A in pulmonary fibrosis. *Am. J. Respir. Crit. Care Med.* 177:638–645.

Newell-Litwa, K.A., R. Horwitz, and M.L. Lamers. 2015. Non-muscle myosin II in disease: mechanisms and therapeutic opportunities. *Dis. Model. Mech.* 8:1495–1515.

Nobes, C.D., and A. Hall. 1995. Rho, Rac, and Cdc42 GTPases regulate the assembly of multimolecular focal complexes associated with actin stress fibers, lamellipodia, and filopodia. *Cell*. 81:53–62.

Olumi, A.F., G.D. Grossfeld, S.W. Hayward, P. Epithelium, A.F. Olumi, G.D. Grossfeld, S.W. Hayward, P.R. Carroll, T.D. Tlsty, and G.R. Cunha. 1999. Carcinoma-associated Fibroblasts Direct Tumor Progression of Initiated Human Prostatic Epithelium Carcinoma-associated Fibroblasts Direct Tumor Progression of Initiated Human. 5002–5011.

Orimo, A., P.B. Gupta, D.C. Sgroi, F. Arenzana-Seisdedos, T. Delaunay, R. Naeem, V.J. Carey, A.L. Richardson, and R.A. Weinberg. 2005. Stromal fibroblasts present in invasive human breast carcinomas promote tumor growth and angiogenesis through

elevated SDF-1/CXCL12 secretion. *Cell*. 121:335–348.

Östman, A. 2004. PDGF receptors-mediators of autocrine tumor growth and regulators of tumor vasculature and stroma. *Cytokine Growth Factor Rev.* 15:275–286.

Oyanagi, J., N. Kojima, H. Sato, S. Higashi, K. Kikuchi, K. Sakai, K. Matsumoto, and K. Miyazaki. 2014. Inhibition of transforming growth factor-β signaling potentiates tumor cell invasion into collagen matrix induced by fibroblast-derived hepatocyte growth factor. *Exp. Cell Res.* 326:267–279.

Pankov, R., E. Cukierman, B.Z. Katz, K. Matsumoto, D.C. Lin, S. Lin, C. Hahn, and K.M. Yamada. 2000. Integrin dynamics and matrix assembly: Tensin-dependent translocation of a5b1 integrins promotes early fibronectin fibrillogenesis. *J. Cell Biol.* 148:1075–1090.

Pankov, R., and K. Yamada. 2002. Fibronectin at a glance. *J. Cell Sci.* 115:3861–3863.

Parsons, J.T., A.R. Horwitz, and M. a Schwartz. 2010. Cell adhesion: integrating cytoskeletal dynamics and cellular tension. *Nat. Rev. Mol. Cell Biol.* 11:633–43.

Paszek, M.J., N. Zahir, K.R. Johnson, J.N. Lakins, G.I. Rozenberg, A. Gefen, C.A. Reinhart-King, S.S. Margulies, M. Dembo, D. Boettiger, D.A. Hammer, and V.M. Weaver. 2005. Tensional homeostasis and the malignant phenotype. *Cancer Cell*. 8:241–254.

Petrie, R.J., A.D. Doyle, and K.M. Yamada. 2009. Random versus directionally persistent cell migration. *Nat. Rev. Mol. Cell Biol.* 10:538–49.

Peuhu, E., R. Kaukonen, M. Lerche, M. Saari, C. Guzmán, P. Rantakari, N. De Franceschi, A. Wärri, M. Georgiadou, G. Jacquemet, E. Mattila, R. Virtakoivu, Y. Liu, Y. Attieh, K.A. Silva, T. Betz, J.P. Sundberg, M. Salmi, M.-A. Deugnier, K.W. Eliceiri, and J. Ivaska. 2017. SHARPIN regulates collagen architecture and ductal outgrowth in the

developing mouse mammary gland. *EMBO J.* 36:165–182.

Polacheck, W.J., I.K. Zervantonakis, and R.D. Kamm. 2013. Tumor cell migration in complex microenvironments. *Cell. Mol. Life Sci.* 70:1335–1356.

Pouwels, J., J. Nevo, T. Pellinen, J. Ylanne, and J. Ivaska. 2012. Negative regulators of integrin activity. *J. Cell Sci.* 125:3271–3280.

Provenzano, P.P., D.R. Inman, K.W. Eliceiri, S.M. Trier, and P.J. Keely. 2008. Contact guidance mediated three-dimensional cell migration is regulated by Rho/ROCK-dependent matrix reorganization. *Biophys J.* 95:5374–5384.

Qian, F., Z.C. Zhang, X.F. Wu, Y.P. Li, and Q. Xu. 2005. Interaction between integrin α5 and fibronectin is required for metastasis of B16F10 melanoma cells. *Biochem. Biophys. Res. Commun.* 333:1269–1275.

Rasanen, K., and A. Vaheri. 2010. Activation of fibroblasts in cancer stroma. *Exp. Cell Res.* 316:2713–2722.

Ridley, A.J. 2003. Cell Migration: Integrating Signals from Front to Back. *Science (80-.).* 302:1704–1709.

Rizwani, W., A.E. Allen, and J.G. Trevino. 2015. Hepatocyte growth factor from a clinical perspective: A pancreatic cancer challenge. *Cancers (Basel).* 7:1785–1805.

Roca-Cusachs, P., N.C. Gauthier, A. Del Rio, and M.P. Sheetz. 2009. Clustering of alpha(5)beta(1) integrins determines adhesion strength whereas alpha(v)beta(3) and talin enable mechanotransduction. *Proc. Natl. Acad. Sci. U. S. A.* 106:16245–16250.

Roca-Cusachs, P.P., T.T. Iskratsch, and M.P.M.P. Sheetz. 2012. Finding the weakest link: exploring integrin-mediated mechanical molecular pathways. *J. Cell Sci.* 125:3025–3038.

Rokhlin, O.W., and M.B. Cohen. 1995. Expression of cellular adhesion molecules on human prostate tumor cell lines. *Prostate*. 26:205–12.

Ross, R., J. Glomset, B. Kariya, and L. Harker. 1974. A platelet-dependent serum factor that stimulates the proliferation of arterial smooth muscle cells in vitro. *Proc. Natl. Acad. Sci. U. S. A.* 71:1207–10.

Ross, T.D., B.G. Coon, S. Yun, N. Baeyens, K. Tanaka, M. Ouyang, and M.A. Schwartz. 2013. Integrins in mechanotransduction. *Curr. Opin. Cell Biol.* 25:613–618.

Ruoslahti, E. 1996. Rgd and Other Recognition Sequences for Integrins. *Annu. Rev. Cell Dev. Biol.* 12:697–715.

Sabass, B., M.L.M.L. Gardel, C.M.C.M. Waterman, and U.S.U.S. Schwarz. 2008. High resolution traction force microscopy based on experimental and computational advances. *Biophys. J.* 94:207–220.

Sawada, K., A.K. Mitra, A.R. Radjabi, V. Bhaskar, E.O. Kistner, M. Tretiakova, S. Jagadeeswaran, A. Montag, A. Becker, H.A. Kenny, M.E. Peter, V. Ramakrishnan, S.D. Yamada, and E. Lengyel. 2008. Loss of E-cadherin promotes ovarian cancer metastasis via alpha(5)-integrin, which is a therapeutic target. *Cancer Res.* 68:2329–2339.

Schäfer, M., and S. Werner. 2008. Cancer as an overhealing wound: an old hypothesis revisited. *Nat. Rev. Mol. Cell Biol.* 9:628–38.

Schaffner, F., A.M. Ray, and M. Dontenwill. 2013. Integrin ??5??1, the fibronectin receptor, as a pertinent therapeutic target in solid tumors. *Cancers (Basel).* 5:27–47.

Schor, S.L., I.R. Ellis, S.J. Jones, R. Baillie, K. Seneviratne, J. Clausen, K. Motegi, B. Vojtesek, K. Kankova, E. Furrie, M.J. Sales, A.M. Schor, and R.A. Kay. 2003. Migration-Stimulating Factor: A Genetically Truncated Onco-Fetal Fibronectin

Isoform Expressed by Carcinoma and Tumor-Associated Stromal Cells. *Cancer Res.* 63:8827–8836.

Schwartz, M.A. 2010. Integrins and extracellular matrix in mechanotransduction. *Cold Spring Harb. Perspect. Biol.* 2:1–13.

Schwartz, M.A., and D.W. DeSimone. 2008. Cell adhesion receptors in mechanotransduction. *Curr. Opin. Cell Biol.* 20:551–556.

Schwarzbauer, J.E., and D.W. DeSimone. 2011. Fibronectins, their fibrillogenesis, and in vivo functions. *Cold Spring Harb. Perspect. Biol.* 3:1–19.

Sechler, J.L., A.M. Cumiske, D.M. Gazzola, and J.E. Schwarzbauer. 2000. A novel RGD-independent fibronectin assembly pathway initiated by α4β1 integrin binding to the alternatively spliced V region. *J. Cell Sci.* 113:1491–1498.

Seewaldt, V. 2014. ECM stiffness paves the way for tumor cells. *Nat. Med.* 20:332–333.

Sellers, J.R. 2000. Myosins: A diverse superfamily. *Biochim. Biophys. Acta - Mol. Cell Res.* 1496:3–22.

Shao, Z.-M., M. Nguyen, and S.H. Barsky. 2000. Human breast carcinoma desmoplasia is PDGF initiated. *Oncogene*. 19:4337–4345.

Shi, C., M.K. Washington, R. Chaturvedi, Y. Drosos, F.L. Revetta, C.J. Weaver, E. Buzhardt, F.E. Yull, T.S. Blackwell, B. Sosa-pineda, R.H. Whitehead, R.D. Beauchamp, K.T. Wilson, and A.L. Means. 2014. Fibrogenesis in pancreatic cancer is a dynamic process regulated by macrophage – stellate cell interaction. *Lab. Investig.* 94:409–421.

Shi, F., and J. Sottile. 2008. Caveolin-1-dependent beta1 integrin endocytosis is a critical regulator of fibronectin turnover. *J. Cell Sci.* 121:2360–71.

Shimao, Y.S., K.N. Abeshima, T.I. Noue, and M.K. Oono. 1999. Role of Fibroblasts in Hgf

/ Sf-Induced Cohort Migration of Human Colorectal Carcinoma Cells : Fibroblasts Stimulate Migration Associated With Increased Fibronectin Production. *Int. J. Cancer*. 458:449–458.

Singh, P., C. Carraher, and J.E. Schwarzbauer. 2010. Assembly of fibronectin extracellular marix. *Annu Rev Cell Dev Biol*. 26:397–419.

Sitaras, N.M., E. Sariban, M. Bravo, P. Pantazis, and H.N. Antoniades. 1988. Constitutive Production of Platelet-derived Growth Factor-like Proteins by Human Prostate Carcinoma Cell Lines. *Cancer Res.* 48:1930–1935.

Sottile, J. and Chandler, J. 2004. Fibronectin Matrix Turnover Occurs through a Caveolin-1-dependent Process. *Mol. Biol. Cell*. 16:757–768.

Stanisavljevic, J., J. Loubat-Casanovas, M. Herrera, T. Luque, R. Pena, A. Lluch, J. Albanell, F. Bonilla, A. Rovira, C. Pe??a, D. Navajas, F. Rojo, A. Garcia De Herreros, and J. Baulida. 2015. Snail1-expressing fibroblasts in the tumor microenvironment display mechanical properties that support metastasis. *Cancer Res.* 75:284–295.

Steeg, P.S. 2006. Tumor metastasis : mechanistic insights and clinical challenges. *Nat. Med.* 12:895–904.

Sutherland, M., A. Gordon, S.D. Shnyder, L.H. Patterson, and H.M. Sheldrake. 2012a. RGD-binding integrins in prostate cancer: Expression patterns and therapeutic prospects against bone metastasis. *Cancers (Basel)*. 4:1106–1145.

Sutherland, M., A. Gordon, S.D. Shnyder, L.H. Patterson, and H.M. Sheldrake. 2012b. RGD-binding integrins in prostate cancer: Expression patterns and therapeutic prospects against bone metastasis. *Cancers (Basel)*. 4:1106–1145.

Taddei, M.L., E. Giannoni, G. Comito, and P. Chiarugi. 2013. Microenvironment and tumor

cell plasticity: An easy way out. *Cancer Lett.* 341:80–96.

Tani, N., S. Higashiyama, N. Kawaguchi, J. Madarame, I. Ota, Y. Ito, Y. Ohoka, S. Shiosaka, Y. Takada, and N. Matsuura. 2003. Expression level of integrin α5 on tumour cells affects the rate of metastasis to the kidney. *Br. J. Cancer*. 88:327–333.

Taverna, D., M. Ullman-Cullere, H. Rayburn, R.T. Bronson, and R.O. Hynes. 1998. A test of the role of alpha5 integrin/fibronectin interactions in tumorigenesis. *Cancer Res*. 58:848–853.

Tejada, M.L., L. Yu, J. Dong, K. Jung, G. Meng, F. V Peale, G.D. Frantz, L. Hall, X. Liang, H.-P. Gerber, and N. Ferrara. 2006. Tumor-driven paracrine platelet-derived growth factor receptor alpha signaling is a key determinant of stromal cell recruitment in a model of human lung carcinoma. *Clin. Cancer Res.* 12:2676–88.

Teng, F., W.-Y. Tian, Y.-M. Wang, Y.-F. Zhang, F. Guo, J. Zhao, C. Gao, and F.-X. Xue. 2016. Cancer-associated fibroblasts promote the progression of endometrial cancer via the SDF-1/CXCR4 axis. *J. Hematol. Oncol.* 9:8.

To, W.S., and K.S. Midwood. 2011. Plasma and cellular fibronectin: distinct and independent functions during tissue repair. *Fibrogenesis Tissue Repair*. 4:21.

Tojkander, S., G. Gateva, and P. Lappalainen. 2012. Actin stress fibers - assembly, dynamics and biological roles. *J. Cell Sci.* 125:1855–1864.

Topalovski, M., and R.A. Brekken. 2016. Matrix control of pancreatic cancer: New insights into fibronectin signaling. *Cancer Lett.* 381:252–258.

Tripathi, M., S. Billet, and N. a. Bhowmick. 2012. Understanding the role of stromal fibroblasts in cancer progression. *Cell Adh. Migr.* 6:231–235.

Tschumperlin, D.J. 2013. Fibroblasts and the Ground They Walk On. *Physiology*. 28:380–

390.

Tuxhorn, J. a, G.E. Ayala, M.J. Smith, V.C. Smith, T.D. Dang, and D.R. Rowley. 2002. Reactive Stroma in Human Prostate Cancer : Induction of Myofibroblast Phenotype and Extracellular Matrix Remodeling Reactive Stroma in Human Prostate Cancer : Induction of Myofibroblast Phenotype and Extracellular. *Clin. Cancer Res.* 8:2912–2923.

Valastyan, S., and R.A. Weinberg. 2011. Tumor metastasis: Molecular insights and evolving paradigms. *Cell*. 147:275–292.

Veevers-Lowe, J., S.G. Ball, A. Shuttleworth, and C.M. Kielty. 2011. Mesenchymal stem cell migration is regulated by fibronectin through α5β1-integrin-mediated activation of PDGFR-β and potentiation of growth factor signals. *J. Cell Sci.* 124:1288–1300.

Velling, T., J. Risteli, K. Wennerberg, D.F. Mosher, and S. Johansson. 2002. Polymerization of type I and III collagens is dependent on fibronectin and enhanced by integrins a11b1 and a2b1. *J. Biol. Chem.* 277:37377–37381.

Vicente-Manzanares, M., and A.R. Horwitz. 2010. Myosin light chain mono- and di-phosphorylation differentially regulate adhesion and polarity in migrating cells. *Biochem. Biophys. Res. Commun.* 402:537–542.

Vicente-Manzanares, M., X. Ma, R.S. Adelstein, and A.R. Horwitz. 2009. Non-muscle myosin {II} takes centre stage in cell adhesion and migration. *Nat. Rev. Mol. Cell Biol.* 10:778–790.

Vicente-Manzanares, M., D.J. Webb, and a R. Horwitz. 2005. Cell migration at a glance. *J. Cell Sci.* 118:4917–4919.

Wang, J.P., and A. Hielscher. 2017. Fibronectin: How its aberrant expression in tumors may

improve therapeutic targeting. *J. Cancer*. 8:674–682.

Wang, Y., K. Appiah-Kubi, M. Wu, X. Yao, H. Qian, Y. Wu, and Y. Chen. 2016. The platelet-derived growth factors (PDGFs) and their receptors (PDGFRs) are major players in oncogenesis, drug resistance, and attractive oncologic targets in cancer. *Growth Factors*. 34:64–71.

Webb, D.J., K. Donais, L.A. Whitmore, S.M. Thomas, C.E. Turner, J.T. Parsons, and A.F. Horwitz. 2004. FAK–Src signalling through paxillin, ERK and MLCK regulates adhesion disassembly. *Nat. Cell Biol.* 6:154–161.

Webb, D.J., H. Zhang, and A.F. Horwitz. 2012. Cell migration. *Methods Mol. Biol.* 294:2369–2392.

De Wever, O., Q.-D. Nguyen, L. Van Hoorde, M. Bracke, E. Bruyneel, C. Gespach, and M. Mareel. 2004. Tenascin-C and SF/HGF produced by myofibroblasts in vitro provide convergent pro-invasive signals to human colon cancer cells through RhoA and Rac. *FASEB J.* 18:1016–1018.

White, E.S., F.E. Baralle, and A.F. Muro. 2008. New insights into form and function of fibronectin splice variants. *J. Pathol.* 216:1–14.

White, E.S., and A.F. Muro. 2011. Fibronectin splice variants: Understanding their multiple roles in health and disease using engineered mouse models. *IUBMB Life*. 63:538–546.

Wierzbicka-Patynowski, I., and J.E. Schwarzbauer. 2003. The ins and outs of fibronectin matrix assembly. *J. Cell Sci.* 116:3269–3276.

Woods, A. 2001. Syndecans: Transmembrane modulators of adhesion and matrix assembly. *J. Clin. Invest.* 107:935–941.

Wu, M.H., H.C. Hong, T.M. Hong, W.F. Chiang, Y.T. Jin, and Y.L. Chen. 2011. Targeting

galectin-1 in carcinoma-associated fibroblasts inhibits oral squamous cell carcinoma metastasis by downregulating MCP-1/CCL2 expression. *Clin. Cancer Res.* 17:1306–1316.

Wyckoff, J.B., Y. Wang, E.Y. Lin, J.F. Li, S. Goswami, E.R. Stanley, J.E. Segall, J.W. Pollard, and J. Condeelis. 2007. Direct visualization of macrophage-assisted tumor cell intravasation in mammary tumors. *Cancer Res.* 67:2649–2656.

Xia, Y., and G.M. Whitesides. 1998. Soft Lithography. *Annu. Rev. Mater. Sci.* 28:153–184.

Xiao, Q., X. Hu, Z. Wei, and K.Y. Tam. 2016. Cytoskeleton molecular motors: Structures and their functions in neuron. *Int. J. Biol. Sci.* 12:1083–1092.

Yamada, K.M., and S. Even-Ram. 2002. Integrin regulation of growth factor signalling and adhesion. *Nat. Cell Biol.* 4:E75E–76.

Yamaguchi, H., N. Yoshida, M. Takanashi, Y. Ito, K. Fukami, K. Yanagihara, M. Yashiro, and R. Sakai. 2014. Stromal fibroblasts mediate extracellular matrix remodeling and invasion of scirrhous gastric carcinoma cells. *PLoS One*. 9:1–12.

Yang, J.T., and R.O. Hynes. 1996. Fibronectin receptor functions in embryonic cells deficient in alpha 5 beta 1 integrin can be replaced by alpha V integrins. *Mol. Biol. Cell*. 7:1737–1748.

Yang, N., R. Mosher, S. Seo, D. Beebe, and A. Friedl. 2011. Syndecan-1 in breast cancer stroma fibroblasts regulates extracellular matrix fiber organization and carcinoma cell motility. *Am. J. Pathol.* 178:325–335.

Yeung, T., P.C. Georges, L.A. Flanagan, B. Marg, M. Ortiz, M. Funaki, N. Zahir, W. Ming, V. Weaver, and P.A. Janmey. 2005. Effects of substrate stiffness on cell morphology, cytoskeletal structure, and adhesion. *Cell Motil. Cytoskeleton*. 60:24–34.

Yilmaz, M., and G. Christofori. 2010. Mechanisms of motility in metastasizing cells. *Mol. Cancer Res.* 8:629–642.

Yu, Y., C.-H. Xiao, L.-D. Tan, Q.-S. Wang, X.-Q. Li, and Y.-M. Feng. 2014. Cancer-associated fibroblasts induce epithelial-mesenchymal transition of breast cancer cells through paracrine TGF-β signalling. *Br. J. Cancer*. 110:724–32.

Zaidel-Bar, R., S. Itzkovitz, A. Ma'ayan, R. Iyengar, and B. Geiger. 2007. Functional atlas of the integrin adhesome. *Nat. Cell Biol.* 9:858–867.

Zaman, M.H., L.M. Trapani, A.L. Sieminski, D. Mackellar, H. Gong, R.D. Kamm, A. Wells, D.A. Lauffenburger, and P. Matsudaira. 2006. Migration of tumor cells in 3D matrices is governed by matrix stiffness along with cell-matrix adhesion and proteolysis. *Proc. Natl. Acad. Sci. U. S. A.* 103:10889–10894.

Zemskov, E.A., E. Loukinova, I. Mikhailenko, R.A. Coleman, D.K. Strickland, and A.M. Belkin. 2009a. Regulation of platelet-derived growth factor receptor function by integrin-associated cell surface transglutaminase. *J Biol Chem*. 284:16693–16703.

Zemskov, E.A., E. Loukinova, I. Mikhailenko, R.A. Coleman, D.K. Strickland, and A.M. Belkin. 2009b. Regulation of Platelet-derived Growth Factor Receptor Function by Integrin-associated CellSurfaceTransglutaminase. *J. Biol. Chem.* 284:16693–16703.

Zhai, L., J. Madden, W.-C. Foo, V. Mouraviev, T.J. Polascik, M.L. Palmeri, and K.R. Nightingale. 2010. Characterizing Stiffness of Human Prostates Using Acoustic Radiation Force. *Ultrason. Imaging*. 32:201–213.

Zhang, J., X. Tian, and J. Xing. 2016. Signal Transduction Pathways of EMT Induced by TGF-β, SHH, and WNT and Their Crosstalks. *J. Clin. Med.* 5:41.

Zhang, Q., W.J. Checovich, D.M. Peters, R.M. Albrecht, and D.F. Mosher. 1994. Modulation

of cell surface fibronectin assembly sites by lysophosphatidic acid. *J. Cell Biol.* 127:1447–1459.

Zhong, C., M. Chrzanowska-Wodnicka, J. Brown, A. Shaub, A.M. Belkin, and K. Burridge. 1998. Rho-mediated contractility exposes a cryptic site in fibronectin and induces fibronectin matrix assembly. *J. Cell Biol.* 141:539–551.

Zhuang, J., Q. Lu, B. Shen, X. Huang, L. Shen, X. Zheng, R. Huang, J. Yan, and H. Guo. 2015. TGFβ1 secreted by cancer-associated fibroblasts induces epithelial-mesenchymal transition of bladder cancer cells through lncRNA-ZEB2NAT. *Sci. Rep.* 5:11924.